FATIGUE CRACK GROWTH PREDICTION AND ANALYSIS

by

Turgut AKYÜREK

B.S. in M.E., Boğaziçi University

Submitted to the Institute for Graduate Studies in Science and Engineering in partial fulfillment of the requirements for the degree of

Master of Science

in

Mechanical Engineering

Boğaziçi University

1984

FATIGUE CRACK GROWTH PREDICTION AND ANALYSIS

APPROVED BY

Doç.Dr. Öktem VARDAR ....
(Thesis supervisor)

Doç.Dr. Burak ERMAN ....

Doç.Dr. Sabri ALTINTAŞ ....

DATE OF APPROVAL

ACKNOWLEDGEMENTS

I would like to express my gratitude and sincere thanks to Assoc. Prof. Öktem VARDAR, thesis supervisor, for his kind interest and guidance in the production of this work.

I am also indepted to Turkish Army that gave me opportunity to get my entire graduate education in the Faculty of Engineering at Boğaziçi University.

FATIGUE CRACK GROWTH PREDICTION AND ANALYSIS

In this thesis, A computer program predicting the fatigue life of the specimens subjected to randomized black loading is prepared. A detailed description of fatigue crack growth and predictive models are reviewed.

The computer program AKYÜREK-I takes also the retardation phenomenon into consideration. The Wheeler and Willenborg retardation models are used.

In the program, center-crack panel, single and double edge cracked specimens, compact tension specimen, bend specimen and surface flawed plates are considered. A cycle-by-cycle integration scheme is used.

The results of some experiments are used to review the existing crack growth prediction models.

YORULMA ÇATLAĞI İLERLEMESİ TAHMİN VE ANALİZİ

Bu tez çalışmasında, düzensiz blok yükleme tatbik edilen deney numunelerinin yorulma sürelerini tahmin eden bir bilgisayar programı hazırlanılmıştır. Ayrıca yorulma çatlak ilerlemesi ve yorulma süresi tahmin modellerini içeren geniş bir derleme yapılmıştır.

AKYÜREK-I bilgisayar programı çatlak ilerlemesindeki gecikme olgusunu da göz önüne almaktadır. Wheeler ve Willenborg gecikme modelleri kullanılmıştır.

Program merkez çatlaklı, tek ve çift kenar çatlaklı deney numuneleri, standard ufak çekme numunesi, bükme numunesi ve yüzey çatlaklı plakalara uygulanan yükleme durumlarını değerlendirmektedir. Çatlak ilerlemesi; yükleme dalgaları bir bir göz önüne alınarak, her bir yüklemenin neden olduğu ilerlemelerin toplamı olarak düşünülmüştür.

Bazı deney sonuçlarını kullanarak, programdaki çatlak ilerleme metotlarının değerlendirmeleri yapılmıştır.

TABLE OF CONTENTS

LIST OF FIGURES

LIST OF TABLES

LIST OF SYMBOLS

a	Crack length
a/w	Crack length-the width of specimen ratio
A(f)	Some function of frequency
a_i	Current crack length
a_o	Crack length at the overload
a_p	a_o+r_{po} (plastic zone size due to overload)
B	Thickness of the specimen
C	Material constant in crack-growth equations.
c	Crack length in the major axis direction of the surface flaw
COD	Crack opening displacement
C_p	Retardation factor
da/dN	Crack growth rate
(da/dN)lin.	Linear crack growth rate
(da/dN)ret.	Retarded crack growth rate
ds	A segment of crack border
du	Strain energy change
E	Youngs modulus
$\mathcal{G}$	Crack extension force
h	Step size in the simpson's integration formula
K	Stress intensity factor
K_I	Stress intensity factor for mode-I
K_{IC}	Plane-strain fracture toughness
$K_{max.i}$	Maximum stress intensity factor at the current cycle
$K_{min.i}$	Minimum stress intensity factor at the current cycle
$K_{max.eff}$	Max. effective stress intensity factor
$K_{min.eff}$	Min. effective stress intensity factor

m	Walker's exponent, Wheeler's retardation exponent
M_K	Front-free surface correction
n	Material constant
N	Cycles of load
p.c.f.	Plastic constraint factor
P_{max}	Maximum applied load
P_{min}	Minimum applied load
Q	Flaw shape parameter
r_{pi}	Plastic zone size at the current cycle
R	Cycle ratio ($= K_{min}/K_{max}$)
r_p^*	Plastic zone correction
S	Distance between the supports in bend specimen
U	Elber's stress intensity ratio ($= \Delta K_{eff} / \Delta K$)
Y	A polynomial in (a/w)
W	Width of the specimen
α	Constant used in plastic zone size evaluation
Φ	Elliptic integral of the second kind
η	Crack opening displacement in y direction
η_o	Half the total separation of the wall at the origin
σ_{cl}	Closure stress
σ_{max}	Maximum stress
σ_{min}	Minimum stress
σ_a	Stress amplitude ($\sigma_{max} - \sigma_{min})/2$
σ_{res}	Residual stress
σ_y	Stress in the y direction
σ_{ys}	Yield strength
σ_r	Stress range ($= \sigma_{max} - \sigma_{min}$)
ΔK	Stress intensity range

ΔK_{eff}	Effective stress intensity range
$\Delta\sigma$	Stress range ($= \sigma_{max} - \sigma_{min}$)

I. INTRODUCTION

Fatigue of materials is a common problem that affects everything that moves, and even apparently stationary objects may fail in fatigue if they experience cyclically imposed forces or deformations. There are innumerable problem areas. Automobiles fatigue from rough roads, airplane wings flutter in flight, bridges deflect under each passing vehicle, ships are heaved by the waves, and nuclear reactors are damaged by cyclic temperature changes.

The goal of this study is to prepare a computer program using the Wheeler and the Willenborg retardation models. This program predicts the cyclic life of the edge-cracked, center-cracked, double-edge-cracked, surface flawed, ASTM standard compact-tension and bend specimens under randomized block loading. Since the computer program requires a high knowledge of fatigue crack propagation detailed review of that subject is given in Chapters II, III, and IV.

In reality materials experience variable amplitude load fatigue. Because of the difficulty in treating the problem in real conditions, research has been devoted to predict the variable amplitude behavior from the constant amplitude data.

The subject of linear crack growth is reviewed in Chapter II. Since stress intensity factor range is the governing parameter in crack propagation, stress intensity evaluations are presented. The crack tip plasticity is the basis of the Wheeler and the Willenborg retardation models, therefore it is also reviewed in Chapter II.

Many models have been developed to take into account the retardation phenomenon in variable amplitude fatigue. The best known four models; the Wheeler model-the Willenborg model-the crack closure model-the root mean square approach, are presented in Chapter III.

The models usually overestimate or underestimate the fatigue life. In orde to understand the reasons of that, the factors affecting crack propagation should be known. They are reviewed in Chapter IV.

The computer program, AKYÜREK-I, is given in Chapter V. Sample calculations using AKYÜREK-I, their comparisons with the test data and the reasons of difference between calculations and the test data are presented in Chapter VI.

Chapter VII presents the conclusion of the study. Users manual for AKYÜREK-I is given in Appendix-D.

II. FATIGUE CRACK PROPAGATION

2.1. Fatigue Crack Growth Under Constant Amplitude Loading

Linear Elastic Fracture Mechanics (LEFM) regards the stress intensity factor as a sufficient parameter to describe the whole stress field at the tip of a crack. When there is a plastic zone at the crack tip, the stress intensity factor may still give a good indication of the stress environment of the crack tip, provided the size of the zone is small compared to the crack length. If two different cracks have the same stress environment, i.e. the same stress intensity factor, they behave in the same manner and show equal rates of growth (1)*. The rate of fatigue crack propagation per cycle, da/dN, is governed by the stress intensity factor range, ΔK;

$$da/dN = f(\Delta K) = f\{(\sigma_{max} - \sigma_{min})\sqrt{\pi a}\} = f\{2\sigma_a\sqrt{\pi a}\} \quad (2.1)$$

Where σ_{max} and σ_{min} are the maximum and minimum stresses in a cycle, and σ_a is the stress amplitude.

---

* Parenthetical references placed superior to the line of text refer to the bibliography.

Paris (2) and Paris, Gomez and Anderson (3) were first to point this out. Data obtained from specimens tested at various stress levels should all be on a single curve. Figure 2.1. shows a plot of data (4) obtained at three different stress levels, but with the minimum stress in a cycle always virtually zero (the cycle ratio $R = \sigma_{min} / \sigma_{max} = 0.05$).

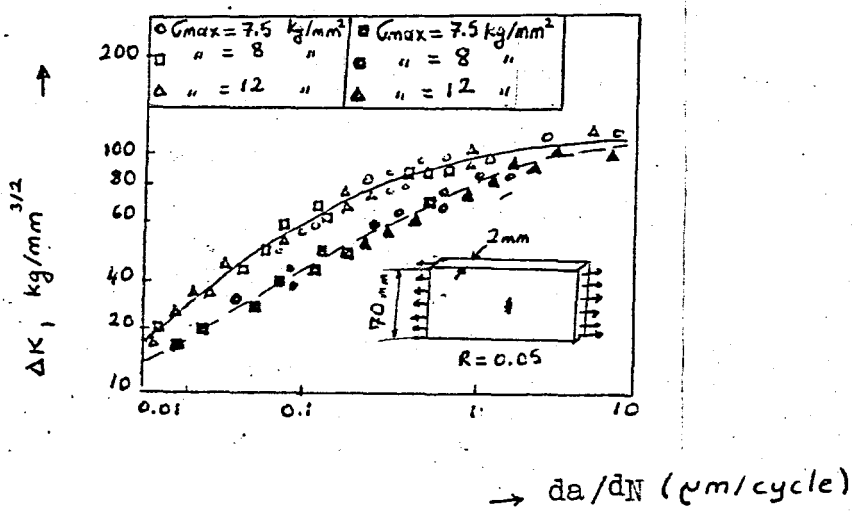

Figure 2.1. Relation between stress intensity factor and crack propagation rate (4).

The data in this figure indeed obey eq(2.1).

Equation (2.1) is sometimes assumed to be a simple power function:

$$da/dN = C\,(\Delta K)^n \qquad (2.2)$$

in which C and n are supposed to be material constants. A double logarithmic plot of da/dN versus ΔK would then be a straight line. However, eq(2.2) does not fully represent reality. Actual data fall on a S-shaped curve, or on a line with varying slope (5,6), as shown in figures 2.1 and 2.2. At low ΔK values crack propagation is extremely slow. Conceivably there is a threshold value of ΔK below which there is no crack growth at all (e.g.7). Experimental

verification of the existence of this threshold is difficult. A growing crack of some length has to be arrested by gradually decreasing ΔK until below the threshold, e.g. by decreasing the stress amplitude. The interpretation of the results presents often difficulties in view of history effects.

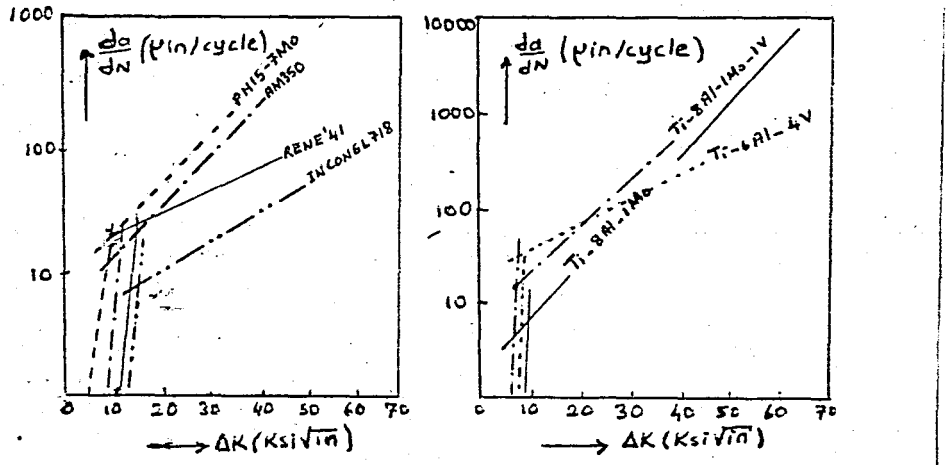

Figure 2.2. Crack growth rate versus stress intensity factor range (5).

According to the mechanism of fatigue crack growth, the amount of growth per cycle is closely related to the crack tip opening displacement. Therefore, attempts have been made (8,9) to correlate the crack propagation rate with the crack opening displacement. This leads to relations of the form

$$\frac{da}{dN} = \frac{C(\Delta K)^2}{E\,\sigma_{ys}} \quad \text{or} \quad \frac{da}{dN} = C\left(\frac{\Delta K}{E}\right)^2 \tag{2.3}$$

in which E is Young's modulus and σ_{ys} is the cyclic yield stress. These equations are interesting, because crack propagation can be considered as a geometric consequence of crack tip opening (10, 11, 12). It has been shown (e.g.13) that data for a large variety of

materials fall within one large scatter band when plotted on the basis of $\Delta K/E$ versus da/ dN, as suggested by the second expression in eqs (2.3). However, a mere glance at figures 2.1 and 2.2 shows how materials with virtually the same Young's modulus can have widely different crack propagation properties. This is probably due to the fact that many more parameters are involved than those occured in eq(2.3).

Many other equations have been proposed. They are analyzed in a concise paper by Pelloux (14). Further work to derive an equation with a sound physical basis is certainly needed; it must be anticipated that this final equation will be a complicated one if it is to have a general validity. For the technical problem of fatigue crack propagation the simple knowledge that da/ d N is a function of the stress intensity factor will often be sufficient.

A fatigue cycle is defined by a frequency and two stress parameters. These can be the mean stress σ_m and the stress amplitude σ_a, the minimum stress in a cycle ($\sigma_{min} = \sigma_m - \sigma_a$) and the maximum stress ($\sigma_{max} = \sigma_m + \sigma_a$), or other combinations of two of these four parameters. As long as the cycle ratio ($R = \sigma_{min} / \sigma_{max}$) equals zero, one can speak unambiguously about the stress intensity factor of the fatigue cycle, since $\sigma_{max} = 2\sigma_a = \Delta\sigma$. The hypothesis that the rate of crack propagation is a function of stress intensity factor presents no difficulties. When $R \neq 0$ the range of the stress intensity $\Delta K = 2\sigma_a\sqrt{\pi a}$ is an insufficient description of the stress environment of the crack tip. The question arises whether da/ d N will now be a function of ΔK, or of the maximum stress intensity in a cycle ($K_{max} = \sigma_{max}\sqrt{\pi a}$) or of both.

It appears (15,16) that the rate of crack propagation is a function of both ΔK and K_{max}. This can be appreciated from figure 2.3. It can be concluded that

$$da/dN = f_1(\Delta K, R) = f_2(K_{max}, R) = f_3(\Delta K, K_{max}) \quad (2.4)$$

Several investigators have tried to establish empirical relations which attempt to incorporate the effect of the cycle ratio such that all data could be condensed to a single curve. Broek and Schijve (15) proposed a complicated relation, but also the following more simple one:

$$da/dN = C\, K_{max}^2 \Delta K \quad (2.5)$$

A similar equation was given by Erdoğan (16). Walker (17,18) used the more general equation

$$da/dN = C\, K_{max}^m \Delta K^n \quad (2.6)$$

which he modified by introducing an effective $\overline{\Delta K}$, yielding

$da/dN = C\, \overline{\Delta K}^n$ where $\overline{\Delta K}$ is defined as

$$\overline{\Delta K} = S_{max}\,(1-R)^m \sqrt{\pi a} \quad (2.7)$$

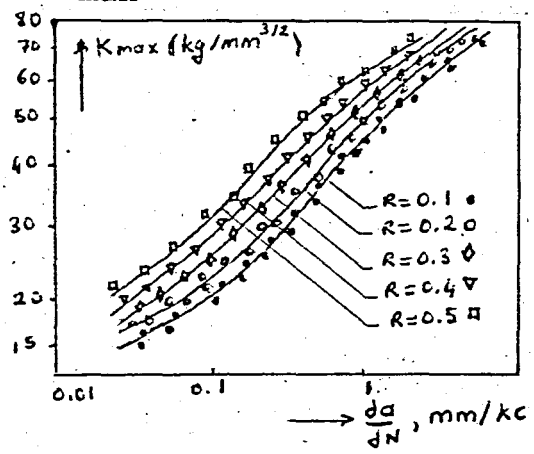

Figure 2.3. Effect of cycle ratio on the relation between crack growth rate and stress intensity factor (15), 2024-T3-alloy.

Forman et al. (19) argued that da/dN should become infinite when the crack reaches a critical crack size, i.e. when K_{max} reaches K_{1C}. They arrived at

$$\frac{da}{dN} = \frac{C\,\Delta K^n}{(1-R)K_{1C} - \Delta K} = \frac{C\,\Delta K^n}{(1-R)(K_{1C}-K_{max})} \qquad (2.8)$$

which can be rearranged to give:

$$\frac{da}{dN} = \frac{C\,\Delta K^m\,K_{max}}{K_{1C} - K_{max}} \qquad (2.9)$$

The differences among these expressions are not large, and none of them has a general applicability. Each one may be found reasonably satisfactory in a limited region or for limited sets of data.

The question arises whether eq(2.4) still holds for $R < 0$, i.e. when the stresses go into compression. A crack is not a stress raiser in compression and the expressions for ΔK lose their meaning. This suggests that

$$da/dN = f\,(K_{max}) \text{ for } R < 0 \qquad (2.10)$$

There have been many arguments about the validity of eq(2.10). The data (20) plotted in figure 2.4 seem to support the equation. A crack will not always close exactly at the moment the stress reverses from tension into compression.

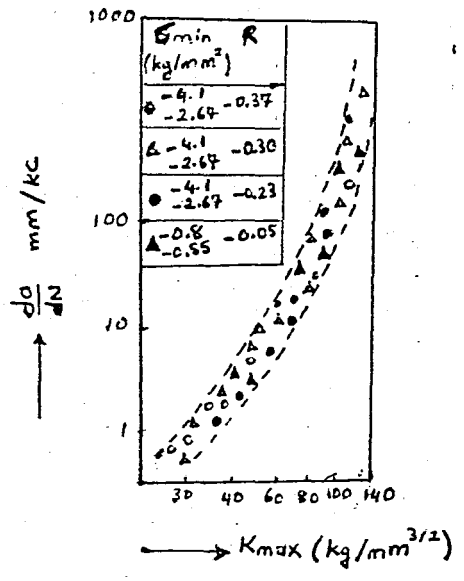

Figure 2.4. Crack propagation rate at negative cycle ratios (20). 7075-T6 Al-alloy.

The moment of closure depends upon the magnitude of the crack tip opening attained in the tension part of the cycle, and upon the plastic deformation properties of the material (20). Therefore, eq(2.10) should probably be modified to

$$da/dN = f_1(\Delta K, K_{max}) = f_2(K_{max}, R) \text{ for } R > \delta$$

$$da/dN = f_3(K_{max}) \text{ for } R < \delta$$

$$= f_4(\text{material properties}) \approx 0. \qquad (2.11)$$

2.2. Stress intensity formulations and the effect of finite size.

Cracks in a plate of finite size are of great practical interest, but for these cases no closed form solutions are available. The problems are difficult because of the boundary conditions. An

approximate solution can be obtained for a strip of finite width loaded in tension and containing an edge crack or a central crack (22).

First consider an infinite sheet with an infinite row of evenly spaced collinear cracks as depicted in figure 2.5. Solutions for this case were given by Westergard (23), Irwin (24) and Koiter (25). The result is:

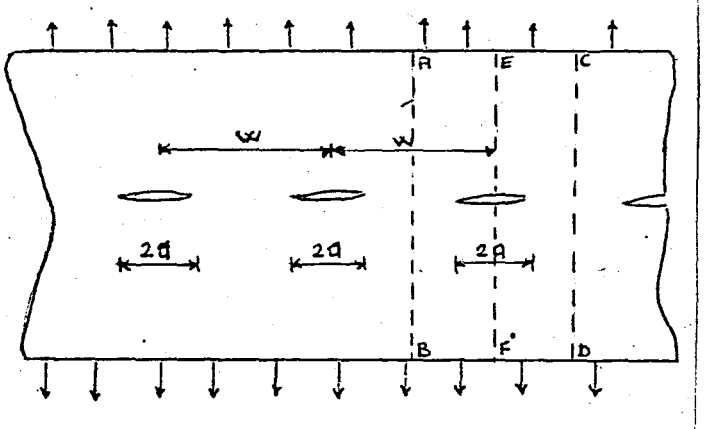

Figure 2.5. Infinite plate with collinear cracks.

$$K_I = \sigma\sqrt{\pi a}\left(\frac{w}{\pi a}\tan\frac{\pi a}{w}\right)^{1/2} \qquad (2.12)$$

If the plate is cut along the lines AB and CD one obtains a strip of finite width w, containing a central crack $2a$. It is likely that the solution of eq (2.12) is approximately valid for the strip. In the case of collinear cracks a strip of width w bears stresses (note that shear stresses are zero because of symmetry) along its edges AB and CD (figure 2.6), where as the edges of a plate of finite size are stress free. Supposedly, the stresses parallel to the crack do not contribute much to K and consequently eq (2.12) can be used as an approximate solution for the strip of finite size.

It appears that

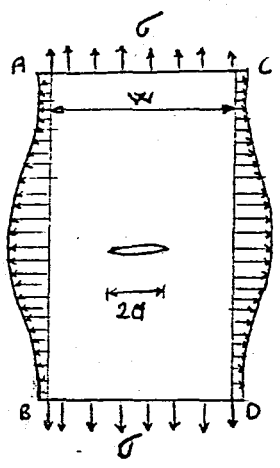

Figure 2.6. Stresses on the edges of strip cut from infinite plate with collinear cracks.

eq (2.12) reduces to $K_I = \sigma\sqrt{\pi a}$ if (a/w) approaches zero. This means that the finite strip behaves as an infinite plate if the cracks are small.

Isida (26) has developed mapping functions to derive stress concentration factors. These can be used (27) to compute stress intensity factors for finite plates to any degree of accuracy. Usually the result is presented as:

$$K = Y\sigma\sqrt{a} \tag{2.13}$$

where Y is a polynomial in a/w. The factor $\sqrt{\pi}$ is often incorporated in Y, sometimes it is not. Fedderson (28) discovered that the solution of Isida is very closely appoximated by $\sqrt{\sec \pi a/w}$. Therefore a convenient formula for the stress intensity factor for a strip in tension is

$$K_I = \sigma\sqrt{\pi a}\ \sqrt{\sec \pi a/w} \tag{2.14}$$

A comparison of a finite width correction factors of Irwin, Isida and Fedderson is made in Figure 2.7.

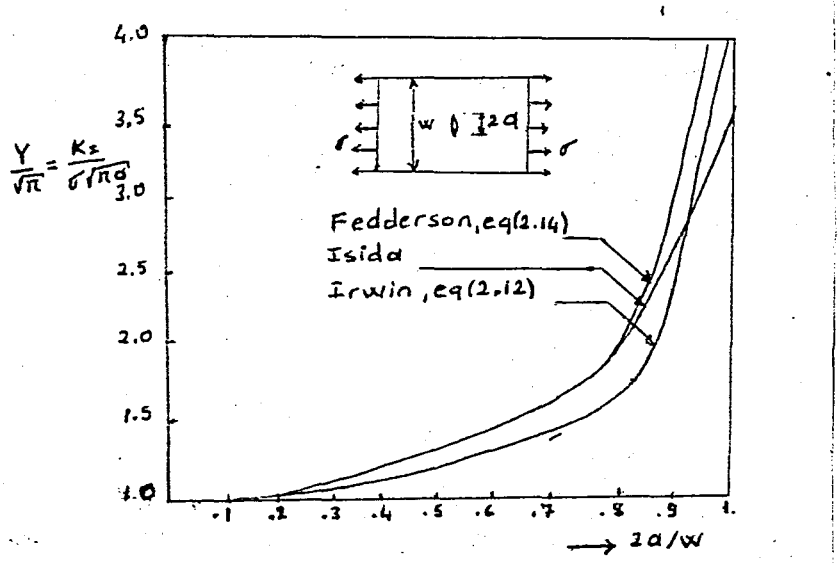

Figure 2.7. Finite width corrections for center cracked plate.

Cutting the plate with collinear cracks (figure 2.5) along EF and CD, one similarly arrives at a strip with an edge crack. Analogous to the central crack problem the solution of eq(2.12) can be used as an approximation for the edge crack. Again K reduces to $K = \sigma\sqrt{\pi a}$ for small a/w. However, the stresses acting on the edge EF tend to slightly close the crack. Absence of these stresses in the strip of finite size results in a somewhat larger displacement of the crack edges. Consequently K is somewhat higher due to these free edges. The correction factor is in the order of 12 percent (27). Thus, for a small edge crack K is given by

$$K_I = 1.12\,\sigma\sqrt{\pi a} \qquad (2.15)$$

Stress intensity factors and the finite size polynomials for a number of practical configurations are collected in table 2.1.

TABLE 2.1.

K expressions for some practical geometries.

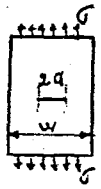

$$K_I = \sigma \sqrt{\pi a}\,(\sec \pi a/w)^{1/2}$$

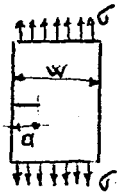

$$K_I = 1.12\,\sigma \sqrt{\pi a} \quad \text{(small } a/w\text{)}$$

or $$K_I = Y \sigma \sqrt{a}$$

with $$Y = 1.99 - 0.41\frac{a}{w} + 18.7\left(\frac{a}{w}\right)^2 - 38.8\left(\frac{a}{w}\right)^3 + 53.85\left(\frac{a}{w}\right)^4$$

$$(1.99 = 1.12\sqrt{\pi})$$

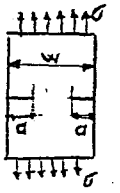

$$K_I = 1.12\,\sigma \sqrt{\pi a} \quad \text{(small } a/w\text{)}$$

or $$K_I = Y \sigma \sqrt{a}$$

with $$Y = 1.99 + 0.76\frac{a}{w} - 8.48\left(\frac{a}{w}\right)^2 + 27.36\left(\frac{a}{w}\right)^3$$

$$(1.99 = 1.12\sqrt{\pi})$$

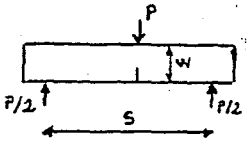

ASTM BEND SPECIMEN

$$K_I = \frac{PS}{BW^{3/2}}\left[2.9\left(\frac{a}{w}\right)^{1/2} - 4.6\left(\frac{a}{w}\right)^{3/2} + 21.8\left(\frac{a}{w}\right)^{5/2} - 37.6\left(\frac{a}{w}\right)^{7/2} + 38.7\right.$$

Thickness: B

ASTM COMPACT TENSION SPECIMEN

$$K_I = \frac{P}{BW^{1/2}}\left[29.6\left(\frac{a}{w}\right)^{1/2} - 185.5\left(\frac{a}{w}\right)^{3/2} + 655.7\left(\frac{a}{w}\right)^{5/2} - 1017\left(\frac{a}{w}\right)^{7/2} + 63.9\right.$$

Thickness: B

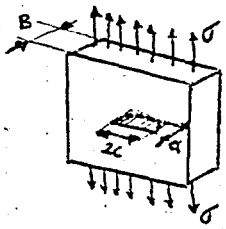

$$K_{Imax} = 1.12\,\frac{\sigma}{\Phi}\sqrt{\pi a}$$

$$K_{Imin} = 1.12\,\frac{\sigma}{\Phi}\sqrt{\pi a^2/c}$$

$$\Phi = \int_0^{\pi/2}\left[1 - \frac{c^2 - a^2}{c^2}\sin^2\phi\right]d\phi \approx \frac{3\pi}{8} + \frac{\pi}{8}\,\frac{a^2}{c^2}$$

2.3. Stress Intensity Evaluations in Semi-elliptical Surface Flaws.

Natural cracks occuring in practice are often initiated at corners and edges. They tend to grow inwards and assume a quarter-elliptical or semi-elliptical shape. The application of fracture mechanics to these "corner cracks" (quarter elliptical) and to "surface flaws" or "part-through" cracks (semi-elliptical) requires knowledge of the stress intensity factor for a crack with a curved front. Because of its technical significance this problem has received ample attention in the literature (29-40). A widely used approximate solution is discussed in the following paragraphs.

Sneddon (29) treated the problem of a circular internal crack of radius a (penny-shaped crack) embedded in an infinite solid subjected to uniform tension (figure 2.8).

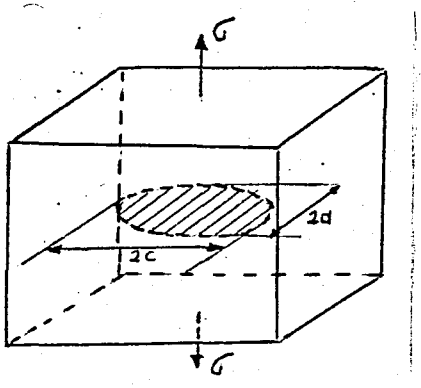

Figure 2.8. Embedded penny-shaped crack.

He arrived at:

$$K_I = \frac{2}{\pi} \sigma \sqrt{\pi a} \qquad (2.16)$$

A solution for an embedded elliptical flaw not being available, Irwin (24) derived a useful expression on the basis of the stress field around an ellipsoidal cavity as derived by Green and Sneddon (30). The displacements found from the latter solution were rela-

ted (29) to the stress intensity factor in the same way as in the case of through-the-thickness cracks.

Studies of the flat elliptical crack problem by Green and Sneddon (30) provide principally the information that tension normal to the crack produces an ellipsoidal crack opening shape. Assume the crack lies in the X-Z plane with its major dimension 2c along the Z-axis and its minor dimension 2a along the X-axis in such a way that border points X_1, Z_1 of the crack correspond to

$$\frac{x_1^2}{a^2} + \frac{Z_1^2}{c^2} = 1 \qquad (2.17)$$

If the crack opening displacements in the y-direction are represented by η then the Green-Sneddon result may be expressed as

$$\eta = \eta_o\left(1 - \frac{x^2}{a^2} - \frac{Z^2}{c^2}\right)^{1/2} \qquad (2.18)$$

where η_o is half the total separation of the walls of the crack at the origin.

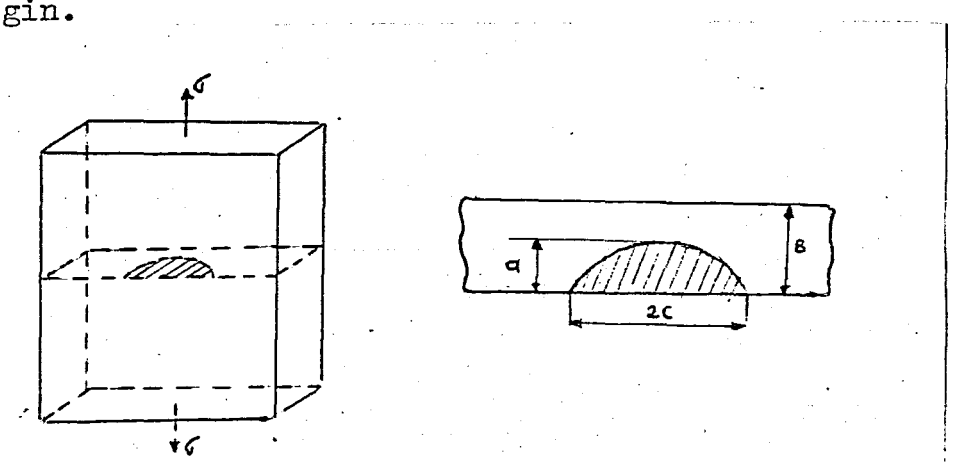

Figure 2.9. Part-through crack in a plate showing dimensions a and c of crack and plate thickness, B.

The desired expressions for $\mathcal{G}$ and K will be derived from eq (2.18) rather than from stress equations for two reasons: (a) The stress relations given by the Green-Sneddon paper are not in a form convenient for the calculation of σ_y near the border of the crack; (b) The author wishes to establish the point that the general shape of the crack opening provides sufficient information to determine $\mathcal{G}$ and K.

The procedure to be followed consists first in a discussion of the variation around the border of the crack of the elastic opening displacements of the crack. It will be noted that deviations of the stress state from plane strain become negligible in the limit of small separations from the crack border. Plane strain relations for $\mathcal{G}$ and K associated with crack-opening displacement then permit the desired calculations.

The position variables X_1 and Z_1 which lie on the crack borders may be represented in parametric form by

$$X_1 = a \operatorname{Sin} \phi \tag{2.19}$$

$$Z_1 = c \operatorname{Cos} \phi \tag{2.20}$$

A change $d\phi$ then corresponds to a segment ds of crack border given by

$$ds = (a^2 \operatorname{Cos}^2 \phi + c^2 \operatorname{Sin}^2 \phi)\, d\phi \tag{2.21}$$

At a small normal separation r (inward from the crack border) straight forward algebraic steps from eq(2.18) lead to the expression

$$\eta^2 = \eta_o^2 \frac{2r}{ac} (a^2 \operatorname{Cos}^2 \phi + c^2 \operatorname{Sin}^2 \phi)^{1/2} \tag{2.22}$$

The variation of displacement η at fixed distance r from the crack border as a function of ϕ will be considered in terms of the variation with ϕ of

$$\rho = \eta^2 / 2r \tag{2.23}$$

Thus

$$\rho = \frac{\eta_o^2}{ac} (a^2 \cos^2 \phi + c^2 \sin^2 \phi)^{1/2} \tag{2.24}$$

Differentiating with respect to ϕ and using eq(2.21) one finds

$$\frac{d\rho}{ds} = \left(\frac{\eta_o^2}{ac}\right) \frac{(c^2-a^2) \sin \phi \cos \phi}{a^2 \cos^2 \phi + c^2 \sin^2 \phi} \tag{2.25}$$

At the value of ϕ where $d\rho/ds$ is largest the fractional change of ρ across the segment ds is

$$d\rho/\rho = \frac{(c^2-a^2)(a^2+c^2)^{1/2} ds}{2\sqrt{2}\, a^2 c^2} \tag{2.26}$$

putting $c = 2a$ for specific illustration, the value of $d\rho/\rho$ becomes

$$d\rho/\rho = 0.6\, ds/a \tag{2.27}$$

The quantity ρ can be interpreted as the root radius of the elastic crack opening along the crack border. As a reference point approaches the crack border, ρ becomes the principal length factor associated with the crack. If we know a solution for stresses and strains valid along a crack-border length δs large enough so that the dimension ρ is negligible in comparison, then such a solution can be used to supply an expression for η for substitution into eq(2.22)

In crack stress-field analysis problems ρ is always equal to (σ / E^2) times a dimension comparable to the crack size. Bearing in mind that linear elasticity analysis regards σ / E as an infinitesimal in comparison to unity, we can for example, choose.

$$\delta s = (\frac{E}{\sigma})\rho \tag{2.28}$$

or, say,

$$\delta s = (\frac{\sigma}{E})\, a \tag{2.29}$$

Such a crack-border-length segment is obviously short compared to crack size and long compared to ρ, substituting δs from eq(2.29) for ds in eq(2.27) gives

$$d\rho / \rho = 0.6\,(\sigma / E) \tag{2.30}$$

which can be regarded as meaning ρ changes only by an infinitesimal fraction across the border length segment δs. The changes of displacements and stresses near the crack border must possess a similar degree of constancy relative to a coordinate parallel to the crack border. Since the problem is symmetrical about the plane containing the crack, a plane strain stress field fits the conditions of the problem in local crack-border regions comparable to dimensions to δs.

The three crack-border stress fields for which the displacements are independent of the co-ordinate prallel to the border are discussed in reference (41). The first of these, opening mode plane strain, is appropriate here and provides the relations

$$\gamma = \frac{2(1-\nu^2)}{E}\,(2r)^{1/2} K \tag{2.31}$$

$$\mathcal{G} = \frac{\pi}{E}(1-\nu^2)\,K^2 \tag{2.32}$$

Inserting γ^2 from eq(2.31) to σ, a and c from reference (31) or find this relation by computing the strain energy change for a small expansion of the crack boundary. The latter is not difficult. If the ellipse is expanded by adding fa to a and fc to c where f is very small, the normal outward displacement, r, of any point on the elliptical boundary is

$$r = \frac{acf}{(a^2\cos^2\phi + c^2\sin^2\phi)^{1/2}} \tag{2.33}$$

Computation of the strain energy change dU from

$$du = 4\int_0^{\pi/2} \mathcal{G}\, r \frac{ds}{d\phi}\, d\phi \tag{2.34}$$

leads to

$$du = \frac{\pi E cf\, \gamma_0^2 \Phi}{(1-\nu^2)} \tag{2.35}$$

where Φ is the elliptic integral

$$\Phi = \int_0^{\pi/2} \left[\sin^2\phi + \left(\frac{a}{c}\right)^2 \cos^2\phi\right]^{1/2} d\phi \tag{2.36}$$

we also know the strain energy change is one half of σ times the change in crack volume. From this

$$du = 2\pi\sigma acf\gamma_0 \tag{2.37}$$

The value of γ_0 found by equating the two relations for du equations (2.35) and (2.37) may be substituted into (2.32) with the result that

$$\mathcal{G} = \frac{\pi(1-\nu^2)a^2}{E\,\Phi^2}\left(\frac{a}{c}\right)\left(a^2\cos^2\phi + c^2\sin^2\phi\right)^{1/2} \qquad (2.38)$$

By inspection of eq(2.38) one observes that $\mathcal{G}$ is greatest where the crack-boundary intersects the minor axis. Thus with increase of tension on a flat elliptical crack, the crack extension should, barring anisotropy, tend to produce a circular crack boundary shape.

The function Φ increases with $(\frac{a}{c})$. When a is infinitesimal compared to c, Φ is unity. When crack shape is circular Φ is $\pi/2$. Other values of Φ are easily found from published tables of elliptical integrals. Taking $\phi = \pi/2$ it is readily seen that the values of unity and $\pi/2$ for Φ correspond, respectively, to the Griffith equation

$$\mathcal{G} = \frac{\pi\sigma^2 a}{E}(1-\nu^2) \qquad (2.39)$$

and to the energy-release rate for the penny-shaped crack

$$\mathcal{G} = \frac{4\sigma^2 a}{\pi E}(1-\nu^2) \qquad (2.40)$$

The results of Irwin's analysis is

$$K_I = \frac{\sigma\sqrt{\pi a}}{\Phi}\left(\sin^2\phi + \frac{a^2}{c^2}\cos^2\phi\right)^{1/4} \qquad (2.41)$$

in which Φ is an elliptical integral of the second kind, given by

$$\Phi = \int_0^{\pi/2}\left[1-\frac{c^2-a^2}{c^2}\sin^2\phi\right]^{1/2} d\phi \qquad (2.42)$$

where a and c are as defined in figure 2.10. If a = c

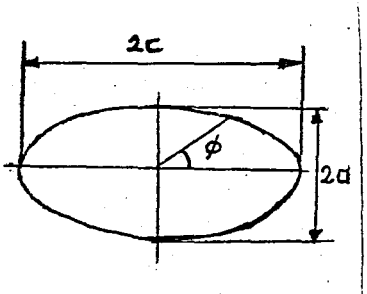

Figure 2.10. Elliptical crack

eq (2.41) reduces to eq(2.16), as should be the case. Values for Φ can be found in mathematical tables or in a graph as in figure 2.11. It is possible to develop a series expansion for Φ

$$\Phi = \frac{\pi}{2}\left\{1 - \frac{1}{4}\,\frac{c^2 - a^2}{c^2} - \frac{3}{64}\left(\frac{c^2 - a^2}{c^2}\right)^2 - \cdots\right\} \qquad (2.43)$$

Even for a ratio a/c approaching zero the third term contributes only about 5 per cent and therefore it can be neglegted in most cases, yielding

$$\Phi = \frac{3\pi}{8} + \frac{\pi}{8}\,\frac{a^2}{c^2} \qquad (2.44)$$

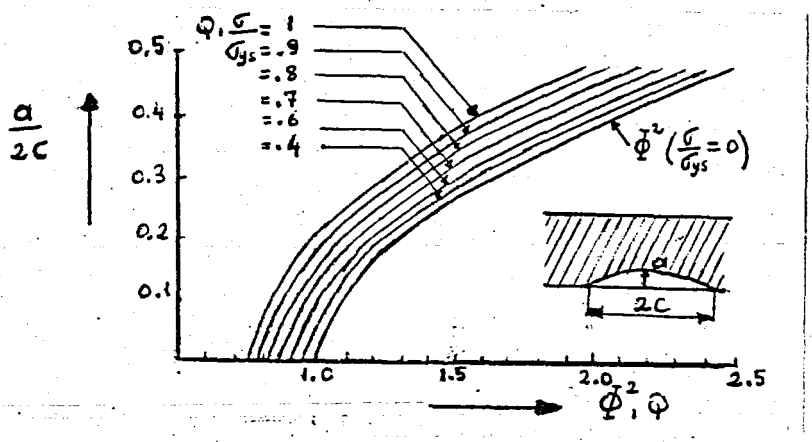

Figure 2.11. Surface flaw parameter.

and also:

$$K_I = \frac{\sigma\sqrt{\pi a}}{\frac{3\pi}{8} + \frac{\pi}{8}\,\frac{a^2}{c^2}}\left(\mathrm{Sin}^2\phi + \frac{a^2}{c^2}\,\mathrm{Cos}^2\phi\right)^{1/4} \qquad (2.45)$$

With only slight modifications eqs(2.41) and (2.45) can be applied to semielliptical surface flaws and to a quarter-elliptical corner cracks. Therefore the equations are of great practical interest. It turns out that K_I varies along the crack front. At the end of the minor axis ($\phi = \pi/2$) the stress intensity is the largest. At the end of major axis ($\phi = o$) it is the lowest. Therefore;

$$K_I(\phi = \pi/2) = \frac{\sigma\sqrt{\pi a}}{\Phi} \quad ; \quad K_I(\phi = o) = \frac{\sigma\sqrt{\pi a^2/c}}{\Phi} \qquad (2.46)$$

Usually a number of correction factors are applied to these K-expressions. A surface flaw is comparable to an edge crack, and it was argued that this requires a correction factor of about 12 percen to K. This is called the back free-surface correction. Also, a plastic zone correction is often applied to take account of the fact that plastic deformation takes place at the crack tip. This plastic deformation makes the crack behave as if it were slightly longer than its physical size. Because of this, the plastic zone correction r_p^* is a correction to the crack size;

$$K_I = 1.12 \frac{\sigma}{\Phi}\sqrt{\pi\,(a + r_p^*)}\,(\mathrm{Sin}^2\phi + \frac{a^2}{c^2}\mathrm{Cos}^2\phi)^{1/4} \qquad (2.47)$$

By taking

$$r_p^* = \frac{K_I^2}{4\pi\sqrt{2}\sigma_{ys}^2} \quad (\sigma_{ys} \text{ is the yield stress}) \qquad (2.48)$$

the resulting expression for K is :

$$K_I = \frac{1.12\,\sigma\sqrt{\pi a}}{\sqrt{\Phi^2 - 0.212\,\sigma^2/\sigma_{ys}^2}}(\mathrm{Sin}^2\phi + \frac{a^2}{c^2}\mathrm{Cos}^2\phi)^{1/4} \qquad (2.49)$$

The maximum stress intensity is:

$$K_{Imax} = 1.12\,\sigma\sqrt{\pi a/Q} \qquad (2.50)$$

The quantity $Q = \Phi^2 - 0.212\,\sigma^2/\sigma_{ys}^2$ is called the flaw shape parameter. Values for Q are presented graphically in figure 2.11 for various values of the ratio σ/σ_{ys}.

Finally, a correction is often necessary to account for the proximity of the free surface in front of the crack. For this front free-surface correction, use can be made of the tangent formula of eq(2.12). It is preferable, however, to use the front free-surface correction due to Kobayashi et al. (31), which is given in graphical form in figure 2.12. The resulting maximum stress intensity for a surface flaw becomes:

$$K_{Imax} = 1.12\, M_K\, \sigma \sqrt{\pi a/Q} \qquad (2.51)$$

where M_K is the front free-surface correction of figure 2.12.

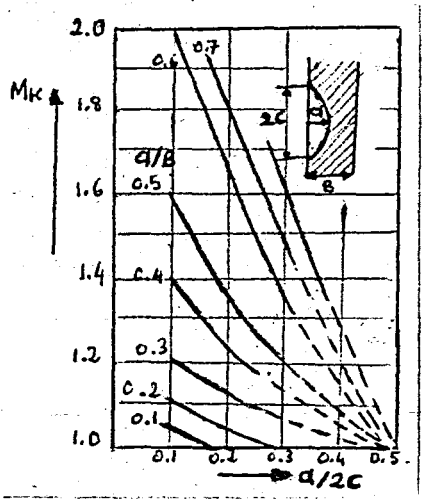

Figure 2.12. Kobayashi correction (M_K) for proximity of front free-surface.

For the case where a semi-elliptical flaw extends deep into the material, the back free-surface correction should be decreased from 1.12 to unity. For the case of a quarter-elliptical crack having two free surfaces, the back free-surface correction should

be applied twice. However, it appears that this is a slight over-correction. Therefore the back free-surface correction for a corner crack is usually taken as 1.2.

The previous equations for surface flaws were obtained indirectly (24) from the solution for an embedded elliptical cavity. Rice (32) and Rice and Levy (33) have directly analysed the problem of a surface crack. Their final equations can be treated to give numerical data for K, which are particularly useful because the bending case was also solved. It turns out that for shallow flaws (2c/B large) the stress intensity factor approaches the value for an edge crack ($2c \longrightarrow \infty$). The same result is obtained from eq(2.51) since $Q = 1$ for $a/2c = 0$. Stress intensity factors for surface cracks in bending were also calculated by Grandt and Sinclair (34). The foregoing discussion serves as an illustration of the variation of the stress intensity factor along the crack front of a surface flaw. Information about stress intensity factors of elliptical cracks can be found elsewhere (31-40).

2.4. The Crack Tip Plastic zone

2.4.1. Irwin Plastic Zone Correction

According to the elastic stress field solutions a stress singularity exists at the tip of an elastic crack. In practice, materials (especially metals) tend to exhibit a yield stress, above which they deform plastically. This means that there is always a region around the tip of a crack in a metal, where plastic deformation occurs, and hence a stress singularity cannot exist. The plastic region is known as the crack tip plastic zone. A rough estimate of the size of the plastic zone, whether in plane strain

or plane stress, is simple to make. To start with, the considerations in this section are limited to plane stress.

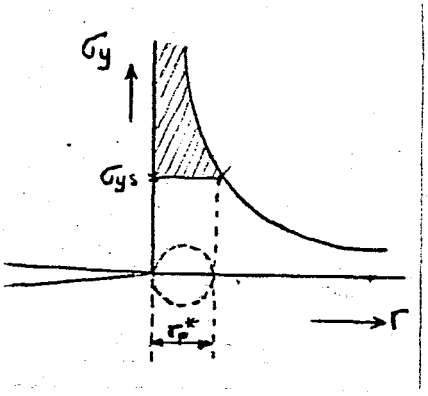

Figure 2.13. First estimate of plastic zone size.

Figure 2.13 shows the magnitude of the stress σ_y in the plane $\theta = 0$. Until a distance r_p^* from the crack tip the stress is higher than the yield stress σ_{ys}. To a first approximation this distance r_p^* is the size of plastic zone. By substituting σ_{ys} in the equation for σ_y the distance r_p^* can be calculated:

$$\sigma_y = \frac{K_I}{\sqrt{2\pi r_p^*}} = \sigma_{ys} \quad \text{or} \quad r_p^* = \frac{K_I^2}{2\pi \sigma_{ys}^2} = \frac{\sigma^2 \pi a}{2\pi \sigma_{ys}^2} \qquad (2.52)$$

It is quite clear that the actual plastic zone size must be larger than r_p^* : the load represented by the shaded area in figure 2.13 must still be carried through. This can be achieved if the material immediately ahead of the plastic zone carries some more stress which will bring this material above the yield stress.

Irwin (42) has argued that the occurence of plasticity makes the crack behave as if it were longer than its physical size. As a result of crack tip placticity the displacements are larger and the stiffness is lower than in the elastic case. In other words,

the plate behaves as if it contained a crack of somewhat larger size. The effective crack size, aeff, is equal to $a + \delta$, the physical crack size plus a correction δ. An expression for can easily be derived.

In figure 2.14 the physical crack of size a is replaced by a longer crack of size $a + \delta$, and the elastic stress distribution (σ_y) at the tip of the effective crack is given. The stress at the tip of the effective crack is again limited to the yield stress σ_{ys}. Similarly, the stress acting on the part δ in front of the physical crack is equal to the yield stress. Consequently, δ must be large enough to carry the load that is lost by cutting the area A (figure 2.14) from the elastic

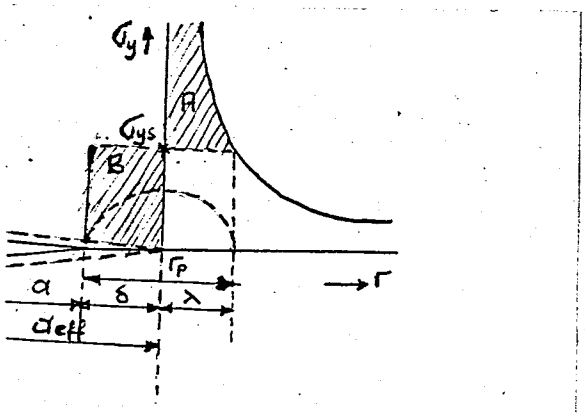

Figure 2.14. Second estimate of plastic zone size.

stress distribution. Hence, area A is equal to area B. The distance λ in figure 2.14 follows from:

$$\sigma_{ys} = \frac{K}{\sqrt{2\pi\lambda}} = \sigma\sqrt{\frac{a+\delta}{2\lambda}} \quad \text{or} \quad \lambda = \frac{\sigma^2 (a+\delta)}{2\sigma_{ys}^2} \approx r_p^* \qquad (2.53)$$

Since δ is small with respect to the crack size it can be neglected, and it follows that $\lambda \approx r_p^*$ as in eq(2.52). The area B is

equal to $\sigma_{ys} \cdot \delta$; hence, the requirement B = A yields:

$$\delta . \sigma_{ys} = \left[\int_0^{\lambda} \sigma \sqrt{\frac{a - \delta}{2r}}\, dr\right] - \sigma_{ys} \lambda . \qquad (2.54)$$

Neglecting δ as compared to a and using eq(2.53) it follows that

$$(\delta + r_p^*)\, \sigma_{ys} = \sigma \sqrt{2ar_p^*} \quad \text{or} \quad (\delta + r_p^*)^2 = \frac{2\sigma^2 a}{\sigma_{ys}^2}\, r_p^* = 4\, r_p^{*2} \qquad (2.55)$$

Hence, it turns out that:

$$\delta = r_p^* \text{ and } r_p = \lambda + \delta = 2r_p^* . \qquad (2.56)$$

The size of the plastic zone r_p is found to be twice as large as the first estimate, r_p^*.

Since $\delta = r_p^*$ it follows that the crack behaves as if its length were a + r_p^*. The quantity r_p^* is known as Irwin's plastic zone correction. Assuming for the time being that the plastic zone has a circular shape, the situation can be represented as in figure 2.15, where the effective crack

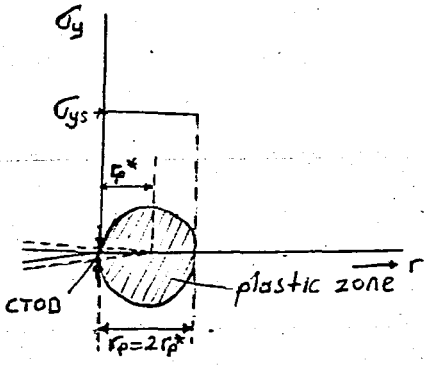

Figure 2.15. Irwin's plastic zone correction.

extends to the centre of the plastic zone. If the plastic zone correction is applied consistently a correction to K is also

necessary:

$$K = C\sigma\sqrt{\pi(a + r_p^*)} = C\sigma\sqrt{\pi\left(a + \frac{K^2}{2\pi\sigma_{ys}^2}\right)} \qquad (2.57)$$

The use of eq(2.57) presents difficulties because K has to be determined by following an iteration procedure. The latter can be avoided if one takes $K = C\sigma\sqrt{\pi a}$ for calculating r_p^* and then determines the corrected K from eq(2.57). Conversely, for a given K one can find the uncorrected stress from $\sigma = K/\sqrt{\pi a}$, which allows determination of r_p^*. The corrected stress then follows from $\sigma = K/\sqrt{\pi(a + r_p^*)}$. In practice the plastic zone correction is seldom applied to K. The plastic zone correction of eq(2.52) is not suitable in plane strain (see sect.2.4.3.).

2.4.2. The Dugdale Approach:

A different approach to finding the extend of the plastic zone was followed by Dugdale (43,44) and (in a slightly different way) by Barenblatt (45). The procedure yields similar results as an analysis by means of a continuous distribution of dislocations (46,47).

Dugdale also considers an effective crack which is longer than the physical crack as in figure 2.16 a. The crack edges, ρ, in front of the physical crack carry the yield stress σ_{ys}, tending to close the crack. (The part ρ is not really cracked; the material can still bear the yield stress). The size of ρ is chosen such that the stress singularity disappears: K should be zero. This means that the stress intensity K_σ

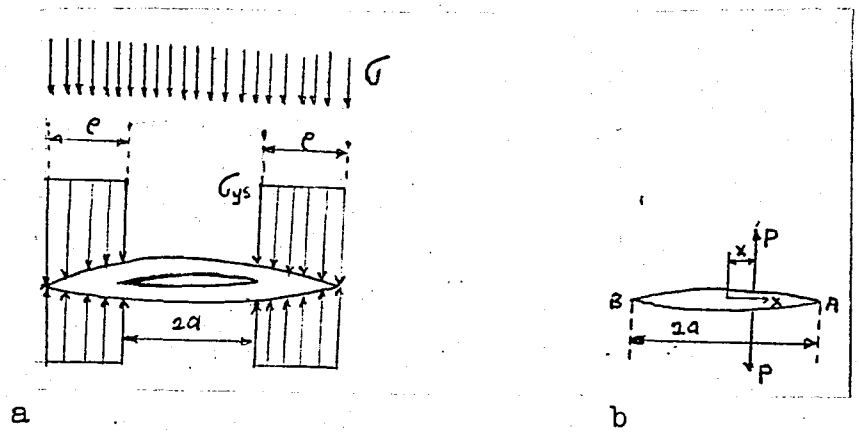

a b

Figure 2.16. Dugdale approach; a. Dugdale crack, b. Wedge forces.

due to the uniform stress σ has to be compensated by the stress intensity K_ρ due to the wedge forces σ_{ys}:

$$K_\sigma = - K_\rho \tag{2.58}$$

The requirement (2.58) permits determination of ρ in the following manner. The stress intensity due to wedge forces p in figure 2.16 b is given as:

$$K_A = \frac{p}{\sqrt{\pi a}} \sqrt{\frac{a+x}{a+x}} \quad \text{and} \quad K_B = \frac{p}{\sqrt{\pi a}} \sqrt{\frac{a-x}{a+x}} \tag{2.59}$$

If the wedge forces are distributed from S to the crack tip (as in the Dugdale case) the stress intensity becomes:

$$K = \frac{p}{\sqrt{\pi a}} \int_S^a \left\{ \sqrt{\frac{a+x}{a-x}} + \sqrt{\frac{a-x}{a+x}} \right\} dx = 2p \sqrt{\frac{a}{\pi}} \int_S^a \frac{dx}{\sqrt{a^2-x^2}} \tag{2.60}$$

The integration can be carried out by substituting $x=a\cos\phi$. The result is:

$$K = 2p \sqrt{\frac{a}{\pi}} \arccos \frac{S}{a} . \tag{2.61}$$

Applying this result to the Dugdale crack in figure 2.16 a the integral has to be taken from $s = a$ to $a + \rho$. Hence a has to be substituted for s and $a + \rho$ for a in eq(2.61), while $p = \sigma_{ys}$. Thus

$$K_\rho = 2\sigma_{ys}\sqrt{\frac{a+\rho}{\pi}} \arccos\frac{a}{a+\rho} . \qquad (2.62)$$

According to eq(2.58) this stress intensity should be equal to K_σ, where the latter is $K_\sigma = \sigma\sqrt{\pi(a+\rho)}$. Then it follows that ρ can be determined from eq(2.58) as

$$\frac{a}{a+\rho} = \cos\frac{\pi\sigma}{2\sigma_{ys}} \qquad (2.63)$$

Neglecting the higher order terms in the series developement of the cosine, ρ is found as:

$$\rho = \frac{\pi^2\sigma^2 a}{8\sigma_{ys}^2} = \frac{\pi K^2}{8\sigma_{ys}^2} \qquad (2.64)$$

This result can be compared with $r_p = 2r_p^* = K^2/\pi\sigma_{ys}^2$ as derived in the previous section. Apparently, the two expressions are almost identical. For high values of σ/σ_{ys} eq(2.63) has to be used instead of (2.64), and the differences with the Irwin plastic zone size become larger.

Duffy et al. (49) used eq(2.63) as a basis for a plastic zone correction. By taking $\rho = r_p^*$ it follows that $a + r_p^* = a\sec\pi\sigma/2\sigma_{ys}$ and $K_I = \sigma\sqrt{\pi\, a\sec\pi\sigma/2\sigma_{ys}}$. Several other plastic zone corrections have been proposed. Correcting for plasticity is not necessary in the event that linear elastic fracture mechanics apply, i.e. when the plastic zone is small compared to the crack

size. If the plastic zone is larger with respect to the crack, the application of a plastic zone correction is doubtful, because of the validity of the expressions for K, which are based on elastic solutions.

2.4.3. Plastic Constraint Factor.

The plane strain plastic zone is significantly smaller than the plane stress plastic zone. This is a result of the fact that the effective yield stress in plane strain is larger than the uniaxial yield stress. The maximum stress in the plane strain plastic zone can be as high as three times the uniaxial yield stress. The ratio of the maximum stress to the yield stress is called the plastic constraint factor (p.c.f.):

$$p.c.f = \frac{\sigma_{max}}{\sigma_{ys}} \qquad (2.65)$$

The quantity (p.c.f.) times σ_{ys} can be considered as an effective yield stress.

The p.c.f. for the plane strain crack problem can be estimated as follows. By taking $\sigma_2 = n\sigma_1$ and $\sigma_3 = m\sigma_1$ the Von Mises yield criterion can be rewritten as:

$$[(1-n)^2 + (n-m)^2 + (1-m)^2]\sigma_1^2 = 2\sigma_{ys}^2 \qquad (2.66)$$

which can be rearranged to:

$$p.c.f. = \frac{\sigma_1}{\sigma_{ys}} = (1-n-m+n^2+m^2-mn)^{-1/2} \qquad (2.67)$$

Eq (2.67) enables calculation of the p.c.f. at any location of the crack tip region. From the stress field equations it follows that $n = (1 - \sin\theta/2)/(1 + \sin\theta/2)$ and $m = 2\nu/(1 + \sin\theta/2)$.

For the plane $\theta = o$ it turns out that $n = 1$ and $m = 2\nu$, by taking $\nu = 1/3$ the plastic constraint factor is according to (2.67): p.c.f. = 3. Similar results are obtained by application of other yield criteria. In the case of plane stress $n = 1$ and $m = o$, which gives the estimate: p.c.f. = 1.

Apparently the normal stress σ_y on the $\theta = o$ plane in plane strain can be as high as three times the yield stress. During plastic deformation the crack tip blunts. Since a stress perpendicular to a free surface cannot exist, it follows that σ_x must tend to zero at the very crack tip. In that case $\sigma_2 = o$, i.e. there is a state of plane stress. Consequently p.c.f. must drop to 1 and stress at the crack tip does

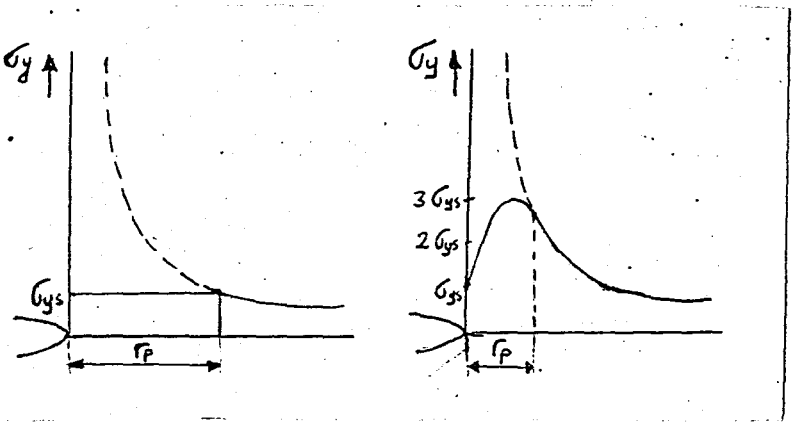

Figure 2.17. Approximate stress distribution in plane stress and plane strain. a.Plane stress; b.Plane strain.

not exceed the yield stress. The resulting stress distribution are shown in figure 2.17. In the plane strain case the stress rises quickly from σ_{ys} at the very crack tip to $3\,\sigma_{ys}$ at a short distance from the crack. This is confirmed by finite elemen calculations(50). Stress and strain distributions in the plastic zone measured as well as calculated, can be found in the literatur

(51-57), but a general elastic-plastic analysis of the crack problem is not yet available.

Figure 2.17 again shows that the plastic zone in the y = o plane in the case of plane stress is nine times larger than for plane strain. Knowledge of the plastic constraint factor enables derivation of a plastic zone correction factor for plane strain in a similar way as in the above equation. If the effective yield stress in plane strain is $3\sigma_{ys}$, the plastic zone correction of eq(2.52) becomes:

$$r_p^* = \frac{K_I^2}{2\pi(3\sigma_{ys})^2} = \frac{K_I^2}{18\pi\sigma_{ys}^2} \qquad (2.68)$$

In a practical case, plane strain does not exist at the specimen surface. As a consequence the average plastic constraint factor is much lower than 3. Irwin (42) uses a p.c.f. of $\sqrt{2\sqrt{2}} = 1.68$, which modifies eq(2.68) into:

$$r_p^* = \frac{K_I^2}{2\pi(1.68\sigma_{ys})^2} \approx \frac{1}{6\pi}\,\frac{K_I^2}{\sigma_{ys}^2} \qquad (2.69)$$

This plastic zone correction is only one third of the plane stress correction. Experimentally determined p.c.f.'s (e.g. 58) are mostly between 1.5 and 2, which confirms the usefulness of eq(2.69).

III. RETARDATION MODELS

A fatigue cycle preceded by a load of higher magnitude produces less crack propagation than it does in the absence of the higher preload. This retardation phenomenon is usually attributed to a combination of compressive residual stresses and crack closure due to residual stresses (59).

The overload has introduced a large plastic zone as is shown in figure 3.1. The material in this zone is streched to a permanent deformation, but after unloading it still has to fit in the surrounding elastic material. The elastic material resumes its original size, but the material in the plastic zone does not. The plastic zone is too large for its elastic surroundings if the latter contract upon load release. Then the

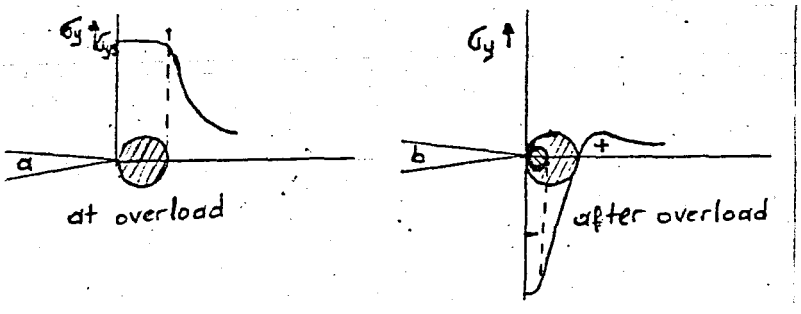

Figure 3.1. Residual compressive stresses at crack tip as a result of overload.

elastic material has to make it fit. Consequently, the surrounding elastic material will exert compressive stresses on the plastically deformed material at the crack tip. The resulting residual stress system is depicted diagrammatically in figure 3.1. As soon as the crack has grown through the area of residual stresses, the original crack propagation curve will be resumed again. The residual compressive stresses tend to close the crack tip over some distance (60). Subsequent cycling can cause crack growth only if the residual stresses are overcome to a degree that the crack tip is opened again. This explains the low growth rate after the overload.

At least five models have been proposed (61-65) to treat retardation in a quantitative fashion. None of the models has a solid physical basis, and most are semiempirical, and contain one or more constants to be derived from variable-amplitude crack growth experiments.

3.1. The Wheeler Model

Wheeler (61) introduces a crack growth reduction factor, C_p,

$$\frac{da}{dN} = C_p \, f(\Delta K) \tag{3.1}$$

where $f(\Delta K)$ is the usual crack growth function. The retardation factor, C_p, is given as (see figure 3.2):

$$C_p = \left(\frac{r_{pi}}{a_o + r_{po} - a_i} \right)^m \tag{3.2}$$

where r_{pi} = current plastic zone in the ith cycle under consideratio
ai = current crack size
r_{po} = size of the plastic zone generated by a previous overloa
ao = crack size at which that overload occured
m = empirical constant (retardation exponent)

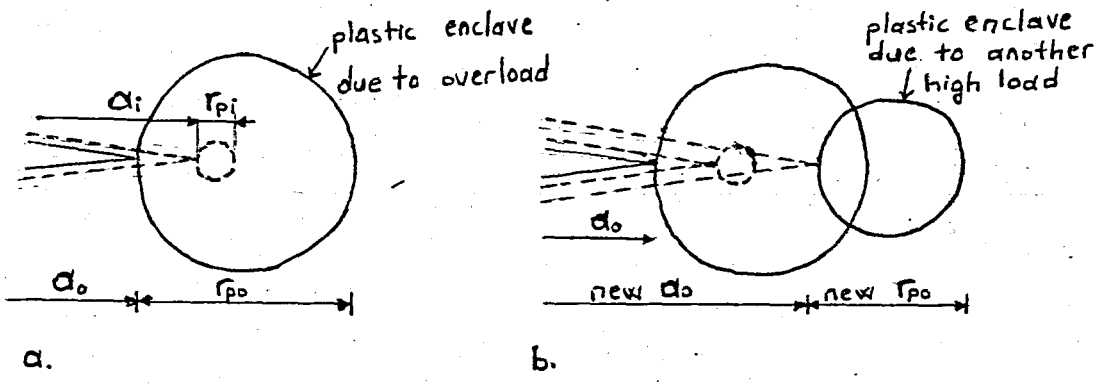

Figure 3.2. The model of Wheeler (61)
a. Situation after overload, b. Situation after second overload.

The size of the plastic zone is:

$$r_{pi} = \frac{K_{max,i}^2}{\alpha \sigma_{ys}^2} = \frac{(\Delta K)_{,i}^2}{(1-R)^2 \alpha \sigma_{ys}^2} \quad ; \quad r_{po} = \frac{K_{max,o}^2}{\alpha \sigma_{ys}^2} \qquad (3.3)$$

where K_{max} is the maximum stress intensity in a given cycle, $\alpha = 2\pi$ for plane stress, and $\alpha = 6\pi$ for plane strain according to Irwin's plastic zone approach.

There is retardation as long as the current plastic zone size is contained within a previously generated plastic zone. If $a_i + r_{pi} \geqslant a_o + r_{po}$ the crack has grown through the overload plastic zone, and the retardation factor becomes $C_p = 1$ by definition. The power m in eq(3.2) has to be determined empirically. Wheeler

finds m = 1.43 for D6ac steel and m = 3.4 for T_i-6Al-4V.

For the case of a single overload in a constant amplitude test the retardation factor gradually decreases to unity while the crack progresses through the plastic enclave. If a second high load occurs, producing a plastic zone extending beyond the border of the existing plastic enclave, the boundary of this new plastic zone will have to be used in the equations (figure 3.2.b), and the instantaneous crack length will then become the new a_o.

The retarded crack-growth rate can be determined from the baseline (constant amplitude) crack growth rate as,

$$(da/dN)\ \text{retarded} = C_p (da/dN)\ \text{linear} \qquad (3.4)$$

where (da/dN) linear follows from constant amplitude data.

Predictions made by Wheeler by using his cycle-by-cycle integration method led to fairly good predictions of block-programme crack propagation tests. But the model does not account for compressive loading. Since the fracture surfaces are pressed together by compressive stresses, stress intensity has no physical meaning under compressive loading and therefore if the stress intensity factor is less than zero it is set at zero. On the other hand, although compressive peak hoad causes acceleration of crack growth rate, the Wheeler model does not account for this.

3.2. The Willenborg Model

The method was proposed by Willenborg, Engle and Wood (62). They also make use of the plastic enclave formed at the overload (figure 3.3). The plastic enclave extends to

$$a_p = a_o + r_{po} = a_o + \frac{1}{\alpha} \frac{K_o^2}{\sigma_{ys}^2} \qquad (3.5)$$

where a_p is the distance from the centre of the crack to the boundary of the plastic enclave and the other symbols have the same meaning as in eqs(3.2) and (3.3). Willenborg et al. consider the stress intensity that would be required to produce a plastic zone (at the tip of the current crack a_i) that would extend to the border of the plastic enclave (figure 3.3).

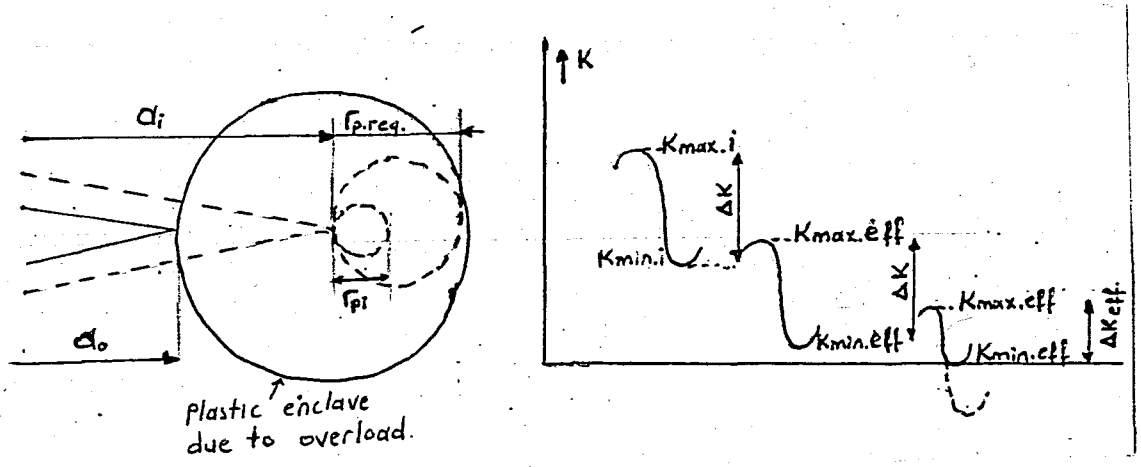

Figure 3.3. The model of Willenborg, Engle and Wood (62)

This means that it has to be determined what magnitude of K_{max} is required to give:

$$a_i + r_{p.req.} = a_o + r_{po} \qquad (3.6)$$

where $r_{p.req}$ is the plastic zone required to reach the boundary of the existing plastic enclave. The $K_{max.\,req}$ to achieve this, is given by:

$$\frac{1}{\alpha} \frac{K_{max.req}^2}{\sigma_{ys}^2} = a_o + r_{po} - a_i. \qquad (3.7)$$

In the first cycle subsequent to the overload, a_i is still equal to

a_o. Hence $K_{max.req}$ would be equal to the stress intensity of the overload, as should be expected.

Willenborg et al. make the rather odd assumption that $K_{max.i}$ actually occuring at the current crack length a_i, will be effectively reduced by an amount K_{red}, given by:

$$K_{red} = K_{max.req} - K_{max,i}. \tag{3.8}$$

The residual compressive stresses introduced by an overload reduce the effective stress at the crack tip. This implies that the effective stress is the difference between the active stress and the residual stress. Eq(3.8) means that Willenborg et al. expect that the magnitude of the residual stress is given by:

$$\sigma_{res} = \frac{K_{max.req}}{\sqrt{\pi a_i}} - \frac{K_{max.i}}{\sqrt{\pi a_i}} \tag{3.9}$$

This means that both $K_{max.i}$ and $K_{min.i}$ in cycle i are reduced by an amount K_{red}. Hence, the effective stress intensity is given by:

$$K_{max.eff.i} = K_{max.i} - K_{red} = 2K_{max.i} - K_{max.req}$$

$$K_{min.eff.i} = K_{min.i} - K_{red} = K_{min.i} + K_{max.i} - K_{max.req}. \tag{3.10}$$

If either $K_{min.eff}$ or both $K_{max.eff}$ and $K_{min.eff}$ would be smaller than zero they are set at zero. If the latter accurs, $\Delta K_{eff.i}$ will be smaller than ΔK_i: if not, $\Delta K_{eff.i} = \Delta K$, as can be seen from figure 3.3. The cycle ratio R_{eff} becomes

$$R_{eff} = \frac{K_{min.i} - K_{red}}{K_{max.i} - K_{red}} = \frac{K_{min.i} + K_{max.i} - K_{max.req}}{2K_{max.i} - K_{max.req}} \tag{3.11}$$

Both ΔK_{eff} and R_{eff} can be calculated and then da/dN can be calculated from the Forman equation based on effective values:

$$da/dN = \frac{C \Delta K_{eff}^{n}}{(1-R_{eff})K_c - \Delta K_{eff}} \qquad (3.12)$$

Willenborg et al. also show integration results of block-programme crack propagation in good agreement test data. An objection against their model is that the assumption regarding the residual compressive stresses is doubtful.

3.3. The Crack Closure Model

Let us consider a growing fatigue crack (figure 3.4). During its growth the plastic zone is moving with the tip of the crack. It is also increasing in size and as a first approximation (central crack).

$$r_p \doteq K^2 \doteq a. \qquad (3.13)$$

That means that the plastic zone size is proportional to the crack length a. The same will be true for

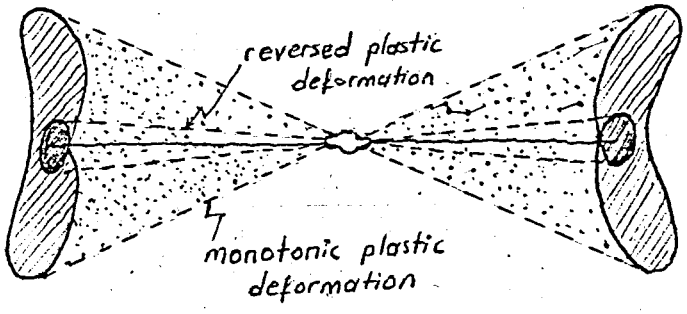

Figure 3.4. Plastic deformation in front of and in the wake of crack

the reversed plastic zone. Since the monotonic plastic zone is considerably larger than the reversed plastic zone, the consequence

of the growing fatigue crack is that monotonic plastic deformation has been left in the wake of the crack. This deformation involves elongation in the loading direction. As a result of this elongation the crack will close (at least partly) during unloading, and after full unloading ($P = o$) compressive residual stresses will be present in the wake of the crack. It means that residual compressive stresses are transmitted through the crack, because the fracture surfaces are pressed together by the plastic deformation left in the wake of the crack.

The phenomenon that the upper and lower fracture surfaces of a fatigue crack come together before complete unloading (i.e. at $p > o$, tensile load) implies that the crack is no longer fully open. This phenomenon in the literature is referred to as "crack closure". It was first observed by Elber (21) and it is sometimes referred to as the Elber mechanism.

The most well known method to indicate crack closure is by COD (crack opening displacement) measurements. For crack opening between two points A and B, close to the edges of the crack and in the center of the panel, the relation for an infinite sheet is:

$$COD = 4a\sigma / E \qquad (3.14)$$

It means that COD is linearly proportional to σ (Hooke's law) and to the crack length a. For a finite sheet a geometry correction factor has to be added. Measurements on panels with fine saw cuts (Figure 3.5)

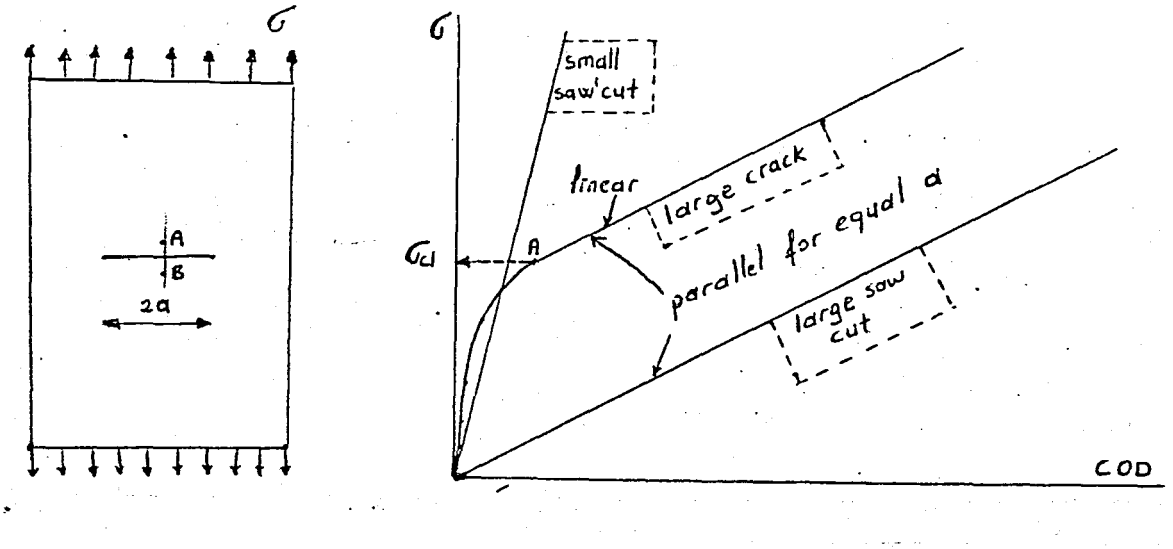

Figure 3.5. Crack closure measurement.

have confirmed the linear relationship with excellent agreement between measured slopes (σ/COD) and theoretical values. If a similar test is carried out on a panel with a fatigue crack the σ-COD record shows a non-linear part. Above point A the record is linear and the slope is in agreement with the crack length, which implies that the crack is fully open. Below point A the slope (tangent to σ - COD record) is larger, which implies that the panel behaves as a panel with a shorter crack. This indicates that the crack is partly closed. The stress corresponding to point A is called the crack closure stress (σ_{cl}) or the crack opening stress (σ_{op}). A full loop of a COD record (figure 3.6) usually shows a slight hysteresis, but there is no doubt about the occurence of full crack opening at A' the onset of crack closure at A''. The existence of a non-linear part followed by a linear part is easily observed, but the problem is to determine accurately the point A where the transition occurs. Measurements suggest that

A' and A'' coincide, however, experience shows that the unloading

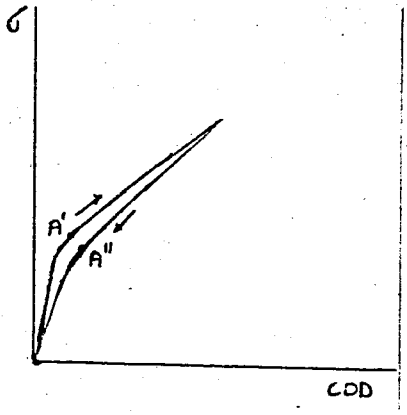

Figure 3.6. A full loop of COD.

branch (A') gives a slightly better reproduction and a more unambiguous determination of the closure stress. Nevertheless it cannot be denied that it is difficult to achieve a high accuracy.

In order to increase the accuracy, Paris suggested a compensation method, illustrated by figure 3.7. Instead of recording the COD signal it is compensated by a signal that would have been obtained under full linear behavior (i.e. no crack closure). This leads to a vertical line as long as the crack is fully open. The compensated COD signal now allows a much larger application which will bring out the transition point A more clearly. If the amplification is selected too high, the linear part (vertical line) may become erratic.

Another possibility to improve the sensitivity of the crack closure measurement is to locate the COD meter more closely to the crack tip. The effect on the σ- COD record is shown in figure 3.8.

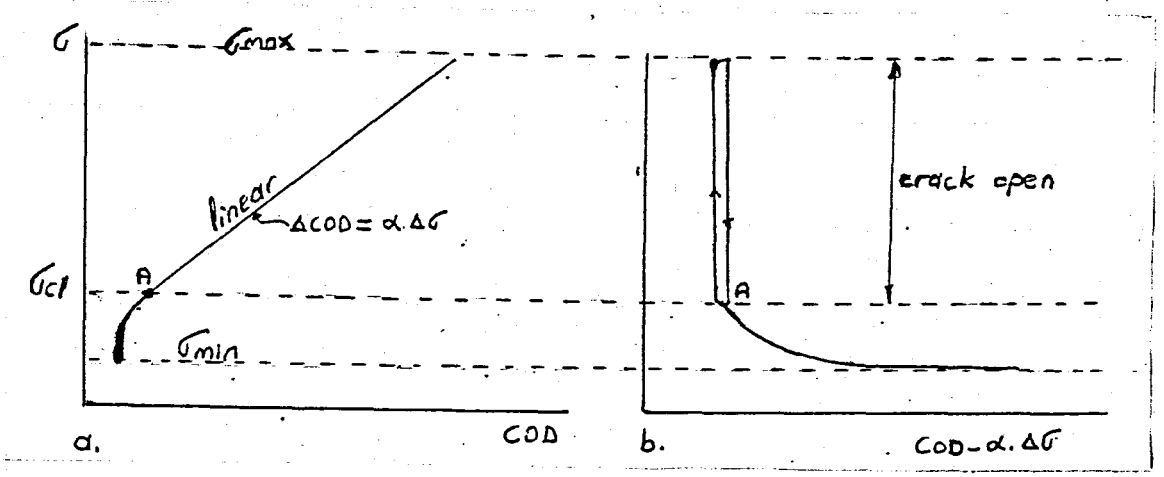

Figure 3.7. COD measurement; a. Normal record, b. compensated record.

The non-linear part ($A'' - A'$) of the record is small and the transition is more easily observed. This method can be used for a particular crack length, but if the crack is growing the COD-meter has to be moved also. If the COD-meter is too close to the crack tip, plasticity effects may obscure the measurements.

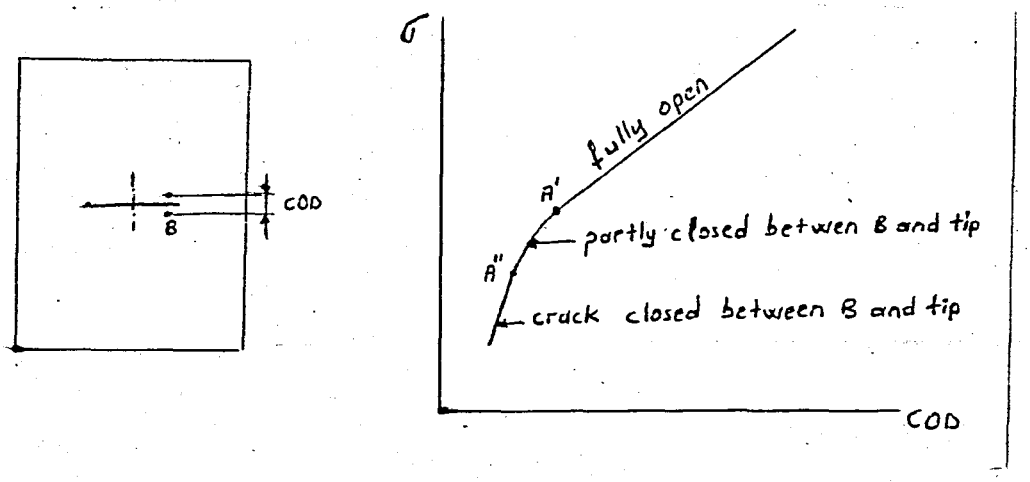

Figure 3.8. The COD-meter is too close to the crack tip.

In 1970 W.Blazewicz carried out fatigue tests in Delf. He made ball impressions on 2024-T3 sheet specimens before the crack growth test was started (figure 3.9) (66). As a result there is a zone between the impressions with residual compressive stresses.

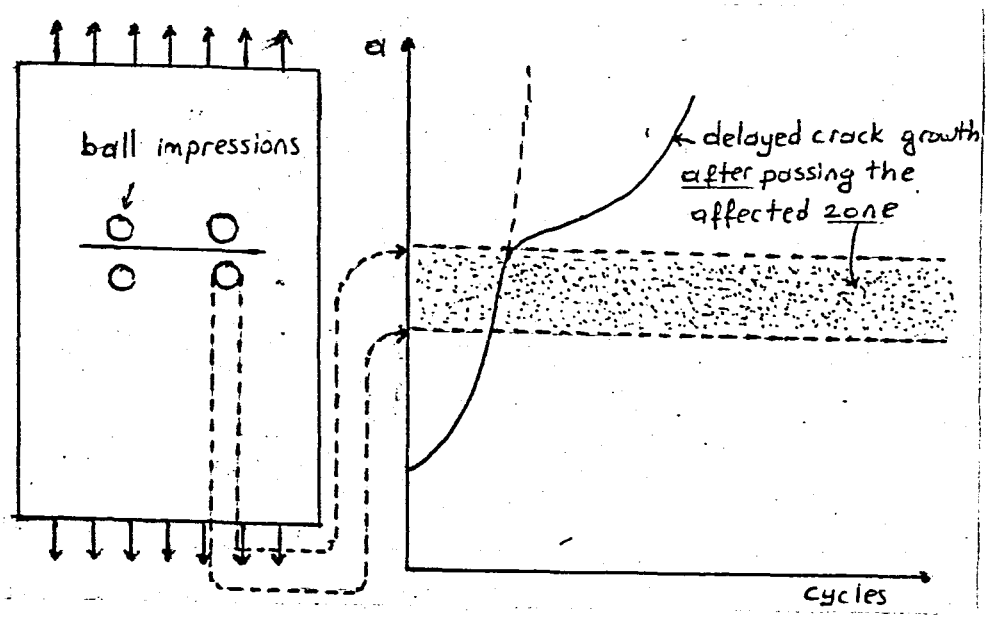

Figure 3.9. The Blazewicz's tests.

This caused a delay in the crack growth, but (surprisingly enough at that time) the delay was small during the growth through the zone between the impressions, whereas it was significant at a later stage. The explanation is that the deformations of the ball impressions were the cause of crack closure after the crack had grown through the affected zone.

Elber (21) suggested the following relation between crack closure and crack growth. During a stress cycle a fatigue crack will be partly or fully closed as long as $\sigma < \sigma_{cl}$ (figure 3.10). He then suggested that the stress variation will contribute to crack extension only if

$$\sigma < \sigma_{cl}$$

which leads to the definition of an effective stress range:

$$\Delta\sigma_{eff} = \sigma_{max} - \sigma_{cl} \qquad (3.15)$$

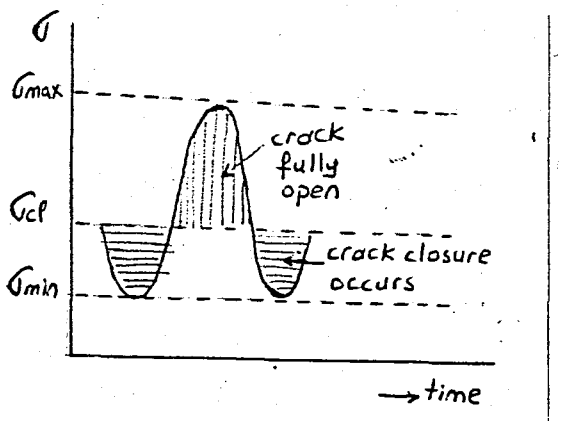

Figure 3.10. The crack closure model.

and an effective stress intensity factor:

$$\Delta K_{eff.} = C \Delta \sigma_{eff.} \sqrt{\pi a} \qquad (3.16)$$

The crack rate was supposed to be dependent on $\Delta K_{eff.}$ only.

$$da/dN = f(\Delta K_{eff.}) \qquad (3.17)$$

This relation includes the effect of the stress ratio R because crack closure (and thus $\Delta K_{eff.}$) will depend on R. For 2024-T3 material Elber found that σ_{cl} was approximately constant during a fatigue test, implying that σ_{cl} was independent of the crack length a. This is an empirical result. He defined the ratio:

$$U = \frac{\Delta K_{eff.}}{\Delta K} \left(= \frac{\Delta \sigma_{eff.}}{\Delta \sigma} \right) \qquad (3.18)$$

and the test results indicated the relation:

$$U = 0.5 + 0.4\, R \qquad (3.19)$$

This is again an empirical result. Combining the above equations leads to

$$\log \Delta K_{eff.} = \log \Delta K + \log (0.5 + 0.4\ R) \qquad (3.20)$$

Figure 3.11 includes a schematic of a simple spectrum in which the opening stress is seen to vary. The success

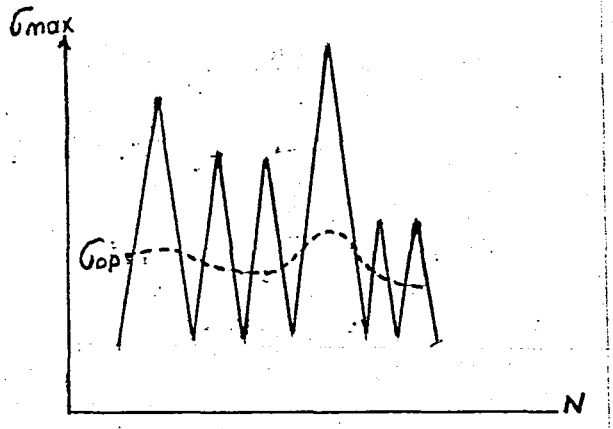

Figure 3.11. The variation of opening stress during variable amplitude cycling as described by Elber (21).

in using a closure model for the prediction of delay following an overload depends upon the assumptions made regarding the stabilization of closure load following the overload and the number of cycles of load required to accomplish "equilibrium" (67). For example, following one or a few overloads (figure 3.12) closure load of the subsequent series of cycles would be effected by the presence of the overload. If the overload would cause the opening load of the subsequent cycles to be increased, under these assumptions, crack growth could be completely arrested for some conditions. Assuming growth of a retarded nature did occur following the overload, some assumptions would have to be made as to the length of crack or zone over which the retardation would apply. As a first approximation, the yield zone produced by the overload might be tried.

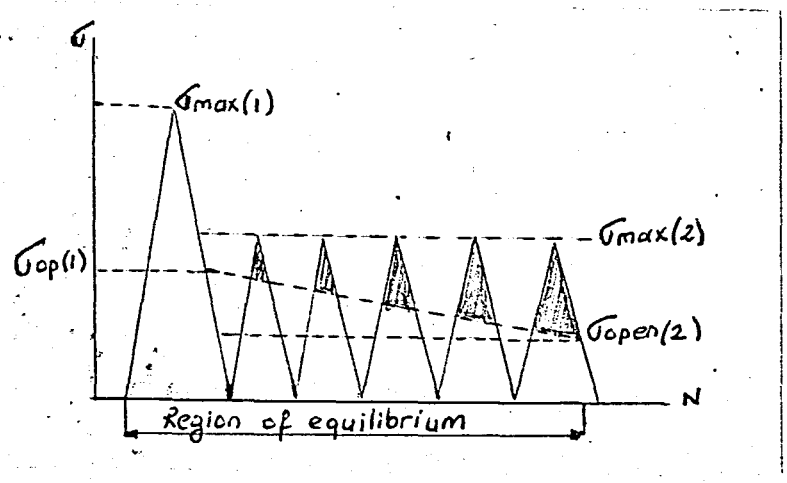

Figure 3.12. Schematic of closure load variation following the application of a single overload.

Shih and Wei (68) have reported evidence to refute closure as the only phenomenon responsible for retardation.

In summary, closure appears to be a real phenomena, which can be rather readilyobserved, measured and quantified. It apparently is not the only phenomena which causes delay. Results from past studies have differed because of specimen type, thickness, precracking procedure, notch geometry and instrumentation.

3.4. The Root Mean Square (RMS) Approach

Barsom (69) attempted to determine the magnitude of constant-amplitude cyclic-load fluctuation that results in the same a versus N curve obtained under variable-amplitude cyclic-load fluctuation when both spectra are applied to identical specimens (including initial crack length). In other words, one of the objectives of his investigation was to find a single stress-intensity parameter, such as mean, modal, or root mean square, that can be used to define the crack-growth rate under both constant-and vari-

able-amplitude loadings. The selected parameter must characterize the probability-density curve.

A good correlation between data obtained under constant amplitude and variable-amplitude random-sequence load spectra was obtained on the basis of the root mean square of the load distribution, where the root mean square is the square root of the mean of the squares of the individual load cycles in a spectrum. The combined crack-growth-rate data are presented in figure 3.13 as a function of ΔK_{rms}. The data show that, within the limits of the experimental work, the average fatigue-crack-growth rates per cycle, da/dN, under variable-amplitude random-sequence stress spectra can be represented by

$$da/dN = C(\Delta K_{rms})^n \tag{3.21}$$

where C and n are constants and

$$\Delta K_{rms} = \sqrt{\frac{\sum_{i=1}^{k} \Delta K_i^2}{n}} \tag{3.22}$$

The root-mean-square value of the stress-intensity factor under constant-amplitude cyclic-load fluctuation is equal to the stress-intensity-factor fluctuation. Consequently, the average fatigue-crack-growth rate can be predicted from constant-amplitude data by using eq(3.21).

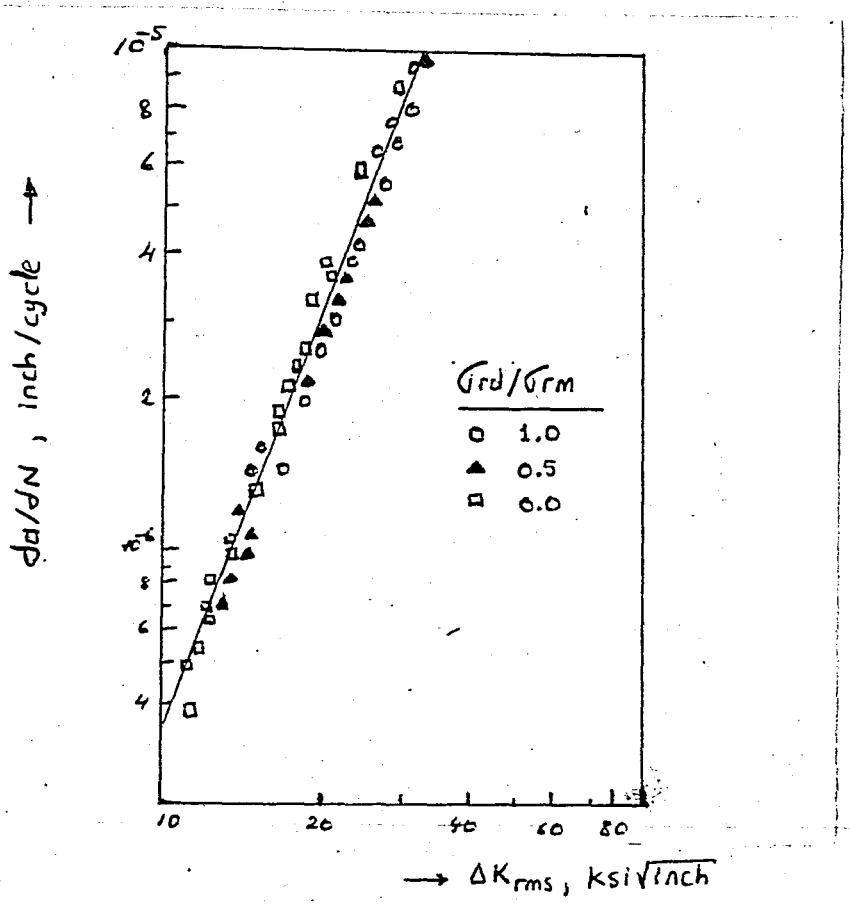

Figure 3.13. Crack-growth rate as a function of the root-mean -square stress-intensity factor.

The root-mean-square stress-intensity factor, ΔK_{rms}, is characteristic of the load-distribution curve and is independent of the cyclic-load fluctuations (70).

Smith (71) and Swanson (72) have also obtained good correlations with similar spectrum characterizations for random loadings. In these studies of random-loading crack growth, stress spectra were all represented by a continuous, unimodal distribution, in particular, by a Rayleigh distribution function. (see appendix-C). The use of an RMS type of characterization to predict fatigue-crack growth should probabily be restricted to load histories which can be described by such distributions and in which sequence effects are not expected to be significant.

IV. FACTORS AFFECTING CRACK PROPAGATIONS

When predictions of crack propagation have to be made, data should be available relavent to the conditions prevailing in service. Such data may be hard to find. Fatigue crack propagation is affected by an endless number of parameters and the circumstances during the test will seldom be the same as in service. The influence of the environment is the most conspicuous. Tests are usually not performed under controlled environmental conditions and part of the scatter in fatigue data may be attributed to this fact.

4.1. Effect of specimen thickness :

Apart from the effects due to the transition from a 90° to a 45° plane, thickness has little effect on the rate of crack growth, provided that the crack front is sensibly straight through the thickness. Some tests (73) showed that, at short crack lengths, the crack growth rates tended to increase with sheet thickness, but were not affected at longer crack lengths.

The crack growth rate may increase as the maximum stress intensity factor in the fatigue cycle, $K_{max.}$, approaches K_c, the fracture toughness of the material. K_c in general decreases as the thickness increa-

ses, reaching a minimum K_{1c} under plane strain conditions. This change in K_c with thickness can cause a corresponding thickness effect at high crack growth rates as illustrated in Fig.4.1

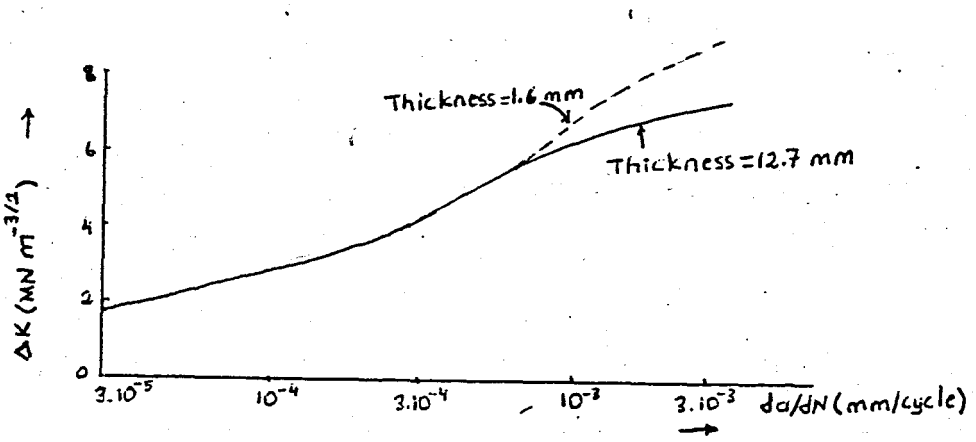

Figure 4.1. Effect of thickness on crack growth in RR58 aluminum alloy.

4.2 The effect of specimen orientation

(For the specimen orientation notation, see appendix E.) Figure 4.2 shows the rate of propagation to be somewhat higher for transverse (T-L) than for longitudinal (L-T) specimens from 7075-T73510 extrusions ; this was generally true for both plate and extrusions of all alloys and tempers. For the hand forgings, the rates were highest for specimens oriented in the short-transverse

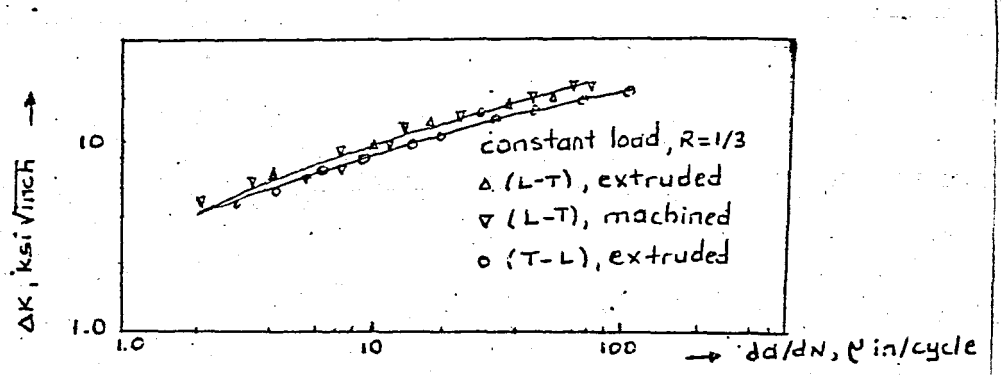

Figure 4.2. Effect of specimen direction on fatigue-crack propagation rate for 7075-T73510 extruded panel (73).

direction. These directional relationships were generally consistent with relative ratings with regard to fracture toughness (73). Data in figure 4.2 also illustrate the results of comparisons of specimens with machined and as-fabricated surfaces ; no significant differences in rate of crack propagation were detected.

Figure 4.3 shows that fatigue crack in long.- transverse specimens propagate substantially slower through the thickness (T-S) than in the longitudinal direction of the forging (T-L). Rates of propagation through the thickness were also shown to be lower for longitudinal (L-S)

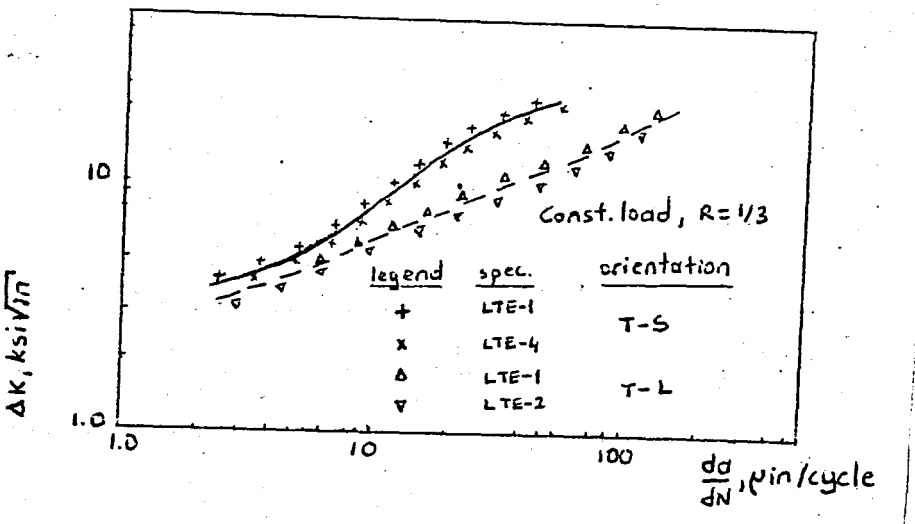

Figure 4.3. Effect of orientation on rate of crack propagation of a 7079-T652 hand forging.

7079-T652 and long-transverse (T-S) 7075-T7352 specimens from the forgings than for the comparable flatwise directions (L-T and T-L, respectively). In the short transverse direction (data not shown), the rate of propagation was found to be slightly lower for S-T specimens than for S-L specimens for both alloys. K_{1c} values were not determined for the L-S , T-S or S-T orientations so K_{1c} crack growth rate comparisons cannot be made. Davis et al. (74) did report lower values of K_{1c} for propagation in the L-S and T-S orientations than

in the L-T and T-L orientations for both 7075-T6 and 7079-T6 hand forgings, so for these orientations, the consistency in ratings may not exist.

4.3. The effect of stress ratio and K_{max}

The effect of stress (or cycle) ratio, R, and the maximum stress intensity, K_{max}, was studied in chapter II. (pp.3-9).

4.4. Effect of temperature.

Temperature has considerable effects on material properties in general. It has a significant influence on fracture toughness also. However, it is impossible to isolate temperature effects from the effects of the many other parameters discussed. As an example consider the thickness effect. A plate of relatively low thickness may show plane stress behavior with inherent high toughness at room temperature. At low temperatures the material has a higher yield stress which causes the plastic zone to be smaller : then the plate may show transitional or even plane-strain behavior, with inherent lower toughness. Apart from the intrinsic effects of temperature on toughness, there is an indirect effect, due to the temperature dependence of yield strength.

The brittle-ductile transition of structural steels is well known from Charpy impact tests. A similar transition may be expected when considering toughness values. In view of the experimental problems of fracture toughness at temperatures different from ambient , attempts have been made (75,76) to estimate K_{Ic} on the basis of the Charpy impact-energy. It seems feasible that a correlation between Charpy energy and fracture toughness exists, since the former is also equivalent to a fracture energy through G_{Ic} . However, this reasoning is doubtful since, the Charpy energy is the integrated energy for complete fracture

of the specimen. On the other hand G_{Ic} is the energy for the first infinitesimal crack growth.

Nevertheless correlations are found between toughness and Charpy energy, particulary in the area of low toughness. Figure 4.4 serves as an illustration. In fact

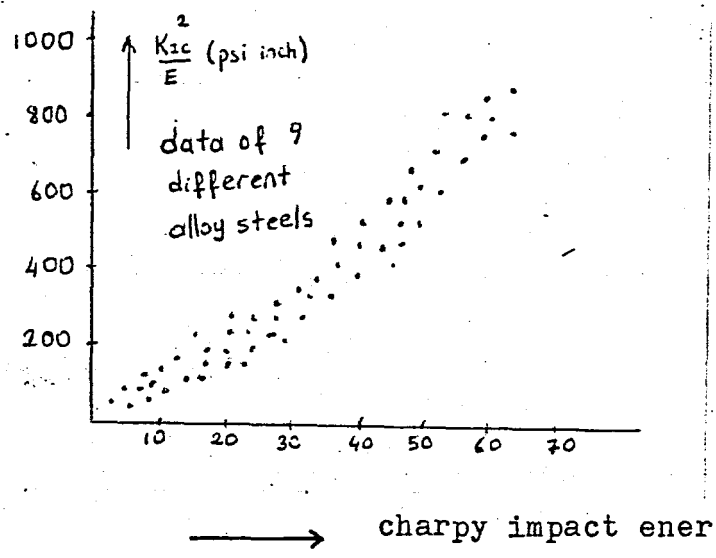

Figure 4.4. Correlation between toughness and charpy impact energy (75).

the charpy test is a dynamic test and it may be more sensible to correlate the impact energy with the dynamic fracture toughness. Although Charpy tests may be able to give an indication of the toughness variation, this type of test is basically not compatible with fracture mechanics principles. Therefore its applicability as a basis for decisions or conclusions concerning fracture behavior in the context of fracture mechanics is debatable.

Figure 4.5 shows that a steel indeed shows a transition from low to high toughness with increasing temperature. Alloy steels and other materials usually show a gradual increase of toughness with temperature, followed by a decrease at temperatures approaching the melting point.

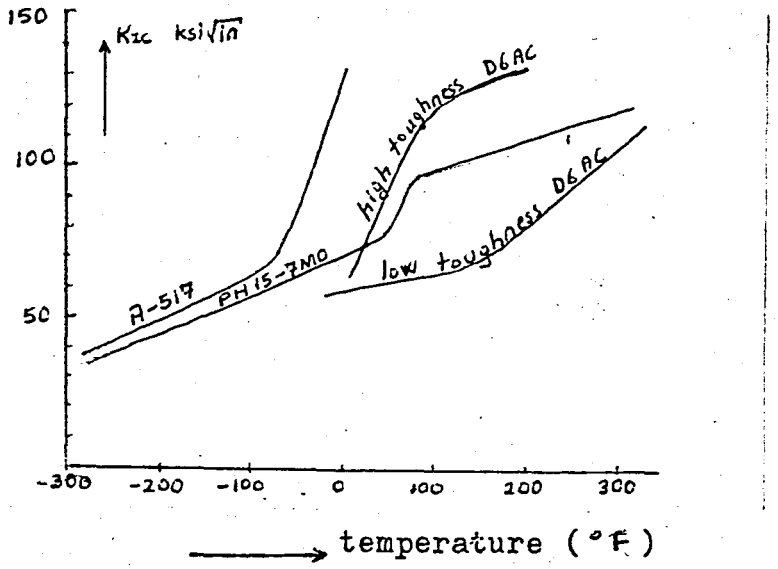

Figure 4.5. Temperature dependence of toughness of various steels (75,77)

4.5. Effect of loading frequency

Four specimens of 2024-T3 aluminum are tested each at a different frequency but with the same load ratio (78). The results show that the threshold decreases with increasing frequency(figure 4.6). This was an unexpected result since no effect of frequency had been previously noted below 200 Hz and it is the reverse of the trend that is expected from environmentally enhanced fatigue crack growth (79).

However, if the possibility of crack tip heating is considered one might expect such a shift. At the higher frequencies, heat may be generated by crack tip plasticity rapidly enough to produce a local rise in temperature. An increase in temperature might produce the lower threshold in 2024-T3 aluminum as it does for A533 steel(7). At lower frequencies heat conduction away from the crack tip would proceed rapidly enough to prevent any appreciable rise in the temperature near the crack tip.

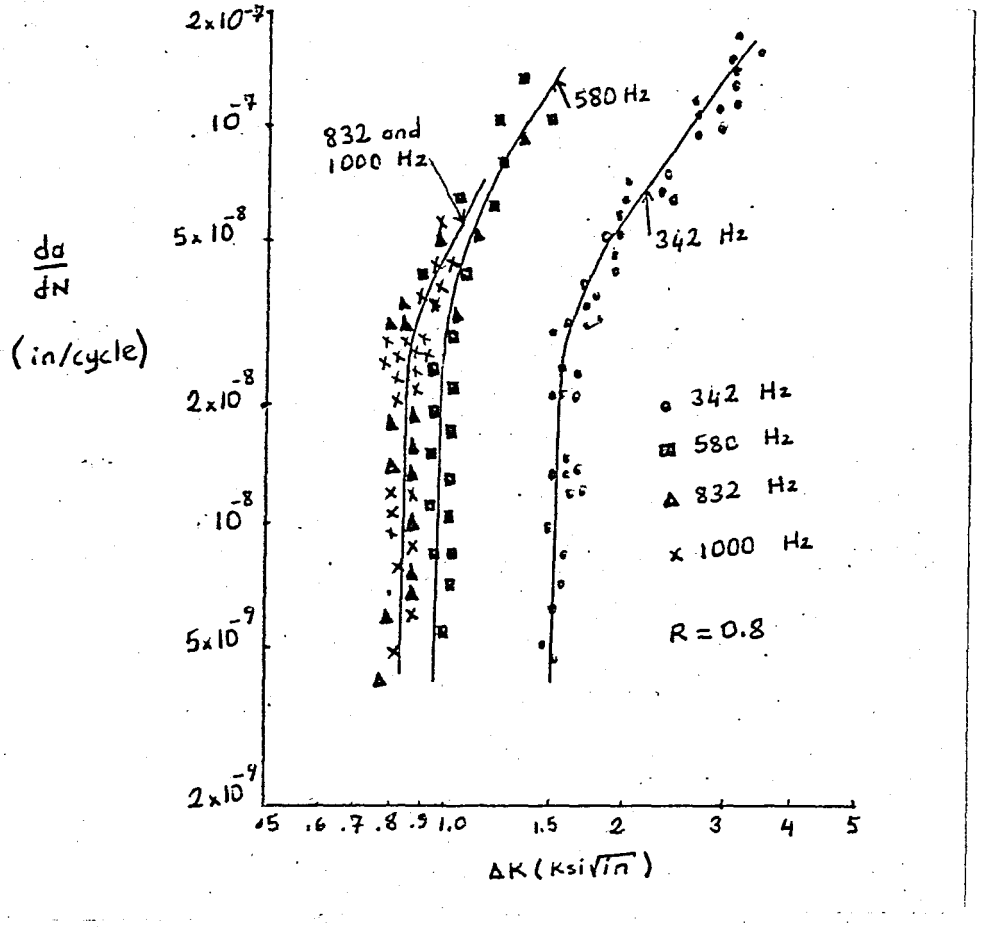

Figure 4.6 Effect of frequency on fatique crack growth rates for 2024-T3 aluminum (78).

James, L.A(80)investigated the effect of frequency upon the fatique-crack growth of type 304 stainless steel at 1000 F. The results of this study are presented in figure 4.7 as a plot of da/dN versus ΔK. Several observations are immediately apparent :

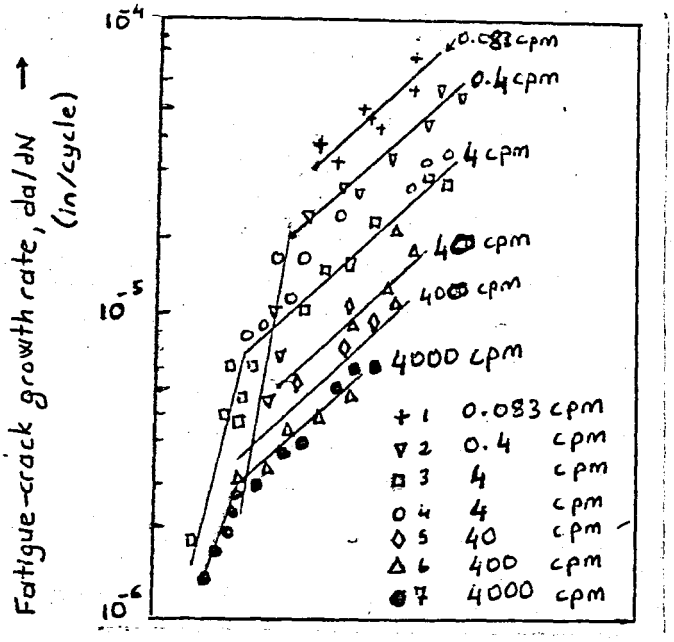

Figure 4.7. The effect of frequency on the crack growth behavior of solution-annealed type 304 stainless steel at 1000°F.

(1) There appears to be a portion of the curve where the fatigue-crack growth rate is independent of cyclic frequency ;

(2) Within the region where the crack growth rate is frequency-dependent, decreasing the cyclic frequency has a profound effect in increasing the rate of crack propagation ;

(3) The scatter of data tends to increase somewhat with decreasing frequency ;

(4) in the region where the crack growth rate is dependent upon the frequency, the slopes of the curves representing the various frequency levels appear to be quite similar

(5) The latter observation suggests that the frequency de - pendent behavior could be represented by a power law of the form

$$\frac{da}{dN} = A(f)[\Delta K]^n \qquad (4.1)$$

where $A(f)$ = some function of frequency, and n = constant for a given material/environment combination.

4.6. Effect of environment :

For the 7079-T652 hand forgings tested in a humidity of about 90 percent, the propagation rate is three times higher in the humid environment. For alloy 7075-T7352, the difference between the rates under the two environments is less even at the higher ΔK values(73). The greater sensitivity of 7079-T652 to moisture seems consistent with evaluations which show 7079-T6-type products to be susceptible to stress-corrosion cracking in normal atmospheres, where as 7075-T73-type products are not (81).

4.7. Effect of loading sequence

A fatigue cycle preceded by a load of higher magnitude produ - ces less crack propagation than it does in the absence of the higher preload. This retardation phenomenon was taken into consideration in detail, in chapter III.

V. COMPUTER PROGRAM EVALUATING FATIGUE LIFE

5.1. Introduction

Because of weight and economy, crack growth retardation gains importance in variable amplitude fatigue. A computer program was developed to predict the crack growth propagation in specimens subjected to randomized block loading. The program also takes into account the retardation phenomenon. The Wheeler and Willenborg models were used for predictions. A cycle-by-cycle integration scheme was used. What the program does is to evaluate the number of cycles, flights or certain repeated stress history untill the critical crack length is reached. For the linear crack growth, Paris-Erdogan eq., Walker's formula and Forman's equations were set to use. Six different types of flaw were taken into consideration ; Center-cracked panel, single-edge notched specimen, double-edge crack, Bend-specimen, compact tension specimen(CTS) and surface flaw(see table 2.1,p.13). Detailed description will be given in Appendix-D.

5.2. Program Outline

The program consists of fifteen routines and a supervisory ro-

utine. Each subroutine will be discussed below. Much of the data transmitted internally in the program AKYÜREK-I is through labeled COMMON blocks.

SUPERVISORY ROUTINE - Overall supervisory routine. This segment controls the calling, in order, all subroutines.

CADATA - Subroutine for the constant amplitude crack growth data and material properties.

SIMPSN - Constant amplitude crack growth integration scheme using simpson's composite integration formula (see Appendix-B)

DATA - Data input subroutine.

SIF - Evaluates the stress intensity factors for a given stress and crack length.

SFSIF - Subroutine for the surface flaw stress intensity evaluation.

PZS - Evaluates the plastic zone size for a given stress intensity and material.

ESIF - Subroutine which calculates the effective stress intensity factors for the Willenborg model.

GROWTH - Subroutine for linear crack growth.

WHEELR - Subroutine for the Wheeler retardation model.

WLLNBG - Subroutine for the Willenborg model.

OUTPUT - Prints out the crack growth information.

MAGFAC - Magnification factor evaluation for surface flaw (see Appendix-A).

DATFIT - Curve fitting subroutine using least squares method (see Appendix-A).

BLOCK - Subroutine for the block by block crack growth integration scheme.

BLOCK DATA - Initializes the labeled common blocks.

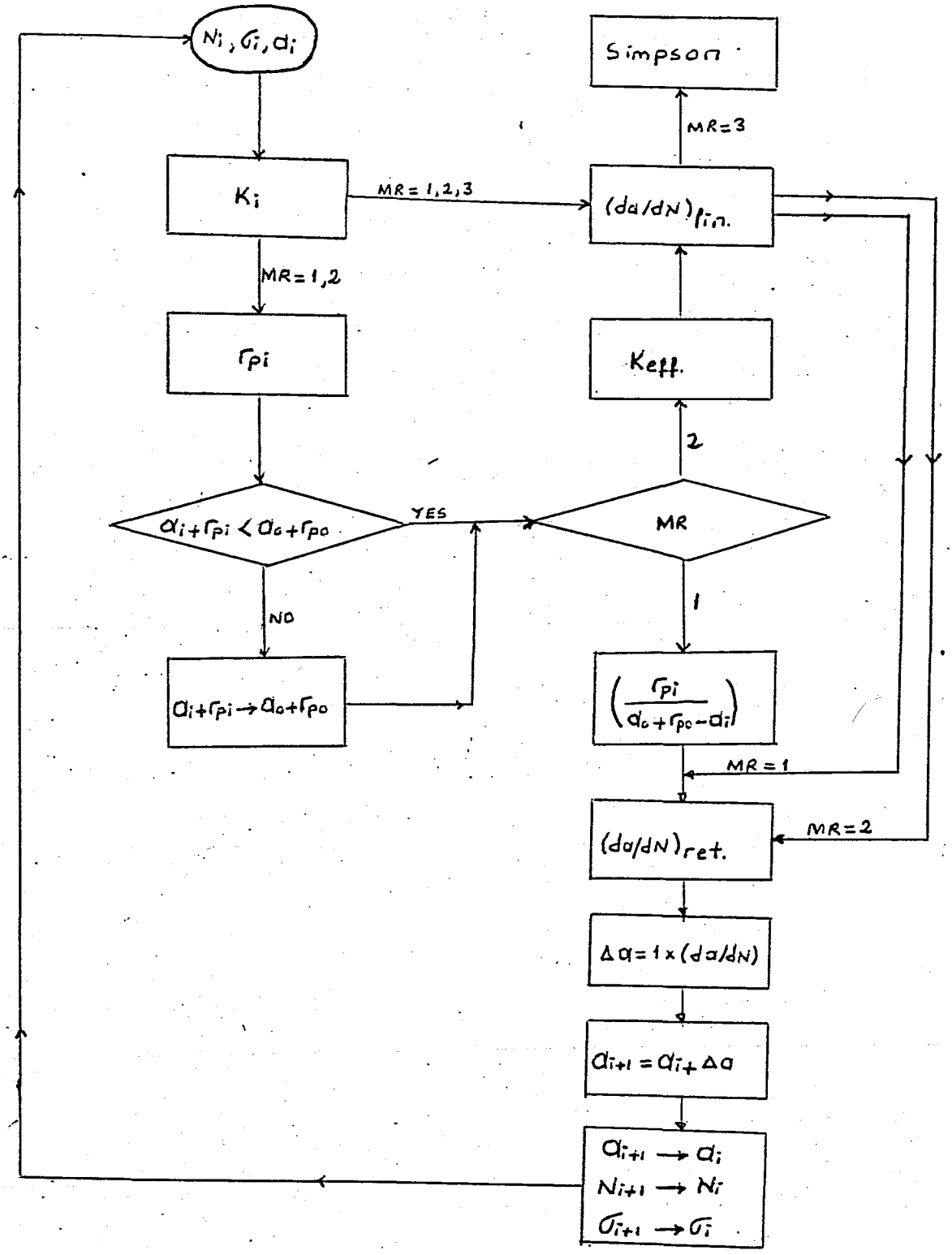

Figure 5.1. Simplified flow diagram for crack growth computation

```
                                                    TTTTTTTTTTTT        RRRRRRRRR
                                                    TTTTTTTTTTTT        RRRRRRRRRR
                                                         TT             RR      RR
                                                         TT             RR      RR
                                                         TT             RR      RR
                                                         TT             RRRRRRRRRR
                                                         TT             RRRRRRRRR
                                                         TT             RR    RR
                                                         TT             RR     RR
                                                         TT             RR      RR
                                                         TT             RR       RR
 *  *  *  UNIVAC 1106  BOGAZICI  UNIVERSITESI  KOMPUTER  MERKEZI  ISTANBUL

    RUNID * TRT          USER ID *                    PART NUMBER * 00      IN

     FILE NAME * CTSpRSSSSSSS          CREATED AT:   17:44:55 MAR 08, 1984

T2345678901234567890123456789012345678901234567890123456789012345678901234567
T001 C      PROGRAM AKYUREK-I
T002        DOUBLE PRECISION ACP,ADAL,ADAR,ADK,AF,AI,AKMAX,AKMAXE,AKMAXO,AKMI
T003       &N,AKMINE,ALPHA,AO,AR,ARPI,ARPO,B,C,CCP,CDAL,CDAR,CF,CI,CKMAX,CKMA
T004       &XO,CKMIN,CN,CO,CR,CRPI,CRPO,F,H,PHI,PI,QMAX,QMIN,SMAX,SMIN,RAB,RA
T005       &C,SKC,SYS,W,WM,WN,Z,BDAL,DDAL
T006        COMMON/TA1/A(8),JB(900),R(8),SMAX(900),SMIN(900)
T007        COMMON/TA2/ADAL,ADK,AF,AI,AKMAX,AKMAXO,AKMIN,ALPHA,AMF,AO,AR,ARPI
T008       &,ARPO,B,C,CDAL,CDK,CI,CKMAX,CKMAXO,CKMIN,CN,CO,CR,CRPI,CRPO,IA,IB
T009       &,IE,IP,J,JA,JE,KB,MN,MP,MR,NC,NFT,NI,NO,NP,PI,SKC,SYS,W,WM,WN,Z,A
T010       &DAR,CDAR,NT,MI
T011 C
T012 C      ************************************************************
T013 C      *PROGRAM FOR THE FATIGUE PROPAGATION LIFE ESTIMATION       *
T014 C      *OF THE SPECIMENS SUBJECTED TO RANDOMIZED BLOCK LOADING    *
T015 C      ************************************************************
T016 C
T017 C      AKYUREK-I TAKES THE RETARDATION INTO CONSIDERATION.IT
T018 C      USES THE WHEELER AND WILLENBORG RETARDATION MODELS.
T019 C
T020 C      ASSIGN DATA SET NUMBERS FOR INPUT,NI,OUTPUT NO
T021        NI=5
T022        NO=6
T023 C
T024 C      ================================================
T025 C      =OVERALL SUPERVISORY ROUTINE.THIS SEGMENT      =
T026 C      =CONTROLS THE CALLING,IN ORDER,ALL SUBROUTINES=
T027 C      ================================================
T028 C
T029 C      SELECTION OF THE RETARDATION MODEL AND
T030 C      CRACK GROWTH INTEGRATION SCHEME.
T031 C      MR IS RETARDATION MODEL NUMBER.
T032 C      MR=1 WHEELER MODEL.
T033 C        =2 WILLENBORG MODEL.
T034 C        =3 CONSTANT AMPLITUDE LOADING(USES SIMPSON'S
T035 C           COMPOSITE INTEGRATION FORMULA)
T036 C      MI IS THE CRACK GROWTH INTEGRATION SCHEME NUMBER.
T037 C      MI=1 CYCLE BY CYCLE CRACK GROWTH INTEGRATION SCHEME.
T038 C        =2 BLOCK BY BLOCK CRACK GROWTH INTEGRATION SCHEME.
T039        READ(NI,5) MR,MI
T040 5      FORMAT(2I10)
T041 C      READ AND WRITE THE MATERIAL PROPERTIES
T042 C      AND CONSTANT AMPLITUDE DATA.
T043        CALL CADATA
T044        GO TO (15,15,10),MR
T045 C
T046 C      EVALUATION OF THE TOTAL NUMBER OF CYCLES REQUIRED FOR
T047 C      THE PROPAGATION OF CRACK FROM INITIAL CRACK LENGTH,
T048 C      AI,TO CRITICAL OR FINAL CRACK LENGTH,AF,USING SIMP-
T049 C      SON'S COMPOSITE INTEGRATION FORMULA.
T050 C
T051 10     CALL SIMPSN
T052        GO TO 36
T053 C      DATA INPUT FOR RANDOM LOAD FATIGUE.
T054 15     CALL DATA
T055        DATA NC,NT/2*0/
T056 C      FOR THE FIRST CYCLE
T057        IA=1
T058 C      STRESS INTENSITY FACTOR EVALUATION.
T059        IF(NFT.NE.6) CALL SIF
T060 C      MAGNIFICATION FACTOR EVALUATION FOR SURFACE FLAW.
T061        IF(NFT.EQ.6) CALL DATFIT
T062 C      STRESS INTENSITY EVALUATION FOR SURFACE FLAW.
T063        IF(NFT.EQ.6) CALL SFSIF
T064 C      PLASTIC ZONE SIZE EVALUATION.
T065        CALL PZS


TURSUT
```

```
C      ASSUME THAT THE FIRST CYCLE IS OVERLOAD CYCLE
       AO=AI
       ARPO=ARPI
       AKMAXO=AKMAX
       IF(NFT.NE.6) GO TO 20
       CO=CI
       CRPO=CRPI
       CKMAXO=CKMAX
C      SELECTION OF THE CRACK GROWTH INTEGRATION SCHEME
20     GO TO (21,6),MI
C      ***BLOCK BY BLOCK CRACK GROWTH INTEGRATION SCHEME
6      CALL BLOCK
       GO TO 36
C      ***CYCLE BY CYCLE CRACK GROWTH INTEGRATION SCHEME
C      START THE APPLICATION OF THE LOADS AND
C      EVALUATION OF CURRENT CRACK LENGTHS
C
C      JE IS THE TOTAL NUMBER OF FLIGTHS,GROUP
C         OF BLOCKS OR NUMBER OF REPEATING SPECTRA
21     DO 1 IE=1,JE
       JH=0
C      JA IS THE TOTAL NUMBER OF BLOCKS OR NUMBER
C         OF CYCLES IN A FLIGTH OR SPECTRA
       DO 2 IA=1,JA
       JH=JH+1
C      JB(JH) IS THE TOTAL NUMBER OF CYCLES IN THE JH.TH BLOCK
       KB=JB(JH)
       DO 3 IB=1,KB
C      NT IS THE TOTAL NUMBER OF CYCLES
       NT=NT+1
C      STRESS INTENSITY EVALUATION IN AI DIRECTION
       IF(NFT.NE.6) CALL SIF
C      STRESS INTENSITY EVALUATION FOR SURFACE FLAW
       IF(NFT.EQ.6) CALL SFSIF
C      PLASTIC ZONE SIZE EVALUATION FOR THE CURRENT CYCLE
       CALL PZS
C      ***CONTROL OF THE PLASTIC ENCLAVE
C      FOR RETARDATION IN AI DIRECTION
       IF(AO+ARPO-AI=ARPI) 25,25,26
C      CURRENT CYCLE IS THE NEW OVERLOAD
25     AO=AI
       AKMAXO=AKMAX
       ARPO=ARPI
26     IF(NFT.NE.6) GO TO 30
C      ***CONTROL OF THE PLASTIC ENCLAVE FOR RETARDATION
C      IN THE MAJOR AXIS DIRECTION OF THE SURFACE FLAW
       IF(CO+CRPO-CI=CRPI) 29,29,30
C      CURRENT CYCLE IS THE NEW OVERLOAD IN THE
C      MAJOR AXIS DIRECTION OF THE SURFACE FLAW
29     CO=CI
       CRPO=CRPI
       CKMAXO=CKMAX
C      ***APPLICATION OF THE RETARDATION MODELS
C      THE WHEELER RETARDATION MODEL
30     IF(MR.EQ.1) CALL WHEELR
C      THE WILLENBORG RETARDATION MODEL
       IF(MR.EQ.2) CALL WLLNBG
C      PRINT OF THE CURRENT INFORMATION(EVALUATIONS)
       CALL OUTPUT
C      NEW CRACK LENGTH AFTER THE CYCLE APPLIED
       AI=AI+ADAR
       IF(NFT.NE.6) GO TO 32
       CI=CI+CDAR
C
C      HAS THE CURRENT CRACK LENGTH REACHED THE CRITICAL
C      VALUE?IF YES,STOP THE EVALUATIONS
C
32     IF(AI=AF) 3,35,35
3      CONTINUE
2      CONTINUE
1      CONTINUE
       IF(AI=AF) 47,35,35
47     WRITE(NO,48)
48     FORMAT(2X,'CRACK HAS NOT REACHED THE CRITICAL VALUE,INCREASE JE')
C      INFORMATION AT THE LAST CYCLE
35     WRITE(NO,40) NT,AI
40     FORMAT(1X,3HNT=,I20,4X,3HAI=,D20.14)
       IF(NFT.NE.6) GO TO 36
       WRITE(NO,45) CI
45     FORMAT(2X,3HCI=,D20.14)
36     STOP
       END
C
```

TURBUT

```
C      ==========================================================
C      =SUBROUTINE FOR THE CONSTANT AMPLITUDE LOAD FATIGUE=
C      =CRACK GROWTH DATA AND MATERIAL PROPERTIES          =
C      ==========================================================
C
      SUBROUTINE CADATA
      DOUBLE PRECISION ACP,ADAL,ADAR,ADK,AF,AI,AKMAX,AKMAXE,AKMAXO,AKMI
     &N,AKMINE,ALPHA,AO,AR,ARPI,ARPO,B,C,CCP,CDAL,CDAR,CF,CI,CKMAX,CKMA
     &XO,CKMIN,CN,CO,CR,CRPI,CRPO,F,H,PHI,PI,QMAX,QMIN,SMAX,SMIN,RAB,RA
     &C,SKC,SYS,W,WM,WN,Z,BDAL,DDAL
      COMMON/TA1/A(8),JB(900),R(8),SMAX(900),SMIN(900)
      COMMON/TA2/ADAL,ADK,AF,AI,AKMAX,AKMAXO,AKMIN,ALPHA,AMF,AO,AR,ARPI
     &,ARPO,B,C,CDAL,CDK,CI,CKMAX,CKMAXO,CKMIN,CN,CO,CR,CRPI,CRPO,IA,IB
     &,IE,IP,J,JA,JE,KB,MN,MP,MR,NC,NFT,NI,NO,NP,PI,SKC,SYS,W,WM,WN,Z,A
     &DAR,CDAR,NT
      DIMENSION TITLE(20)
C     READ AND WRITE THE PROBLEM TITLE
      READ(NI,100) TITLE
      WRITE(NO,100) TITLE
100   FORMAT(20A4)
      PI=0.31415927D01
C     BOUNDS ON THE PROBLEM;INITIAL AND CRITICAL CRACK LENGTHS,
      READ(NI,105) AI,AF
105   FORMAT(2D20.14)
      WRITE(NO,110)
110   FORMAT(//,7X,20HINITIAL CRACK LENGTH,16X,21HCRITICAL CRACK LENGTH)
      WRITE(NO,115) AI,AF
115   FORMAT(//,12X,F10.6,27X,F10.6)
      IF(MR.NE.3) GO TO 126
C     ***CONSTANT AMPLITUDE LOADING*
      IA=1
C     READ AND WRITE THE MAXIMUM AND MINIMUM STRESSES
      READ(NI,105) SMAX(IA),SMIN(IA)
      WRITE(NO,125) SMAX(IA),SMIN(IA)
125   FORMAT(//,2X,5HSMAX=,D20.14,2X,5HSMIN=,D20.14)
C     ***SELECTION OF THE LINEAR CRACK GROWTH EQUATION,
C     MN=1 PARIS-ERDOGAN EQUATION*
C       =2 FORMAN'S EQUATION,
C       =3 WALKER'S CALCULATION FORMULA*
126   READ(NI,130) MN
130   FORMAT(I10)
C     LINEAR CRACK GROWTH DATA AND MATERIAL PROPERTIES,
C
C     C IS THE CONSTANT IN THE LINEAR CRACK GROWTH EQUATIONS,
C     CN IS THE POWER CONSTANT IN THE LINEAR CRACK GROWTH EQUATIONS*
C     SKC IS THE FRACTURE TOUGHNESS OF THE SPECIMEN*
      READ(NI,135) C,CN,SKC
135   FORMAT(3D20.14)
C     SYS IS THE YIELD STRENGTH OF THE SPECIMEN*
C     W IS THE WIDTH OF THE SPECIMEN,
C     B IS THE THICKNESS OF THE SPECIMEN,
C     NFT IS THE NUMBER OF FLAW TYPE,
C     NFT=1 CENTER CRACK PANEL,
C       =2 SINGLE EDGE NOTCH,
C       =3 DOUBLE EDGE CRACK*
C       =4 BEND SPECIMEN*
C       =5 COMPACT TENSION SPECIMEN(CTS)*
C       =6 SURFACE FLAW,
      READ(NI,136) SYS,W,B,NFT
136   FORMAT(3D20.14,I10)
      WRITE(NO,140) C,CN,SKC,SYS,W,B,MN,NFT
140   FORMAT(//,5X,2HC=,D20.14,2X,3HCN=,D20.14,2X,4HSKC=,D20.14,//,3X,4
     &HSYS=,D20.14,10X,2HW=,D20.14,4X,2HB=,D20.14,//,4X,3HMN=,I10,18X,4
     &HNFT=,I10)
      IF(MN.NE.3) GO TO 155
C     WN IS WALKER'S EXPONENT IN THE WALKER'S FORMULA*
      READ(NI,145) WN
145   FORMAT(D20.14)
      WRITE(NO,150) WN
150   FORMAT(//,4X,3HWN=,D20.14)
155   IF(NFT.NE.6)GO TO 165
C
C     CI IS THE SEMI-CRACK LENGTH IN THE
C     MAJOR AXIS DIRECTION IN SURFACE FLAW,
      READ(NI,145) CI
      IF(NFT.NE.4) GO TO 170
C     DISTANCE BETWEEN THE SUPPORTS IN BEND SPECIMEN,
      READ(NI,145) Z
170   RETURN
      END
C     ==========================================================================
C     =EVALUATION OF THE TOTAL NUMBER OF CYCLES REQUIRED TO PROPAGATE=
```

```
C      =THE CRACK FROM INITIAL CRACK LENGTH,AI,TO CRITICAL OR FINAL   =
C      =CRACK LENGTH,AF,USING SIMPSON'S COMPOSITE INTEGRATION SCHEME. =
C      ================================================================
C
      SUBROUTINE SIMPSN
C
      DIMENSION F(9999)
      DOUBLE PRECISION ACP,ADAL,ADAR,ADK,AF,AI,AKMAX,AKMAXE,AKMAXO,AKMI
     &N,AKMINE,ALPHA,AO,AR,ARPI,ARPO,B,C,CCP,CDAL,CDAR,CF,CI,CKMAX,CKMA
     &XO,CKMIN,CN,CO,CR,CRPI,CRPO,F,H,PHI,PI,QMAX,QMIN,SMAX,SMIN,RAB,RA
     &C,SKC,SYS,W,WM,WN,Z,BDAL,DDAL
      COMMON/TA1/A(8),JB(900),R(8),SMAX(900),SMIN(900)
      COMMON/TA2/ADAL,ADK,AF,AI,AKMAX,AKMAXO,AKMIN,ALPHA,AMF,AO,AR,ARPI
     &,ARPO,B,C,CDAL,CDK,CI,CKMAX,CKMAXO,CKMIN,CN,CO,CR,CRPI,CRPO,IA,IB
     &,IE,IP,J,JA,JE,KB,MN,MP,MR,NC,NFT,NI,NO,NP,PI,SKC,SYS,W,WM,WN,Z,A
     &DAR,CDAR,NT
C      H IS THE STEP SIZE FOR NUMERIC INTEGRATION.
      H=0.1D-01
      DATA SUM,TOT/2*0.0/
C      2*N NUMBER OF STEPS
      N=(AF-AI)/(2.*H)
      IR=2*N+1
      DO 21 IQ=1,IR
      IF(IQ.EQ.1) GO TO 200
      AI=AI+H
200   CALL SIF
      CALL GROWTH
      F(IQ)=1./ADAL
21    CONTINUE
      IS=2*N
      DO 22 JR=2,IS,2
      SUM=SUM+F(JR)
22    CONTINUE
      SUM=4.*SUM+F(1)+F(IR)
      IT=2*N-1
      DO 23 IU=3,IT,2
      TOT=TOT+F(IU)
23    CONTINUE
      TOT=2.*TOT
      NTOTAL=(SUM+TOT)*H/3.
      WRITE(NO,205) NTOTAL
205   FORMAT(//,2X,21HLIFE OF THE SPECIMEN=,I20,2X,6HCYCLES)
      RETURN
      END
C
C      ========================
C      =DATA INPUT SUBROUTINE  =
C      ========================
C
      SUBROUTINE DATA
      DOUBLE PRECISION ACP,ADAL,ADAR,ADK,AF,AI,AKMAX,AKMAXE,AKMAXO,AKMI
     &N,AKMINE,ALPHA,AO,AR,ARPI,ARPO,B,C,CCP,CDAL,CDAR,CF,CI,CKMAX,CKMA
     &XO,CKMIN,CN,CO,CR,CRPI,CRPO,F,H,PHI,PI,QMAX,QMIN,SMAX,SMIN,RAB,RA
     &C,SKC,SYS,W,WM,WN,Z,BDAL,DDAL
      COMMON/TA1/A(8),JB(900),R(8),SMAX(900),SMIN(900)
      COMMON/TA2/ADAL,ADK,AF,AI,AKMAX,AKMAXO,AKMIN,ALPHA,AMF,AO,AR,ARPI
     &,ARPO,B,C,CDAL,CDK,CI,CKMAX,CKMAXO,CKMIN,CN,CO,CR,CRPI,CRPO,IA,IB
     &,IE,IP,J,JA,JE,KB,MN,MP,MR,NC,NFT,NI,NO,NP,PI,SKC,SYS,W,WM,WN,Z,A
     &DAR,CDAR,NT,MI
C      READ AND WRITE THE CONTROL DATA
C      ALPHA IS A CONSTANT USED IN EVALUATING THE PLASTIC ZONE SIZE.
C      ALPHA=1. PLANE STRESS CASE
C           =3. PLANE STRAIN CASE.
C      MP IS PLASTIC ZONE SIZE EVALUATION MODEL NUMBER.
C      MP=1 DUGDALE MODEL.
C        =2 IRWIN MODEL.
      READ(NI,300) ALPHA,MP,JE,JA
300   FORMAT(D20.14,3I10)
      ALPHA=2.*PI*ALPHA
      WRITE(NO,305) ALPHA,MP,MR
305   FORMAT(//,1X,6HALPHA=,D20.14,9X,3HMP=,I10,13X,3HMR=,I10)
      IF(MR.NE.1) GO TO 311
C      WM IS THE WHEELER RETARDATION EXPONENT.
      READ(NI,310) WM
310   FORMAT(D20.14)
      WRITE(NO,312) WM,MI
312   FORMAT(//,4X,3HWM=,D20.14,9X,3HMI=,I10)
C      ***STRESS OR LOAD HISTORY INPUT.
311   WRITE(NO,315)
315   FORMAT(1HO,2X,2HJB,10X,4HSMAX,18X,4HSMIN)
      WRITE(NO,320)
320   FORMAT(1H ,2X,2(1H=),10X,4(1H=),18X,4(1H=))
      DO 31 LA=1,JA
```

TURBUT

```
C      JB(LA) IS THE NUMBER OF CYCLES IN THE LA-TH BLOCK.
C      SMAX(LA) IS THE MAXIMUM STRESS OR LOAD IN THE LA-TH BLOCK.
C      SMIN(LA) IS THE MINIMUM STRESS OR LOAD IN THE LA-TH BLOCK.
       READ(NI,325) JB(LA),SMAX(LA),SMIN(LA)
325    FORMAT(I10,2D20.14)
       WRITE(NO,330) JB(LA),SMAX(LA),SMIN(LA)
330    FORMAT(//,1X,I6,5X,F10.3,12X,F10.3)
31     CONTINUE
       WRITE(NO,335) JE,JA
335    FORMAT(//,3X,3HJE=,I10,2X,3HJA=,I5)
C      ***OUTPUT CONTROL DATA.
       IF(MI.EQ.2) GO TO 337
C      IP=1 PRINTS OUT INFORMATION AT THE END OF EACH BLOCK.
C        =2 PRINTS OUT INFORMATION AT THE END OF EACH FLIGTH
C           OR SPECTRA.
C        =3 PRINTS OUT AT THE END OF EVERY NP CYCLES.NP IS
C           GIVEN AS INPUT.
       READ(NI,340) IP
340    FORMAT(I10)
C
C      OUTPUT HEADLINE PRINT CONTROL.
       GO TO (337,339,337),IP
337    WRITE(NO,336)
336    FORMAT(//,1X,'TOTAL CYCLE',4X,'SPECT.NO.',5X,'CURRENT CRACK LENGTH
     &',3X,'LIN.CRACK GROWTH RATE',4X,'MAX.STRESS INTENSITY',10X,'CUR.PL
     &ASTIC ZONE SIZE',/,1X,11(1H=),4X,9(1H=),5X,20(1H=),3X,21(1H=),4X,2
     &0(1H=),10X,21(1H=),/,1X,'IA,TH BLOCK',4X,'CYC.OF BL.',4X,'CRACK LE
     &NGTH AT O.L.',3X,'RET.CRACK GROWTH RATE',4X,'STRESS INT.RANGE',14X
     &,'PLAS.ZONE SIZE AT O.L.')
       GO TO 344
339    WRITE(NO,341)
341    FORMAT(//,2X,'TOTAL CYCLE',4X,'SPECT.NO.',15X,'CURRENT CRACK LENGT
     &H',5X,'STRESS INT.RANGE',10X,'MAX.STRESS INTENSITY',/,2X,11(1H=),4
     &X,9(1H=),15X,20(1H=),5X,16(1H=),10X,20(1H=))
344    IF(MI.EQ.2) GO TO 345
       IF(IP.NE.3) GO TO 345
C      PRINT IS DONE AT THE END OF EVERY NP CYCLES.
       READ(NI,340)NP
345    RETURN
       END
C
C      ============================================================
C      =SUBROUTINE FOR THE EVALUATION OF THE STRESS INTENSITY=
C      =FACTORS FOR A GIVEN STRESS AND CRACK LENGTH           =
C      ============================================================
C
       SUBROUTINE SIF
       DOUBLE PRECISION ACP,ADAL,ADAR,ADK,AF,AI,AKMAX,AKMAXE,AKMAXO,AKMI
     &N,AKMINE,ALPHA,AO,AR,ARPI,ARPO,B,C,CCP,CDAL,CDAR,CF,CI,CKMAX,CKMA
     &XO,CKMIN,CN,CO,CR,CRPI,CRPO,F,H,PHI,PI,QMAX,QMIN,SMAX,SMIN,RAB,RA
     &C,SKC,SYS,W,WM,WN,Z,BDAL,DDAL
       COMMON/TA1/A(8),JB(900),R(8),SMAX(900),SMIN(900)
       COMMON/TA2/ADAL,ADK,AF,AI,AKMAX,AKMAXO,AKMIN,ALPHA,AME,AO,AR,ARPI
     &,ARPO,B,C,CDAL,CDK,CI,CKMAX,CKMAXO,CKMIN,CN,CO,CR,CRPI,CRPO,IA,IB
     &,IE,IP,J,JA,JE,KB,MN,MP,MR,NC,NFT,NI,NO,NP,PI,SKC,SYS,W,WM,WN,Z,A
     &DAR,CDAR,NT
       GO TO (400,405,410,415,420),NFT
C      ***CENTER CRACK PANEL(NFT=1).
400    AKMAX=SMAX(IA)*DSQRT(PI*AI)
       AKMIN=SMIN(IA)*DSQRT(PI*AI)
C      CORRECTION FACTOR EVALUATION FOR CCP
       CF=1./((DCOS(PI*AI/W))**0.5)
       GO TO 425
C      ***SINGLE EDGE CRACK(NFT=2).
405    AKMAX=SMAX(IA)*DSQRT(AI)
       AKMIN=SMIN(IA)*DSQRT(AI)
C      CORRECTION FACTOR EVALUATION FOR SEN
       CF=1.99-0.41*(AI/W)+18.7*((AI/W)**2)-38.48*((AI/W)**3)+53.85*((A
     &I/W)**4)
       GO TO 425
C      ***DOUBLE EDGE CRACK(NFT=3).
410    AKMAX=SMAX(IA)*DSQRT(AI)
       AKMIN=SMIN(IA)*DSQRT(AI)
C      CORRECTION FACTOR EVALUATION FOR DEC
       CF=1.99+0.76*(AI/W)-8.48*((AI/W)**2)+27.36*((AI/W)**3)
       GO TO 425
C      ***BEND SPECIMEN(SMAX&SMIN ARE LOADS)(NFT=4).
415    AKMAX=SMAX(IA)*Z/(B*(W**1.5))
       AKMIN=SMIN(IA)*Z/(B*(W**1.5))
C      CORRECTION FACTOR EVALUATION FOR BS
       CF=2.9*((AI/W)**0.5)-4.6*((AI/W)**1.5)+21.8*((AI/W)**2.5)-37.6*((
     &AI/W)**3.5)+38.7*((AI/W)**4.5)
       GO TO 425
```

THESIS

```
C
C     COMPACT TENSION SPECIMEN(CTS)=SMAX AND SMIN ARE THE LOADS=(NFT=5)
C
420   AKMAX=SMAX(IA)/(B*DSQRT(W))
      AKMIN=SMIN(IA)/(B*DSQRT(W))
C     CORRECTION FACTOR EVALUATION FOR CTS
      CF=29.6*((AI/W)**0.5)-185.5*((AI/W)**1.5)+655.7*((AI/W)**2.5)-101.
     &7*((AI/W)**3.5)+638.9*((AI/W)**4.5)
425   AKMAX=CF*AKMAX
      AKMIN=CF*AKMIN
C     ***AVOIDING FROM COMPRESSIVE LOADING.
      IF(AKMIN.LT.0.0) AKMIN=0.0D00
      IF(AKMAX.LT.0.0) AKMAX=0.0D00
C     STRESS INTENSITY RANGE FOR AI DIRECTION.
      ADK=AKMAX-AKMIN
C     CYCLE RATIO FOR AI DIRECTION.
      IF(AKMAX.EQ.0.0) GO TO 426
      AR=AKMIN/AKMAX
      GO TO 430
426   AR=0.0D00
430   RETURN
      END
C
C     ============================================================
C     =SUBROUTINE FOR SURFACE FLAW STRESS INTENSITY EVALUATION=
C     ============================================================
C
      SUBROUTINE SFSIF
      DOUBLE PRECISION ACP,ADAL,ADAR,ADK,AF,AI,AKMAX,AKMAXE,AKMAXO,AKMI
     &N,AKMINE,ALPHA,AO,AR,ARPI,ARPO,B,C,CCP,CDAL,CDAR,CF,CI,CKMAX,CKMA
     &XO,CKMIN,CN,CO,CR,CRPI,CRPO,F,H,PHI,PI,QMAX,QMIN,SMAX,SMIN,RAB,RA
     &C,SKC,SYS,W,WM,WN,Z,BDAL,DDAL
      COMMON/TA1/A(8),JB(900),R(8),SMAX(900),SMIN(900)
      COMMON/TA2/ADAL,ADK,AF,AI,AKMAX,AKMAXO,AKMIN,ALPHA,AMF,AO,AR,ARPI
     &,ARPO,B,C,CDAL,CDK,CI,CKMAX,CKMAXO,CKMIN,CN,CO,CR,CRPI,CRPO,IA,IB
     &,IE,IP,J,JA,JE,KB,MN,MP,MR,NC,NFT,NI,NO,NP,PI,SKC,SYS,W,WM,WN,Z,A
     &DAR,CDAR,NT
C     ELLIPTIC INTEGRAL OF THE SECOND KIND
      PHI=(PI/2.0)*(1.-0.25*((CI**2-AI**2)/CI**2)-(3./64.)*((CI**2-AI**
     &2)/CI**2)**2)
C     FLAW SHAPE PARAMETER EVALUATION
      QMAX=PHI**2-0.212*(SMAX(IA)/SYS)**2
      QMIN=PHI**2-0.212*(SMIN(IA)/SYS)**2
C     MAGNIFICATION FACTOR(AMF) EVALUATION.
      CALL MAGFAC
C     STRESS INTENSITY EVALUATION FOR MINOR AXIS(AI) DIRECTION.
      AKMAX=1.12*AMF*SMAX(IA)*DSQRT(PI*AI/QMAX)
      AKMIN=1.12*AMF*SMIN(IA)*DSQRT(PI*AI/QMIN)
C     STRESS INTENSITY EVALUATION FOR MAJOR AXIS(CI) DIRECTION.
      CKMAX=1.12*SMAX(IA)*DSQRT(PI*(AI**2/CI)/QMAX)
      CKMIN=1.12*SMIN(IA)*DSQRT(PI*(AI**2/CI)/QMIN)
C     AVOIDING FROM COMPRESSIVE LOADING IN AI DIRECTION.
      IF(AKMIN.LT.0.0) AKMIN=0.0D00
      IF(AKMAX.LT.0.0) AKMAX=0.0D00
C     STRESS INTENSITY RANGE IN THE MINOR AXIS DIRECTION.
      ADK=AKMAX-AKMIN
C     CYCLE RATIO IN THE MINOR AXIS DIRECTION.
      IF(AKMAX.EQ.0.0) GO TO 480
      AR=AKMIN/AKMAX
      GO TO 485
480   AR=0.0D00
C     AVOIDING FROM COMPRESSIVE LOADING IN CI DIRECTION.
485   IF(CKMIN.LT.0.0) CKMIN=0.0D00
      IF(CKMAX.LT.0.0) CKMAX=0.0D00
C     STRESS INTENSITY RANGE IN THE MAJOR AXIS DIRECTION.
      CDK=CKMAX-CKMIN
C     CYCLE RATIO IN THE MAJOR AXIS DIRECTION.
      IF(CKMAX.EQ.0.0) GO TO 490
      CR=CKMIN/CKMAX
      GO TO 505
490   CR=0.0D00
505   RETURN
      END
C
C     ================================================
C     =SUBROUTINE WHICH CALCULATES THE PLASTIC ZONE  =
C     =SIZE FOR A GIVEN STRESS INTENSITY AND MATERIAL=
C     ================================================
C
      SUBROUTINE PZS
      DOUBLE PRECISION ACP,ADAL,ADAR,ADK,AF,AI,AKMAX,AKMAXE,AKMAXO,AKMI
     &N,AKMINE,ALPHA,AO,AR,ARPI,ARPO,B,C,CCP,CDAL,CDAR,CF,CI,CKMAX,CKMA
     &XO,CKMIN,CN,CO,CR,CRPI,CRPO,F,H,PHI,PI,QMAX,QMIN,SMAX,SMIN,RAB,RA
```

TURBUT

```
     &C,SKC,SYS,W,WM,WN,Z,BDAL,DDAL
      COMMON/TA1/A(8),JB(900),R(8),SMAX(900),SMIN(900)
      COMMON/TA2/ADAL,ADK,AF,AI,AKMAX,AKMAXO,AKMIN,ALPHA,AMF,AO,AR,ARPI
     &,ARPO,B,C,CDAL,CDK,CI,CKMAX,CKMAXO,CKMIN,CN,CO,CR,CRPI,CRPO,IA,IB
     &,IE,IP,J,JA,JE,KB,MN,MP,MR,NC,NFT,NI,NO,NP,PI,SKC,SYS,W,WM,WN,Z,A
     &DAR,CDAR,NT
C     ***PLASTIC ZONE EVALUATION IN THE DIRECTION OF AI.
      IF(MP.GE.2) GO TO 600
C     DUGDALE MODEL(MP=1)
C     ARPI IS THE RADIUS OF THE PLASTIC ZONE.
      ARPI=(PI/8.)*((AKMAX/SYS)**2)/2.
      GO TO 605
C     IRWIN MODEL(MP=2)
600   ARPI=(AKMAX/SYS)**2/ALPHA
605   IF(NFT.NE.6) GO TO 615
C     ***PLASTIC ZONE EVALUATION IN THE DIRECTION OF CI.
      IF(MP.GE.2) GO TO 610
C     DUGDALE MODEL(MP=1)
C     CRPI IS THE RADIUS OF THE PLASTIC ZONE.
      CRPI=(PI/8.)*((CKMAX/SYS)**2)/2.
      GO TO 615
C     IRWIN MODEL(MP=2)
610   CRPI=(CKMAX/SYS)**2/ALPHA
615   RETURN
      END
C
C     ================================================
C     =SUBROUTINE WHICH CALCULATES THE EFFECTIVE     =
C     =STRESS INTENSITY FACTORS FOR WILLENBORG MODEL=
C     ================================================
C
      SUBROUTINE ESIF
      DOUBLE PRECISION ACP,ADAL,ADAR,ADK,AF,AI,AKMAX,AKMAXE,AKMAXO,AKMI
     &N,AKMINE,ALPHA,AO,AR,ARPI,ARPO,B,C,CCP,CDAL,CDAR,CF,CI,CKMAX,CKMA
     &XO,CKMIN,CN,CO,CR,CRPI,CRPO,F,H,PHI,PI,QMAX,QMIN,SMAX,SMIN,RAB,RA
     &C,SKC,SYS,W,WM,WN,Z,BDAL,DDAL
      COMMON/TA1/A(8),JB(900),R(8),SMAX(900),SMIN(900)
      COMMON/TA2/ADAL,ADK,AF,AI,AKMAX,AKMAXO,AKMIN,ALPHA,AMF,AO,AR,ARPI
     &,ARPO,B,C,CDAL,CDK,CI,CKMAX,CKMAXO,CKMIN,CN,CO,CR,CRPI,CRPO,IA,IB
     &,IE,IP,J,JA,JE,KB,MN,MP,MR,NC,NFT,NI,NO,NP,PI,SKC,SYS,W,WM,WN,Z,A
     &DAR,CDAR,NT
C     EFFECTIVE STRESS INTENSITY EVALUATION FOR AI DIRECTION.
      AKMAXE=2.*AKMAX-SYS*DSQRT(ALPHA*(AO+ARPO-AI))
      AKMINE=AKMIN+AKMAX-SYS*DSQRT(ALPHA*(AO+ARPO-AI))
      AKMAX=AKMAXE
      AKMIN=AKMINE
C     AVOIDING FROM COMPRESSIVE LOADING.
      IF(AKMIN.LT.0.0) AKMIN=0.0000
      IF(AKMAX.LT.0.0) AKMAX=0.0000
C     EFFECTIVE STRESS INTENSITY RANGE IN AI DIRECTION.
      ADK=AKMAX-AKMIN
C     EFFECTIVE CYCLE RATIO IN AI DIRECTION.
      IF(AKMAX.EQ.0.) GO TO 690
      AR=AKMIN/AKMAX
      GO TO 695
690   AR=0.0000
695   IF(NFT.NE.6) GO TO 700
C     EFFECTIVE STRESS INTENSITY EVALUATION FOR CI DIRECTION.
      CKMAXE=2.*CKMAX-SYS*DSQRT(ALPHA*(CO+CRPO-CI))
      CKMINE=CKMIN+CKMAX-SYS*DSQRT(ALPHA*(CO+CRPO-CI))
      CKMAX=CKMAXE
      CKMIN=CKMINE
C     AVOIDING FROM COMPRESSIVE LOADING.
      IF(CKMIN.LT.0.) CKMIN=0.0000
      IF(CKMAX.LT.0.) CKMAX=0.0000
C     EFFECTIVE STRESS INTENSITY RANGE FOR CI DIRECTION.
      CDK=CKMAX-CKMIN
C     EFFECTIVE CYCLE RATIO FOR CI DIRECTION.
      IF(CKMAX.EQ.0.0) GO TO 697
      CR=CKMIN/CKMAX
      GO TO 700
697   CR=0.0000
700   RETURN
      END
C
C     ================================================
C     =SUBROUTINE FOR LINEAR CRACK GROWTH            =
C     ================================================
C
      SUBROUTINE GROWTH
      DOUBLE PRECISION ACP,ADAL,ADAR,ADK,AF,AI,AKMAX,AKMAXE,AKMAXO,AKMI
     &N,AKMINE,ALPHA,AO,AR,ARPI,ARPO,B,C,CCP,CDAL,CDAR,CF,CI,CKMAX,CKMA
     &XO,CKMIN,CN,CO,CR,CRPI,CRPO,F,H,PHI,PI,QMAX,QMIN,SMAX,SMIN,RAB,RA
```

```
      &C,SKC,SYS,W,WM,WN,Z,BDAL,DDAL
       COMMON/TA1/A(8),JB(900),R(8),SMAX(900),SMIN(900)
       COMMON/TA2/ADAL,ADK,AF,AI,AKMAX,AKMAXO,AKMIN,ALPHA,AMF,AO,AR,ARPI
      &,ARPO,B,C,CDAL,CDK,CI,CKMAX,CKMAXO,CKMIN,CN,CO,CR,CRPI,CRPO,IA,IB
      &,IE,IP,J,JA,JE,KB,MN,MP,MR,NC,NFT,NI,NO,NP,PI,SKC,SYS,W,WM,WN,Z,A
      &DAR,CDAR,NT
C      LINEAR CRACK GROWTH EVALUATION FOR AI DIRECTION.
       GO TO (800,805,810),MN
C      PARIS-ERDOGAN CALCULATION FORMULA(MN=1)
800    ADAL=C*(ADK**CN)
       GO TO 815
C      FORMAN'S CALCULATION FORMULA(MN=2)
805    ADAL=C*(ADK**CN)/((1.-AR)*SKC-ADK)
       GO TO 815
C      WALKER'S CALCULATION FORMULA(MN=3)
810    ADAL=C*(AKMAX**WN)*(ADK**CN)
815    IF(NFT.NE.6) GO TO 835
C      LINEAR CRACK GROWTH EVALUATION FOR CI
       GO TO (820,825,830),MN
C      PARIS-ERDOGAN CALCULATION FORMULA(MN=1)
820    CDAL=C*(CDK**CN)
       GO TO 835
C      FORMAN'S CALCULATION FORMULA(MN=2)
825    CDAL=C*(CDK**CN)/((1.-CR)*SKC-CDK)
       GO TO 835
C      WALKER'S CALCULATION FORMULA(MN=3)
830    CDAL=C*(CKMAX**WN)*(CDK**CN)
C      CRACK GROWTH RATE FOR SEMI-CRACK LENGTH OF CENTER CRACK PANEL.
835    IF(NFT.EQ.1) ADAL=ADAL/2.
C      CRACK GROWTH RATE FOR SEMI-CRACK LENGTH IN
C      THE MAJOR AXIS DIRECTION OF THE SURFACE FLAW.
       IF(NFT.EQ.6) CDAL=CDAL/2.
       RETURN
       END
C      ================================================
C      = SUBROUTINE FOR THE WHEELER RETARDATION MODEL =
C      ================================================
C
       SUBROUTINE WHEELR
       DOUBLE PRECISION ACP,ADAL,ADAR,ADK,AF,AI,AKMAX,AKMAXE,AKMAXO,AKMI
      &N,AKMINE,ALPHA,AO,AR,ARPI,ARPO,B,C,CCP,CDAL,CDAR,CF,CI,CKMAX,CKMA
      &XO,CKMIN,CN,CO,CR,CRPI,CRPO,F,H,PHI,PI,QMAX,QMIN,SMAX,SMIN,RAB,RA
      &C,SKC,SYS,W,WM,WN,Z,BDAL,DDAL
       COMMON/TA1/A(8),JB(900),R(8),SMAX(900),SMIN(900)
       COMMON/TA2/ADAL,ADK,AF,AI,AKMAX,AKMAXO,AKMIN,ALPHA,AMF,AO,AR,ARPI
      &,ARPO,B,C,CDAL,CDK,CI,CKMAX,CKMAXO,CKMIN,CN,CO,CR,CRPI,CRPO,IA,IB
      &,IE,IP,J,JA,JE,KB,MN,MP,MR,NC,NFT,NI,NO,NP,PI,SKC,SYS,W,WM,WN,Z,A
      &DAR,CDAR,NT
C      EVALUTION OF LINEAR CRACK GROWTH IN AI&CI DIRECTIONS.
       CALL GROWTH
C      EVALUATION OF RETARDED GROWTH IN THE AI DIRECTION
C
C      ACP IS THE RETARDATION FACTOR IN THE AI DIRECTION.
C      WM IS THE WHEELER RETARDATION EXPONENT.
       ACP=(ARPI/(AO+ARPO-AI))**WM
       ADAR=ACP*ADAL
       IF(NFT.NE.6) GO TO 900
C      EVALUATION OF RETARDED GROWTH IN THE CI DIRECTION.
C      CCP IS THE RETARDATION FACTOR IN THE CI DIRECTION.
C
       CCP=(CRPI/(CO+CRPO-CI))**WM
       CDAR=CCP*CDAL
900    RETURN
       END
C
C      ================================================
C      = SUBROUTINE FOR THE WILLENBORG MODEL          =
C      ================================================
C
       SUBROUTINE WLLNBG
       DOUBLE PRECISION ACP,ADAL,ADAR,ADK,AF,AI,AKMAX,AKMAXE,AKMAXO,AKMI
      &N,AKMINE,ALPHA,AO,AR,ARPI,ARPO,B,C,CCP,CDAL,CDAR,CF,CI,CKMAX,CKMA
      &XO,CKMIN,CN,CO,CR,CRPI,CRPO,F,H,PHI,PI,QMAX,QMIN,SMAX,SMIN,RAB,RA
      &C,SKC,SYS,W,WM,WN,Z,BDAL,DDAL
       COMMON/TA1/A(8),JB(900),R(8),SMAX(900),SMIN(900)
       COMMON/TA2/ADAL,ADK,AF,AI,AKMAX,AKMAXO,AKMIN,ALPHA,AMF,AO,AR,ARPI
      &,ARPO,B,C,CDAL,CDK,CI,CKMAX,CKMAXO,CKMIN,CN,CO,CR,CRPI,CRPO,IA,IB
      &,IE,IP,J,JA,JE,KB,MN,MP,MR,NC,NFT,NI,NO,NP,PI,SKC,SYS,W,WM,WN,Z,A
      &DAR,CDAR,NT
C      EVALUATION OF THE LINEAR CRACK GROWTH IN AI&CI DIRECTIONS.
       CALL GROWTH
       BDAL=ADAL
       IF(NFT.NE.6) GO TO 1000
```

TURSUT

```
      DDAL=CDAL
C     EFFECTIVE STRESS INTENSITY EVALUATION.
 1000 CALL ESIF
C     EVALUATION OF THE RETARDED GROWTH IN AI&CI DIRECTIONS.
      CALL GROWTH
      ADAR=ADAL
      ADAL=BDAL
      IF(NFT.NE.6) GO TO 1005
      CDAR=CDAL
      CDAL=DDAL
 1005 RETURN
      END
C
C     ============================================================
C     =SUBROUTINE WHICH PRINTS OUT CRACK GROWTH INFORMATION=
C     ============================================================
C
      SUBROUTINE OUTPUT
      DOUBLE PRECISION ACP,ADAL,ADAR,ADK,AF,AI,AKMAX,AKMAXE,AKMAXO,AKMI
     &N,AKMINE,ALPHA,AO,AR,ARPI,ARPO,B,C,CCP,CDAL,CDAR,CF,CI,CKMAX,CKMA
     &XO,CKMIN,CN,CO,CR,CRPI,CRPO,F,H,PHI,PI,QMAX,QMIN,SMAX,SMIN,RAB,RA
     &C,SKC,SYS,W,WM,WN,Z,BDAL,DDAL
      COMMON/TA1/A(8),JB(900),R(8),SMAX(900),SMIN(900)
      COMMON/TA2/ADAL,ADK,AF,AI,AKMAX,AKMAXO,AKMIN,ALPHA,AMF,AO,AR,ARPI
     &,ARPO,B,C,CDAL,CDK,CI,CKMAX,CKMAXO,CKMIN,CN,CO,CR,CRPI,CRPO,IA,IB
     &,IE,IP,J,JA,JE,KB,MN,MP,MR,NC,NFT,NI,NO,NP,PI,SKC,SYS,W,WM,WN,Z,A
     &DAR,CDAR,NT
C     IP IS THE OUTPUT PRINT TYPE NUMBER.
      GO TO (1100,1115,1125),IP
C     ***PRINTS OUT AT THE END OF EACH BLOCK(IP=1).
 1100 IF(IB.LT.KB) GO TO 1130
      WRITE(NO,1105) NT,IE,AI,ADAL,AKMAX,ARPI,IA,IB,AO,ADAR,ADK,ARPO
 1105 FORMAT(//,1X,3HNT=,I10,2X,3HIE=,I5,4X,3HAI=,D20.14,1X,5HADAL=,D20
     &.14,1X,6HAKMAX=,D20.14,1X,5HARPI=,D20.14,/,1X,3HIA=,I10,2X,3HIB=,
     &I5,4X,3HAO=,D20.14,1X,5HADAR=,D20.14,3X,4HADK=,D20.14,1X,5HARPO=,
     &D20.14)
      IF(NFT.NE.6) GO TO 1130
      WRITE(NO,1110) CI,CDAL,CKMAX,CRPI,CO,CDAR,CDK,CRPO
 1110 FORMAT(/,28X,3HCI=,D20.14,1X,5HCDAL=,D20.14,1X,6HCKMAX=,D20.14,1X
     &,5HCRPI=,D20.14,/,28X,3HCO=,D20.14,1X,5HCDAR=,D20.14,3X,4HCDK=,D2
     &0.14,1X,5HCRPO=,D20.14)
      GO TO 1130
 1115 IF(IA.GT.JA) GO TO 1130
      IF(IB.LT.KB) GO TO 1130
C     ***PRINTS OUT AT THE END OF EACH FLIGTH(IP=2).
      WRITE(NO,1120) NT,IE,AI,ADK,AKMAX
 1120 FORMAT(//,2X,3HNT=,I10,2X,3HIE=,I10,2X,7HFLIGTHS,2X,3HAI=,D20.14,
     &2X,4HADK=,D20.14,2X,6HAKMAX=,D20.14)
      IF(NFT.NE.6) GO TO 1130
      WRITE(NO,1110) CI,CDAL,CKMAX,CRPI,CO,CDAR,CDK,CRPO
      GO TO 1130
C     ***PRINTS OUT AT THE END OF EVERY NP CYLES(IP=3).
 1125 NC=NC+1
      I=NC/NP
      IF(J.EQ.0) J=1
      IF(I.LT.J) GO TO 1130
      J=J+1
      WRITE(NO,1105) NT,IE,AI,ADAL,AKMAX,ARPI,IA,IB,AO,ADAR,ADK,ARPO
      IF(NFT.NE.6) GO TO 1130
      WRITE(NO,1110) CI,CDAL,CKMAX,CRPI,CO,CDAR,CDK,CRPO
 1130 RETURN
      END
C
C     ================================================
C     = MAGNIFICATION FACTOR EVALUATION SUBROUTINE   =
C     ================================================
C
      SUBROUTINE MAGFAC
      DOUBLE PRECISION ACP,ADAL,ADAR,ADK,AF,AI,AKMAX,AKMAXE,AKMAXO,AKMI
     &N,AKMINE,ALPHA,AO,AR,ARPI,ARPO,B,C,CCP,CDAL,CDAR,CF,CI,CKMAX,CKMA
     &XO,CKMIN,CN,CO,CR,CRPI,CRPO,F,H,PHI,PI,QMAX,QMIN,SMAX,SMIN,RAB,RA
     &C,SKC,SYS,W,WM,WN,Z,BDAL,DDAL
      COMMON/TA1/A(8),JB(900),R(8),SMAX(900),SMIN(900)
      COMMON/TA2/ADAL,ADK,AF,AI,AKMAX,AKMAXO,AKMIN,ALPHA,AMF,AO,AR,ARPI
     &,ARPO,B,C,CDAL,CDK,CI,CKMAX,CKMAXO,CKMIN,CN,CO,CR,CRPI,CRPO,IA,IB
     &,IE,IP,J,JA,JE,KB,MN,MP,MR,NC,NFT,NI,NO,NP,PI,SKC,SYS,W,WM,WN,Z,A
     &DAR,CDAR,NT
      RAC=AI/(2.*CI)
      RAB=AI/B
      IF(RAC.GT.0.05) GO TO 1200
      AMF=A(I)*(RAB**R(I))
      GO TO 1240
 1200 IF(RAC.GT.0.10) GO TO 1205
```

```
TURBOT
      AMF2=A(2)*(RAB**R(2))
      AMF1=A(1)*(RAB**R(1))
      AMF=AMF1+((AMF2-AMF1)/0.05)*(RAC-0.00)
      GO TO 1240
1205  IF(RAC.GT.0.15) GO TO 1210
      AMF2=A(3)*(RAB**R(3))
      AMF1=A(2)*(RAB**R(2))
      AMF=AMF1+((AMF2-AMF1)/0.05)*(RAC-0.10)
      GO TO 1240
1210  IF(RAC.GT.0.20) GO TO 1215
      AMF2=A(4)*(RAB**R(4))
      AMF1=A(3)*(RAB**R(3))
      AMF=AMF1+((AMF2-AMF1)/0.05)*(RAC-0.15)
      GO TO 1240
1215  IF(RAC.GT.0.25) GO TO 1220
      AMF2=A(5)*(RAB**R(5))
      AMF1=A(4)*(RAB**R(4))
      AMF=AMF1+((AMF2-AMF1)/0.05)*(RAC-0.20)
      GO TO 1240
1220  IF(RAC.GT.0.30) GO TO 1225
      AMF2=A(6)*(RAB**R(6))
      AMF1=A(5)*(RAB**R(5))
      AMF=AMF1+((AMF2-AMF1)/0.05)*(RAC-0.25)
      GO TO 1240
1225  IF(RAC.GT.0.35) GO TO 1230
      AMF2=A(7)*(RAB**R(7))
      AMF1=A(6)*(RAB**R(6))
      AMF=AMF1+((AMF2-AMF1)/0.05)*(RAC-0.30)
      GO TO 1240
1230  IF(RAC.GT.0.40) GO TO 1235
      AMF2=A(8)*(RAB**R(8))
      AMF1=A(7)*(RAB**R(7))
      AMF=AMF1+((AMF2-AMF1)/0.05)*(RAC-0.35)
      GO TO 1240
1235  AMF=A(8)*(RAB**R(8))
1240  RETURN
      END
C
C     ============================
C     =CURVE FITTING SUBROUTINE  =
C     =USING LEAST SQUARES METHOD=
C     ============================
C
C     THIS SUBROUTINE IS USED TO EVALUATE THE MAGNIFICATION
C     FACTORS.MAGNIFICATION FACTOR CURVES, FORMULAE ARE OB-
C     TAINED IN THIS SUBROUTINE.
C
      SUBROUTINE DATFIT
      DOUBLE PRECISION ACP,ADAL,ADAR,ADK,AF,AI,AKMAX,AKMAXE,AKMAXO,AKMI
     &N,AKMINE,ALPHA,AO,AR,ARPI,ARPO,B,C,CCP,CDAL,CDAR,CF,CI,CKMAX,CKMA
     &XO,CKMIN,CN,CO,CR,CRPI,CRPO,F,H,PHI,PI,QMAX,QMIN,SMAX,SMIN,RAB,RA
     &C,SKC,SYS,W,WM,WN,Z,BDAL,ODAL
      COMMON/TA1/A(8),JB(900),R(8),SMAX(900),SMIN(900)
      COMMON/TA2/ADAL,ADK,AF,AI,AKMAX,AKMAXO,AKMIN,ALPHA,AMF,AO,AR,ARPI
     &,ARPO,B,C,CDAL,CDK,CI,CKMAX,CKMAXO,CKMIN,CN,CO,CR,CRPI,CRPO,IA,IB
     &,IE,IP,J,JA,JE,KB,MN,MP,MR,NC,NFT,NI,NO,NP,PI,SKC,SYS,W,WM,WN,Z,A
     &DAR,CDAR,NT
      DIMENSION Y1(8),Y2(8),Y3(8),Y4(8),Y5(8),Y6(8),Y7(8),Y8(8),U(8),V
     &1(8),V2(8),V3(8),V4(8),V5(8),V6(8),V7(8),V8(8),X(8),S(8)
      DATA Y1/1.005,1.026,1.060,1.130,1.220,1.335,1.495,1.650/,Y2/1.00
     &05,1.020,1.055,1.110,1.195,1.295,1.435,1.575/,Y3/1.004,1.016,1.0
     &04,1.095,1.170,1.260,1.370,1.490/,Y4/1.004,1.013,1.039,1.085,1.1
     &45,1.220,1.310,1.410/,Y5/1.003,1.010,1.030,1.060,1.120,1.180,1.2
     &50,1.335/,Y6/1.002,1.008,1.025,1.050,1.080,1.130,1.200,1.270
     &/,Y7/1.001,1.007,1.016,1.040,1.060,1.095,1.146,1.200/,Y8/1.001,
     &1.005,1.010,1.020,1.035,1.045,1.080,1.135/,X/0.1,0.2,0.3,0.4,0.5
     &,0.6,0.7,0.8/
      DATA TOTU1,TOTU2,TOTUV1,TOTUV2,TOTUV3,TOTUV4,TOTUV5,TOTUV6,TOTUV
     &7,TOTUV8,TOTV11,TOTV21,TOTV31,TOTV41,TOTV51,TOTV61,TOTV71,TOTV8
     &1/18*0.0/
      DO 131 I1=1,8
      U(I1)=LOG(X(I1))
      V1(I1)=LOG(Y1(I1))
      V2(I1)=LOG(Y2(I1))
      V3(I1)=LOG(Y3(I1))
      V4(I1)=LOG(Y4(I1))
      V5(I1)=LOG(Y5(I1))
      V6(I1)=LOG(Y6(I1))
      V7(I1)=LOG(Y7(I1))
      V8(I1)=LOG(Y8(I1))
131   CONTINUE
      DO 132 I2=1,8
      TOTU2=TOTU2+U(I2)**2
```

```
      TOTU1=TOTU1+U(I2)
      TOTV11=TOTV11+V1(I2)
      TOTV21=TOTV21+V2(I2)
      TOTV31=TOTV31+V3(I2)
      TOTV41=TOTV41+V4(I2)
      TOTV51=TOTV51+V5(I2)
      TOTV61=TOTV61+V6(I2)
      TOTV71=TOTV71+V7(I2)
      TOTV81=TOTV81+V8(I2)
      TOTUV1=TOTUV1+U(I2)*V1(I2)
      TOTUV2=TOTUV2+U(I2)*V2(I2)
      TOTUV3=TOTUV3+U(I2)*V3(I2)
      TOTUV4=TOTUV4+U(I2)*V4(I2)
      TOTUV5=TOTUV5+U(I2)*V5(I2)
      TOTUV6=TOTUV6+U(I2)*V6(I2)
      TOTUV7=TOTUV7+U(I2)*V7(I2)
      TOTUV8=TOTUV8+U(I2)*V8(I2)
  132 CONTINUE
      TOT3=TOTU1**2-8.*TOTU2
      S(1)=(TOTU1*TOTUV1-TOTU2*TOTV11)/TOT3
      S(2)=(TOTU1*TOTUV2-TOTU2*TOTV21)/TOT3
      S(3)=(TOTU1*TOTUV3-TOTU2*TOTV31)/TOT3
      S(4)=(TOTU1*TOTUV4-TOTU2*TOTV41)/TOT3
      S(5)=(TOTU1*TOTUV5-TOTU2*TOTV51)/TOT3
      S(6)=(TOTU1*TOTUV6-TOTU2*TOTV61)/TOT3
      S(7)=(TOTU1*TOTUV7-TOTU2*TOTV71)/TOT3
      S(8)=(TOTU1*TOTUV8-TOTU2*TOTV81)/TOT3
      R(1)=(TOTV11*TOTU1-8.*TOTUV1)/TOT3
      R(2)=(TOTV21*TOTU1-8.*TOTUV2)/TOT3
      R(3)=(TOTV31*TOTU1-8.*TOTUV3)/TOT3
      R(4)=(TOTV41*TOTU1-8.*TOTUV4)/TOT3
      R(5)=(TOTV51*TOTU1-8.*TOTUV5)/TOT3
      R(6)=(TOTV61*TOTU1-8.*TOTUV6)/TOT3
      R(7)=(TOTV71*TOTU1-8.*TOTUV7)/TOT3
      R(8)=(TOTV81*TOTU1-8.*TOTUV8)/TOT3
      DO 133 I3=1,8
      A(I3)=EXP(S(I3))
  133 CONTINUE
      DO 134 LL=1,8
      WRITE(NO,1305) LL,A(LL),LL,R(LL)
 1305 FORMAT(/,2X,2HA(,I1,2H)=,F10.5,9X,2HR(,I1,2H)=,F10.5)
  134 CONTINUE
      RETURN
      END
C
C     ====================================
C     =SUBROUTINE FOR THE BLOCK BY BLOCK=
C     =CRACK GROWTH INTEGRATION SCHEME   =
C     ====================================
C     OVERESTIMATES THE CYCLIC LIFE AND IS NOT USED FOR SURFACE FLAWS
      SUBROUTINE BLOCK
      DOUBLE PRECISION ADAL,ADAR,ADK,AF,AI,AKMAX,AKMAXO,AKMIN,ALPHA,AO,
     &AR,ARPI,ARPO,B,C,CDAL,CDAR,CI,CKMAX,CKMAXO,CKMIN,CN,CO,CR,CRPI,CR
     &PO,PI,SMAX,SMIN,SKC,SYS,W,WM,WN,Z
      COMMON/TA1/A(8),JB(900),R(8),SMAX(900),SMIN(900)
      COMMON/TA2/ADAL,ADK,AF,AI,AKMAX,AKMAXO,AKMIN,ALPHA,AMF,AO,AR,ARPI
     &,ARPO,B,C,CDAL,CDK,CI,CKMAX,CKMAXO,CKMIN,CN,CO,CR,CRPI,CRPO,IA,IB
     &,IE,IP,J,JA,JE,KB,MN,MP,MR,NC,NFT,NI,NO,NP,PI,SKC,SYS,W,WM,WN,Z,A
     &DAR,CDAR,NT
      IF(NFT.NE.6) GO TO 1415
      WRITE(NO,1411)
 1411 FORMAT(/,5X,'BLOCK BY BLOCK CRACK GROWTH INTEGRATION SCHEME IS NO
     &T USED FOR SURFACE FLAWS')
      GO TO 1440
 1415 DO 1400 IE=1,JE
      JH=0
      DO 1405 IA=1,JA
      JH=JH+1
      KB=JB(JH)
      CALL SIF
      CALL PZS
      IF(AO+ARPO-AI-ARPI) 1420,1420,1425
C     THE CASE OF NO RETARDATION.
 1420 CALL GROWTH
      ADAR=ADAL
      AI=AI+(KB-1)*ADAL
      CALL SIF
      CALL PZS
      AO=AI
      ARPO=ARPI
      AKMAXO=AKMAX
      NT=NT+K3
      IB=KB
```

TURSUT

TURSUT

```
      WRITE(NO,1423) NT,IE,AI,ADAL,AKMAX,ARPI,IA,IB,AO,ADAR,ADK,ARPO
1423  FORMAT(//,1X,3HNT=,I10,2X,3HIE=,I5,4X,3HAI=,D20.14,1X,5HADAL=,D20
     &.14,1X,5HAKMAX=,D20.14,1X,5HARPI=,D20.14,/,1X,3HIA=,I10,2X,3HIB=,
     &I5,4X,3HAO=,D20.14,1X,5HADAR=,D20.14,3X,4HADK=,D20.14,1X,5HARPO=,
     &D20.14)
      AI=AI+ADAL
      GO TO 1404
C     THE CASE OF RETARDED GROWTH.
1425  IF(MR.EQ.1) CALL WHEELR
      IF(MR.EQ.2) CALL WLLNBG
C     NR IS THE NUMBER OF REQUIRED CYCLES TO
C     REACH THE PLASTIC ENCLAVE OF THE OVERLOAD.
      NR=(AO+ARPO-AI-ARPI)/ADAR
      IF(NR-KB) 1430,1430,1435
C     RETARDATION ENDS WITHIN THE BLOCK.
1430  AI=AI+NR*ADAR
      CALL SIF
      CALL PZS
      AO=AI
      ARPO=ARPI
      AKMAXO=AKMAX
      NT=NT+NR
      IB=NR
      WRITE(NO,1423) NT,IE,AI,ADAL,AKMAX,ARPI,IA,IB,AO,ADAR,ADK,ARPO
C     LINEAR CRACK GROWTH UNTILL THE END OF THE BLOCK.
      CALL GROWTH
      ADAR=ADAL
      AI=AI+(KB-NR)*ADAL
      CALL SIF
      CALL PZS
      AO=AI
      ARPO=ARPI
      AKMAXO=AKMAX
      NT=NT+(KB-NR)
      IB=KB
      WRITE(NO,1423) NT,IE,AI,ADAL,AKMAX,ARPI,IA,IB,AO,ADAR,ADK,ARPO
      GO TO 1404
C     RETARDATION WILL CONTINUE AT THE NEXT BLOCK.
1435  AI=AI+KB*ADAR
      NT=NT+KB
      IB=KB
      WRITE(NO,1423) NT,IE,AI,ADAL,AKMAX,ARPI,IA,IB,AO,ADAR,ADK,ARPO
C     HAS THE CURRENT CRACK LENGTH REACHED THE CRITICAL
C     VALUE? IF YES,STOP THE EVALUATIONS.
1404  IF(AI-AF) 1405,1445,1445
1405  CONTINUE
1400  CONTINUE
      IF(AI-AF) 1443,1445,1445
1443  WRITE(NO,1444)
1444  FORMAT(2X,'CRACK HAS NOT REACHED THE CRITICAL VALUE,INCREASE JE')
C     INFORMATION AT THE LAST CYCLE.
1445  WRITE(NO,1447) NT,AI
1447  FORMAT(1X,3HNT=,I20,4X,3HAI=,D20.14)
1440  RETURN
      END
C     ==========================
C     =BLOCK DATA SUBPROGRAM   =
C     ==========================
C
C     THIS SUBPROGRAM INITIALIZES THE LABELLED
C     COMMON BLOCK VALUES.
C
      BLOCK DATA
      DOUBLE PRECISION ADAL,ADAR,ADK,AF,AI,AKMAX,AKMAXO,AKMIN,ALPHA,AO,
     &AR,ARPI,ARPO,B,C,CDAL,CDAR,CI,CKMAX,CKMAXO,CKMIN,CN,CO,CR,CRPI,CR
     &PO,PI,SMAX,SMIN,SKC,SYS,W,WM,WN,Z
      COMMON/TA1/A(8),JB(900),R(8),SMAX(900),SMIN(900)
      COMMON/TA2/ADAL,ADK,AF,AI,AKMAX,AKMAXO,AKMIN,ALPHA,AMF,AO,AR,ARPI
     &,ARPO,B,C,CDAL,CDK,CI,CKMAX,CKMAXO,CKMIN,CN,CO,CR,CRPI,CRPO,IA,IB
     &,IE,IP,J,JA,JE,KB,MN,MP,MR,NC,NFT,NI,NO,NP,PI,SKC,SYS,W,WM,WN,Z,A
     &OAR,CDAR,NT
      DATA A,JB,R,SMAX,SMIN,ADAL,ADK,AF,AI,AKMAX,AKMAXO,AKMIN,ALPHA,AO,
     &AR,ARPI,ARPO,B,C,CDAL,CDK,AMF,CI,CKMAX,CKMAXO,CKMIN,CN,CO,CR,CRPI
     &,CRPO,IA,IB,IE,IP,J,JA,JE,KB,MN,MP,MR,NC,NFT,NI,NO,NP,PI,SKC,SYS,
     &W,WM,WN,Z,ADAR,CDAR,NT/8*0.0,900*0,8*0.0,1815*0.0000,2*0.0,9*0.00
     &00,16*0.9*0.0000,1*0/
      END
```

CHANGES FOR CDC :

```
1000  PROGRAM AKYUREK(DATA,OUT,TAPE1=DATA,TAPE2=OUT)
1021  NI=1
1022  NO=2
*CHANGE  DSQRT TO SQRT & DCOS TO COS
*CHANGE  0.0 TO 0. & 0.0000 TO 0.
```

VI. SAMPLE CALCULATIONS

6.1. Introduction

Sample calculations using the program are done. The results are compared with the test results. Obviously, some discrepancy between the test results and the calculations are observed. Considering that the normal scatter in fatigue-crack-growth rates may range from a factor of two to four under identical loading conditions, these results are quite good.

6.2. Sample Calculations.

Broek (82) makes sample calculations with the stress history listed in TABLE 6.1. He uses the formula $K = \sigma\sqrt{\pi a}$ for the stress intensity factor evaluations. Obviously, this is applicable for center-cracked panels with infinite sizes, or when the crack length is very small compared to the width of the specimen. He uses Paris eq'n $da/dN = 3.10^{-10} (\Delta K)^4$ mm/cycle for linear (unretarded) crack growth evaluations. Despite the fact that the crack-growth rate corresponds to the crack length 2a for center-crack panel, some modifications are made in order to be able to compare the com-

puter results with Broek's results.

TABLE 6.1.

Stress History

Number of cyles in the spectra (occurences)	S_{max} (kg/mm^2)	S_{min} (kg/mm^2)	S_{ys} (kg/mm^2)
1	13.5	0	
9	12	0	
90	9	0	50
900	5.8	0	
2000	2.8	0	

The results for the linear crack growth are approximately the same, but Broek's linear crack growth evaluation with fixed crack size per block is a slight overestimation.

Retarded crack growth results are very different. Broek assumes that crack length and crack growth rates are constant throughout the block cycles, to save computer time and so, expenditures. But this results in over-estimation of the fatigue life. Cycle by cycle integration results are much more accurate than block by block evaluation.

Why does Broek overestimate the fatigue life? Both the Wheeler and the Willenborg models show maximum retardation at the cycle which comes just after overload cycle. Retardation decreases as the crack length increases. Broek does not take into consideration that point. He assumes constant amount of retardation as long as the plastic zone of current cycle remains in the over-

load's plastic enclave. But, Broek makes that control just at the first cycle of the loading block. Although he considers retardation, there are some cycles which don't show retardation according to plastic enclave model. Of course this results in overestimation of fatigue life.

For constant amplitude loading; Simpson's composite integration scheme, the Wheeler and the Willenborg models are expected to show same estimations. Control was done with the program AKYÜREK-1. The Wheeler and the Willenborg models estimated the same results. Simpson's integration scheme with 14 steps estimates the result with an error 3.8 per cent. Doubling the number of steps decreases the discrepancy with the cycle by cycle integration scheme to 0.42 per cent error. Step size is chosen such small that error due to integration scheme is negligible.

Porter (83) makes tests with 2024-T3 center cracked panel (CCP) test specimen. Estimation using the Program AKYÜREK-1 for the stress spectrum, he designates as P10, results in an overestimation with a factor of two. The main reason is the lack of accurate constant amplitude data for the specimen. In fact P10 is a good sample spectra for variable amplitude random sequence loading. On the other hand, since the overload ratios are so small that, changing the Wheeler exponent did not show much varience in the amount of retardation. There is another important point which should be carefully considered when using the program AKYÜREK-I;Stress or load spectra should be converted to stress or load history. But small errors in conversion may cause surprising results since the spectrum is repeated more than 2000 times for the case considered. For program P10 (83), the overestimated

cyclic life with a factor of two originates from uncertain knowledge of constant amplitude data. This was verified by program P1 (83). The program AKYÜREK-I overestimated the cyclic life with a factor of two. But, program P1 has constant K_{max} stress spectra. This should result in linear crack growth. It was proved that the program AKYÜREK-I predicted unretarded crack growth without error. That implies uncertain knowledge of constant amplitude data.

Fatigue crack growth test reports usually do not give the all required data about the test, such as yield strength, fracture toughness, specimen orientation, etc. Small variance in those data causes unexpected results. For example, because of the strain hardening process it is very difficult to obtain the yield strength of the specimen if it is not given. But, the retardation models operate according to plastic zone size which is strongly dependent upon yield strength.

On the other hand, in literature fatigue crack growth data are available for certain type of specimen and flaw, such as cracks originating from holes. It is necessary to write stress intensity factor equation for that special flaw type in order to be able to estimate cyclic life of the specimen and to compare the estimation with the test results. That can be done. But, it is not practical only to make such a comparison.

6.4. Restrictions and the Deficiencies of the Program

Of Course this program is in the stage of development, therefore it has some deficiencies and does not cover all types of loadings and flaws. In fact, these deficiencies originate from the retardation models. Weakness of the retardation models is also weakness of the program.

The Wheeler and the Willenborg models do not account for physical observations such as : (1) accelerated crack growth under certain load variations , (2) delayed retardation after a high peak load and (3) a sustained delay after a high peak load even when the crack has already fully penetrated through the plastic zone created by the high peak load.

Although compressive peak load causes accelaration of crack growth rate, the Wheeler and the Willenborg models do not account for this. Compressive stress intensities are set to zero. Johnson, W.S (84) modified the Forman's equation to consider the compressive loading :

$$\frac{C\ \Delta K^{n}}{(1-R^{eff})^{m}\ K_c-\Delta K} \qquad (6.1)$$

where $m = 1$ at $R \geq 0$ and

$m = 2$ at $R < 0$

The equation is exactly that suggested by Forman except for the m-exponent applied to the stress ratio. The exponent equals 2.0 for negative R^{eff} values.

Robin, C. and Pelloux, R.M (85) made experiments to observe the crack growth retardation in an aluminum alloy. Figure 6.1 shows that the test result of constant amplitude loading after a single overload. Figure 6.2 presents the crack growth rates calculated from the Wheeler and Willenborg models.

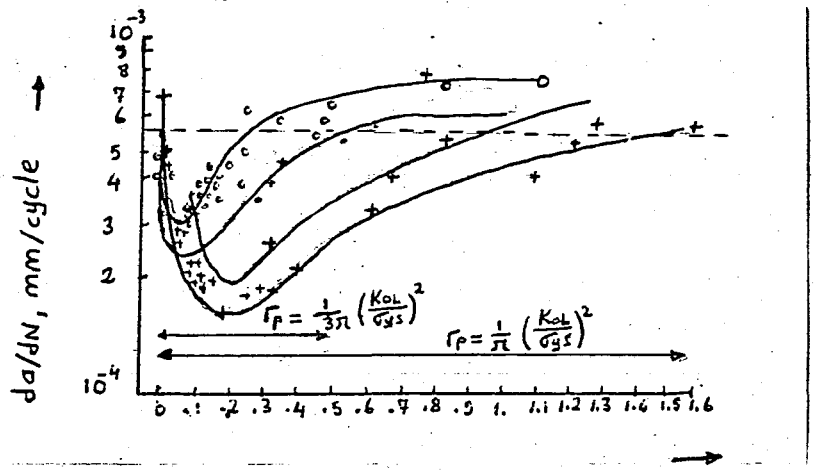

Figure 6.1. Plots of the crack growth rates against the crack length increment for K_{max} = 16.5 MPa $M^{1/2}$ (K_{OL} = 21.45 MPa $M^{1/2}$ O, center measurements : + , edge measurements.(83)

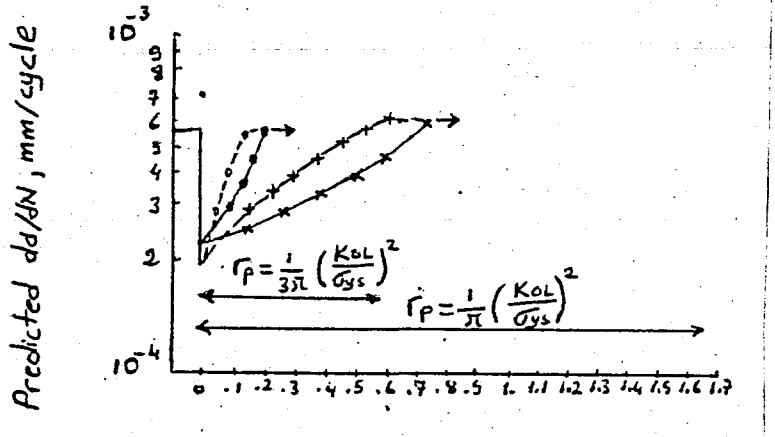

Figure 6.2. The crack growth rates calculated from the Wheeler and Willenborg models at K_{max} = 16.5 MPa $M^{1/2}$

(K_{ol} = 21.45 $MPa\ M^{1/2}$) : _ _ _, o, Willenborg model center measurements : _ _ _ _ +, Willenborg model, edge measurements ; ___ , o , Wheeler model, center measurements ; ___ , x , Wheeler model edge measurements.(85).

Considering Figures 6.6 and 6.7 together, the following observations are made.

(1) The two models do not predict the delayed retardation.

(2) The two models predict the same minimum crack growth rates for plane stress and for plane strain.

(3) The crack length increments over which retardation is predicted are smaller than the crack length increments over which retardation is observed. The two models give a better fit to plane stress data than to the plain strain data.

(4) The two models are quite similar and give a fair representation of the crack retardation phenomenon.

(5) Crack retardation is observed beyond the point at which the plastic zones are tangential. The microscopic crack growth data show that retardation exists until the crack front has reached the elastic-plastic interface of the calculated overload plastic zone.

(6) The two models are conservative, i.e. ,they predict less retardation than is observed.

The two models do not show the short period of crack acceleration after the overload that has been observed after large overload excursions. And, also they don't account for the difference in the retardation between a single peak overload and multiple peak overload

VII. CONCLUSIONS

In this thesis, a computer program evaluating the cyclic life of the specimens subjected to randomized block loading has been prepared. It uses the Wheeler and the Willenborg retardation models.

Either a cycle-by-cyle or block-by-block crack growth integration scheme is used for the fatigue life predictions.

In the program, center-crack panel, single and double edge cracked specimens, ASTM standard compact tension and bend specimens, and surface flawed plates are considered. Other type of flaws can be added to the program by making small changes.

Paris eq., Walker's formula and Forman's eq. are used for linear crack growth evaluations.

Three types of output options are available in the program. Print of the crack growth information can be obtained at the end of each loading block, spectra or every NP cycles (which is given as data).

Simpson's composite integration formula is used for constant amplitude load fatigue evaluations. This requires least computer time among the predictive models. And, also good results can be obtained.

In the computer program AKYÜREK-I; no modification has been made to the retardation models. Therefore, deficiencies of those models may result in overestimation or under estimation of the fatigue life.

For a constant stress intensity range, crack growth rate increases with increasing cycle ratio ($=K_{min}/K_{max}$). Paris and Walker's crack growth equations don't consider that phenomenon, but only Forman's does. The crucial point of the random load fatigue life estimations is to predict the cyclic life from constant amplitude data. If the constant amplitude data are obtained at different cycle ratios and the program AKYÜREK-I is modified to take into account the different cycle ratios, more precise and better predictions can be made.

The most common fatigue flaw type is the surface flaw. Therefore, the main study has been devoted to surface flaws. Detailed information about that flaw type is given for the researchers desiring to study upon that subject.

Block by block crack growth integration scheme overestimates cyclic life of specimens. Since the predictions are sensitive to the Wheeler shaping (retardation) exponent especially in block-by-block integration scheme, better correlations can be done changing the shaping exponent.

A cycle by cycle crack growth integration scheme is favorable but it requires much computer time. To save computer time, block integration scheme can be chosen. A Range-Kutta integration routine should be used to determine the incremental crack growth for each series of discrete load levels. Thus, overestimation in cyclic life predictions can be avoided and the computer time and so, money can be saved. The program AKYÜREK-I can be modified to use a Range-Kutta integration routine, but that will require a tedious study.

Among the retardation models, only the crack closure model has some sort of physical basis. It can be put in the program AKYÜREK-I, as an alternative to the Wheeler and the Willenborg retardation models.

The Root-Mean-Square (RMS) retardation model is the simplest one and requires least computer time. It can be used in the program AKYÜREK-I, by using a new subroutine (e.g., SUBROUTINE RMS) and modifying the SUBROUTINE SIMPSN.

APPENDIX-A

THE METHOD OF LEAST SQUARES (MLS)

Let $q_1, \ldots\ldots, q_n$ be n direct measured values of a magnitude, and let Q represent the sum of squares of their deviations from a number q :

$$Q = \sum_{i=1}^{n} (q_i - q^2) \qquad (A.1)$$

The value of q making Q minimum, is the best value of the measurement, since Q involves squares of devlations which are non-negative. This best value of $\bar{q}$ of $q_1, \ldots\ldots, q_n$ is shown to be the arithmetic of the measured values :

$$\frac{dQ}{dq} = -2 \sum_{i=1}^{n} (q_i - q) = \sum_{i=1}^{n} q_i - nq = 0 \qquad (A.2)$$

resulting.

$$\bar{q} = \frac{q_1 + q_2 + \ldots\ldots + q_n}{n} \qquad (A.3)$$

$\frac{d^2Q}{dq^2} = 2n > 0$. Q is minimum for $\bar{q}$. This process of finding $\bar{q}$ from eq(A.1) is known as the method of least squares(MLS).

Finding the best fitting involves the following steps :

(i) From the distribution guess the type of the function as linear, quadratic, exponential,....

(ii) Write the general form of the function,

(iii) By the use of the MLS, determine the unknown parameters.

The distribution is as given in figure A.1. For instance, for the aspect ratio ; a/2C = 0.05

(i) We observe that the points $P_i(x_i, y_i)$ lie nearly on the function of the form $y = AX^r$.

(ii) Taking the common logarithm of both sides of $y = AX^r$, we get the linear equation.

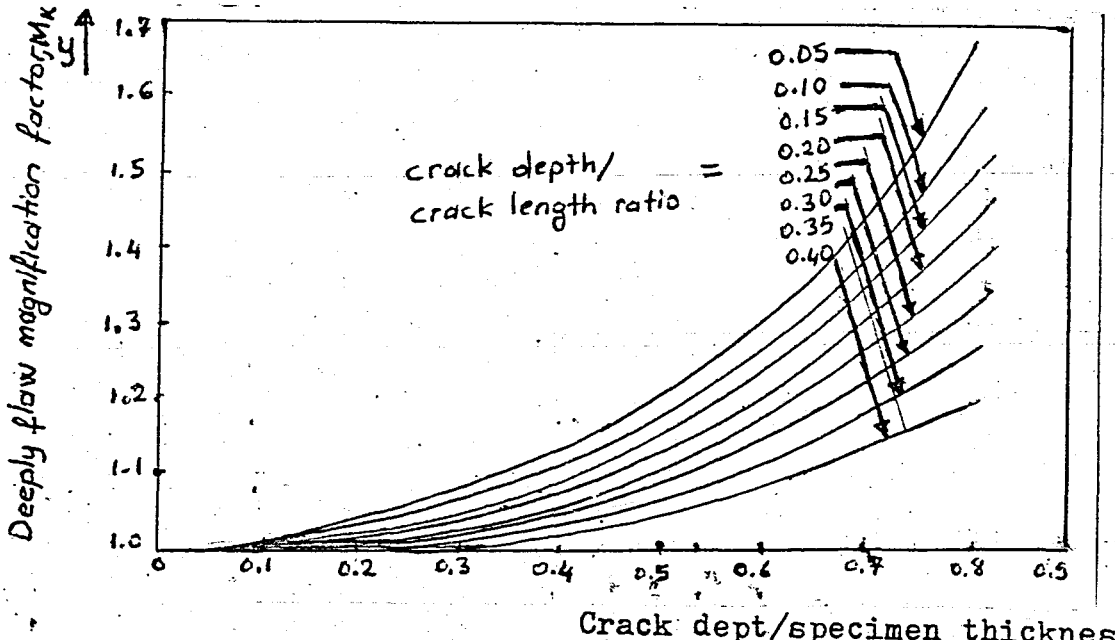

Figure A.1. Deep flaw magnification factor curves

$\log y = \log A + r \log x$ in logy and logx. Then setting $u = \log x$, $v = \log y$, $s = \log A$ we have :

$$v = s + ru \tag{A.4}$$

(iii) By the MLS, we minimize

$$Q(s, r) = \sum_{i=1}^{n} (v_i - ru_i - s)^2 \tag{A.5}$$

in which s,r are the parameters.

$$\frac{\partial Q}{\partial r} = -2\sum_{i=1}^{n}(v_i - ru_i - s)u_i = 0$$

$$\frac{\partial Q}{\partial s} = -2\sum_{i=1}^{n}(v_i - ru_i - s) = 0 \tag{A.6}$$

which yields :

$$(\Sigma u_i)r + ns = \Sigma V_i$$

$$(\Sigma u_i^2)r + (\Sigma u_i)s = \Sigma u_i V_i \tag{A.7}$$

Solutions to these equations :

$$r = \begin{vmatrix} \Sigma V_i & n \\ \Sigma u_i v_i & \Sigma u_i \end{vmatrix} / \Delta, \quad s = \begin{vmatrix} \Sigma u_i & \Sigma V_i \\ \Sigma u_i^2 & \Sigma u_i v_i \end{vmatrix} / \Delta$$

where $$\Delta = \begin{vmatrix} \Sigma u_i & n \\ \Sigma u_i^2 & \Sigma u_i \end{vmatrix}$$

For the case considered, substitute $y = M_k$, $x = a/B$

then $$M_k = A\,(a/B)^r \qquad (A.8)$$

As can be seen in figure A.1 , there are eight curves. For the aspect ratios (a/2c) remaining between the curves, a linear interpolation is used (see figure A.2).

$$M_k = M_{k1} + \frac{(M_{k2} - M_{k1})}{0.05}\left\{\left(\frac{a}{2c}\right) - 0.05\right\} \qquad (A.9)$$

where M_k is the value to be evaluated , corresponding to a/2c . M_{k1} and M_{k2} are the values corresponding to a/2c = 0.05 and a/2c = 0.10 , respectively for the sample case.

Magnification factor, M_k, depends upon the angle ϕ. Since it is necessary to evaluate the stress intensity factors in the major axis and minor axis direction , the magnification factors in these directions are required. Smith (86) showed that the magnification factor in the direction of major axis of the elliptical flaw could be taken as 1. But this is an approximation (87).

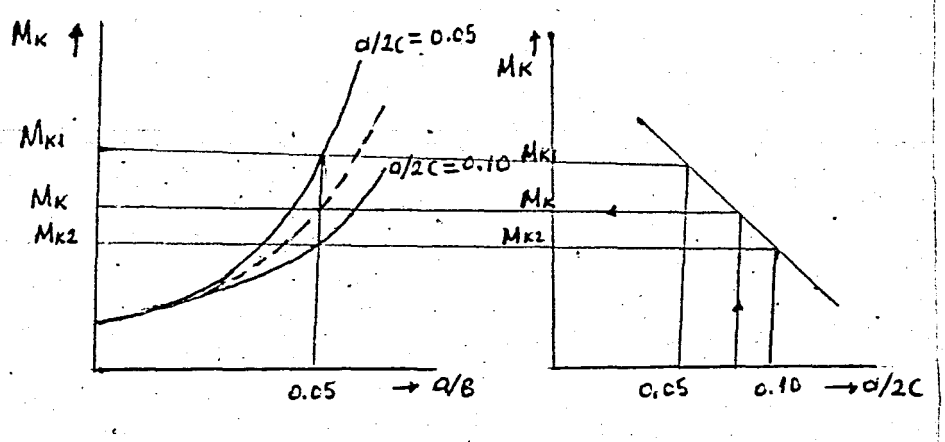

Figure A.2. Linear interpolation for the aspect ratios remaining between the curves.

APPENDIX - B

SIMPSON'S COMPOSITE INTEGRATION FORMULA

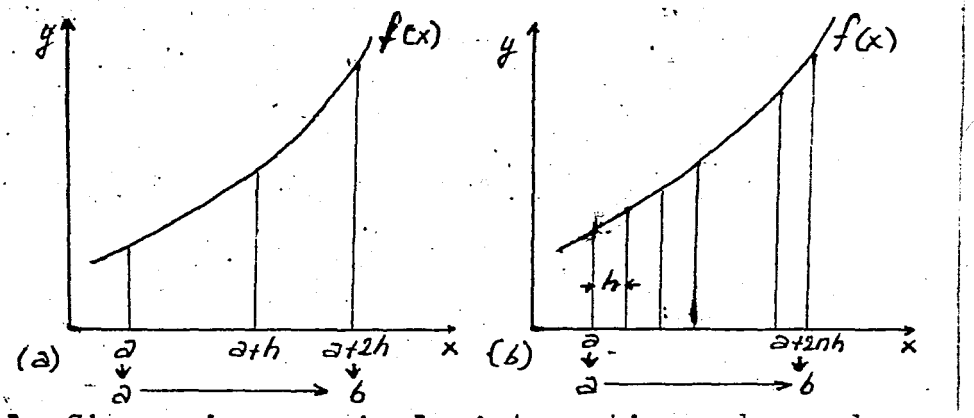

Figure B.1. Simpson's a. simple integration scheme b. composite integration scheme.

Simple formula :
$$\int_a^{b = a+2h} f(x)dx = \frac{h}{3}[\, f(a) + 4f(a+h) + f(a+2h)] \quad \ldots\ldots (B.1)$$

Composite formula :

$$\int_a^{a+2hn} f(x)dx = \frac{h}{3}[\, f(a) + 4f(a+h) + 2f(a+2h) + 4f(a+3h) + \ldots\ldots$$

$$+ f(a+2nh)] \qquad (B.2)$$

Considering the exact matching method (figure B.2)

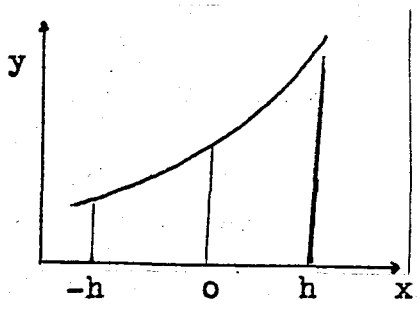

Figure B.2. Figure for the exact matching.

$$\int_{-h}^{h} f(x)dx = W_1\, f(-h) + W_2 f(o) + W_3 f(h) \qquad (B.3)$$

for $f(x) \equiv 1$

$$\int_{-h}^{h} 1.dx = W_1.1 + W_2.1 + W_3.1 \Rightarrow W_1 + W_2 + W_3 = 2h \qquad (B.4)$$

for $f(x) \equiv x$

$$\int_{-h}^{h} xdx = W_1(-h) + W_2.0 + W_3(h) \Rightarrow -W_1 h + W_3 h = 0 \Rightarrow W_1 = W_3 \qquad (B.5)$$

for $f(x) \equiv x^2$

$$\int_{-h}^{h} x^2 dx = W_1(-h)^2 + W_2.0^2 + W_3(h)^2 \Rightarrow W_1 h^2 + W_3 h^2 = \frac{2h^3}{3} \qquad (B.6)$$

from eqs (B.4), (B.5) and (B.6)

$$W_1 = W_3 = \frac{h}{3} \quad \text{and} \quad W_2 = \frac{4h}{3}$$

Substituting these values into eq(B.3) yields :

$$\int_{-h}^{h} f(x)dx = \frac{h}{3}\,(f(-h) + 4f(0) + f(h)) \qquad \text{(B.7)}$$

or

$$\int_{a}^{b=\,d+2h} f(x)dx = \frac{h}{3}\,(f(a) - 4f(a+h) - f(a+2h))$$

for $f(x) \equiv x^3$

$$\int_{-h}^{h} x^3 dx = W_1(-h)^3 + 0 + W_3(h)^3 \Rightarrow W_1 = W_3$$

Simpson's formula is also exact for cubics.

Truncation error (E):

$$E = -\frac{h^5}{90} f^{(iv)}(\theta) \quad \text{- Simple formula} \qquad \text{(B.8)}$$

$$E = -\frac{(b-a)}{90} h^4 f^{(iv)}(\theta) \quad \text{- composite formula} \qquad \text{(B.9)}$$

APPENDIX - C

PROBABILITY - DENSITY DISTRIBUTION

Many engineering structures such as bridges, ships, and others are subjected to variable - amplitude random - sequence load fluctuations. The probability of occurence of the same sequence of stress fluctuations for a given detail in such structures obtained during a given time interval is very small. Consequently, the magnitude of stress fluctuations must be characterized to study the fatigue behavio of components subjected to variable - amplitude random - sequence stress fluctuations. The magnitude of the stress fluctuations should be characterized and described by analytic functions. The use of

probability - density curves to characterize variable - amplitude cyclic - stress fluctuations appear to be very useful (69) .

Stress history, or stress spectrum, for a particular location in a structure subjected to variable - amplitude stress fluctuation can be defined in terms of the frequency of occurence of maximum (peak) stresses. Usually, frequency - of - occurence data are presented as a histogram, or bar graph (figure C.1), in which the height of the bar represents the percentage of recorded maximum stresses that fall with in a certain stress interval represented by the width of the bar. For example, 20.2 % of the maximum stress in

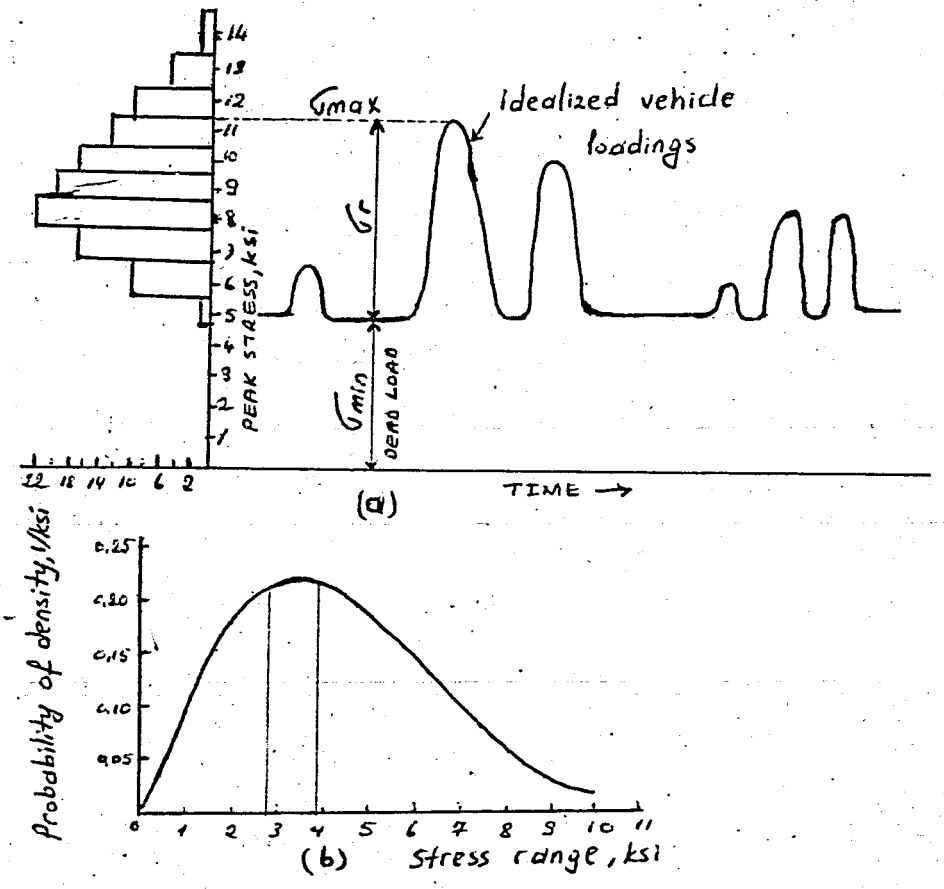

Figure.C.1. Frequency-of-occurence data

figure. C.1.(a) fall within the interval between 7.5 and 8.5 ksi. The frequency of occurence of stress ranges can be represented by similar plots with the vertical scale changed according to the relationship between σ_{max}, σ_{min}, and stress range, σ_r or $\Delta\sigma$. Since stress range is the most important stress parameter controlling the fatigue life of structural components, stress range is used to define the major stress cycles in the following discussion.

The frequency-of-occurence data can be presented in a more general form by dividing the percentage of occurence for each interval, i.e., the height of each bar, in figure C.1.(a) by the interval width to obtain a probability-density curve such as shown in figure C.1(b) . Thus, data from sources that use different stress-range intervals can be compared by using the probability-density curve. The area under the curve between any two values of $\Delta\sigma$ represents the percentage of occurence within that interval.

A single nondimensional mathematical expression can be used to define the probability-density curves for different sets of data. For example, Klippstein and Schilling (88) showed that the following nondimensional mathematical expression,which defines a family of skewed probability-density curves referred to as Rayleigh curves or distribution functions, can be used to accurately fit a probability-density curve to each available set of field data for bridges :

$$p' = 1.011\, x' e^{-\frac{1}{2}(x')^2} \qquad (C.1)$$

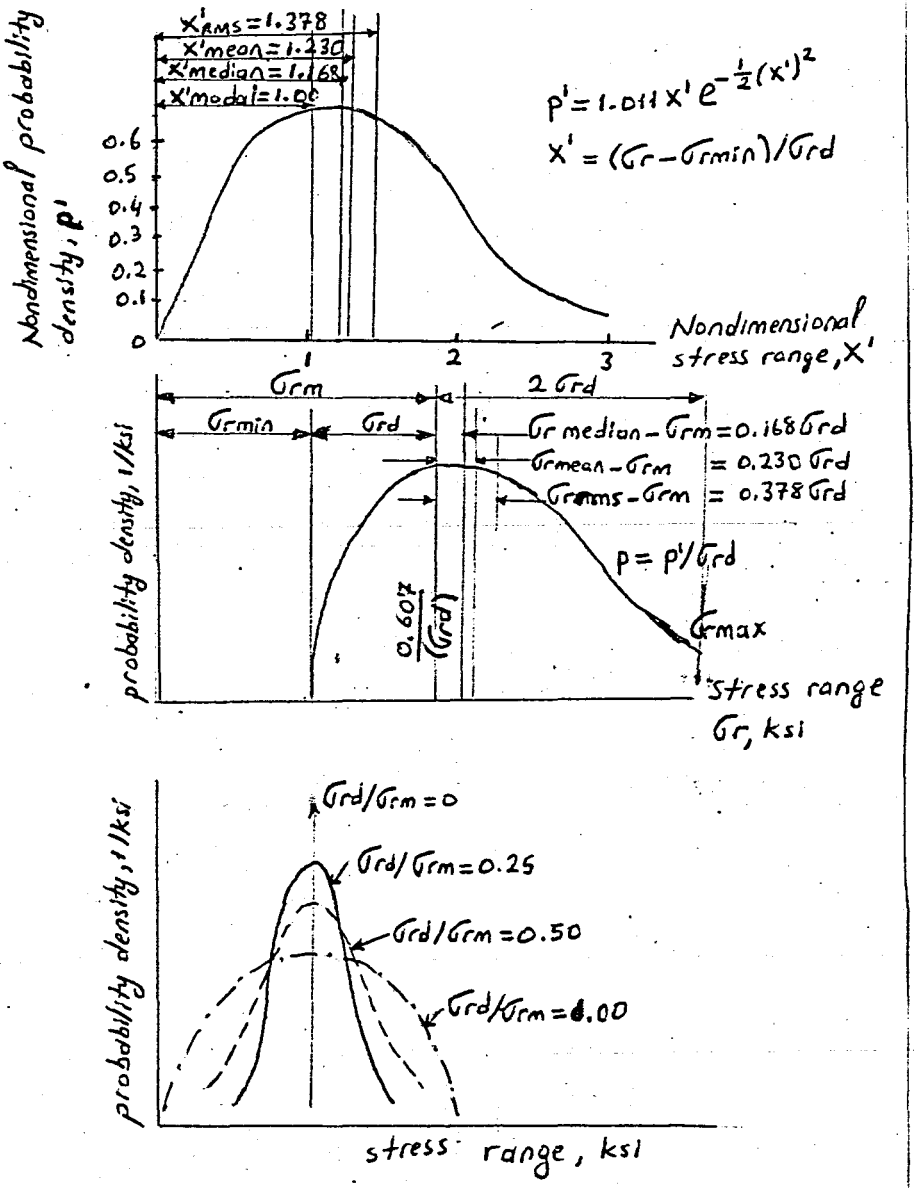

Figure C.2. Characteristics of Rayleigh probability curves

where $x' = (\sigma_r - \sigma_{rmin})/\sigma_{rd}$, $\sigma_r (= \Delta\sigma)$ is the stress range and σ_{rmin} (i.e. $\Delta\sigma_{min}$)

and σ_{rd} (i.e. $\Delta\sigma_d$) are constant parameters that define any particular probability-density curve from the family of curves represented by eq (C.1). Eq (C.1) is plotted in figure C.2(a) . As illustrated in figure C.2(b), a particular curve from the family is defined by two parameters : (1) the modal stress range , σ_{rm} , which corresponds to the peak of the curve ; and (2) the parameter σ_{rd}, which is a measure of the width of the curve or the dispersion of the data. The curve could be shifted sideways by changing σ_{rm}, and the width of the curve could be modified by changing σ_{rd}. Mathematical expressions for the modal, median, mean, and root-mean-square values of the spectrum are given in figure C.2. The root-mean-square (rms) value is defined as the square root of the mean of the squares of the individual values of x^2 or σ_r (70).

APPENDIX-D

AKYUREK - I USERS MANUAL

D.1. Introduction

The computer program AKYUREK - I predicts the fatigue life of the specimens subjected to randomized block loading . It uses the Wheeler and the Willenborg retardation models. Center cracked, edge cracked, surface flawed specimens, standard compact tension and bend specimens are considered . Paris - Erdoğan, Forman and

Walker's linear crack growth calculation formulae are used. Either cycle - by - cycle or block - by - block crack growth integration scheme can be chosen.

AKYÜREK - I is in its developmental stage in terms of new options, more sophisticated models, etc. The program, however , has been designed to be modular in organization which permits additions and changes to be made more easily.

D.2. The Program Outline

The program consists of fifteen routines and a supervisory routine. The outline and simplified flowchart is given in Chapter V (pp 60 - 63)

D.3. Data Preparation

CARD SET 1 : Selection of the retardation model (I 10) - One card.

Columns : (1 - 10) MR Model of retardation.
(= 1 Wheeler model)
(= 2 Willenborg model)
(= 3 Const. amplitude Loading-Simps integration scheme)

Columns : (11 - 20) MI Model of integration scheme .
(=1 Cycle by cycle crak growth integration scheme)
(=2 Block by block integration scheme

NOTE : if MR=3 then MI=2

CARD SET 2 : Title card (20 A 4) - one card.

Columns : (1 - 72) TITLE Title of the problem. It is limited to 72 alphanumeric characters.

CARD SET 3 : Bounds on the problem (2D20. 14) - one card.

Columns : (1 - 20) AI Intial crack length.
(21-40) AF Final (or critical) crack length .
(If the crack length growes to final crack length, the program stops.)

CARD SET 4 : Maximum and Minimum stresses (2D20.14) - one card.
If MR is not equal to 3, Omit this card.

Columns : (1 - 20) SMAX Maximum stress.
(21 - 40) SMIN Minimum stress.
If NFT = 4 or 5 SMAX and SMIN are loads (see card set 6)

CARD SET 5 : Selection of the Linear crack growth eq'n (I10) - one card.

Columns : (1 - 10) MN Linear crack growth equation number
(=1 Paris - Erdoğan equation)
(=2 Forman's equation)
(=3 Walker's calçulation formula)

CARD SET 6 : Linear crack growth data and material properties (3D20.14) - two cards.

Card 1 Col's : (1 - 20) C Material const. in Paris eq.,or Forman's eq. or Walker's formula. Such as in $C(\Delta K)^{CN}$.
(21 - 40) CN Material const. in Paris eq., or Forman's eq. or Walker's formula . Such as in $C(\Delta K)^{CN}$.
(41 - 60) SKC Fracture toughness of the material.

card 2 col's : (1 - 20) SYS Yield strength of the specimen .
(21 - 40) W Width of the specimen.
(41 - 60) B Thickness of the specimen .
(61 - 70) NFT Number of flaw type.
(=1 Center - cracked panel)
(=2 Single edge notched specimen)
(=3 Double edge cracked specimen)
(=4 Standard bend specimen)
(=5 compact tension specimen)

(= 6 Surface flawed specimen)

CARD SET 7 : Material property (D20.14) - one card

If MN is not equal to 3 omit this card

(see card set 5)

Columns : (1 - 20) WN Walker number. (Exponent in the Walker's formula. $da/dN = CK_{max}^{WN} \Delta K^{CN}$)

CARD SET 8 : Flaw size (D20.14) - one card.

If NFT is not equal to 6 omit this card.

(see card set 6)

Columns : (1 - 20) CI half the crack length of the surface flaw in the major axis direction.

CARD SET 9 : Specimen size (D20.14) - one card.

If NFT is not equal to 4 omit this card .

(see card set 6)

Columns : (1 - 20) Z Distance between the supports in the bend specimen.

NOTE : If MR is equal to 3 omit all cards below I

CARD SET 10 : Control data (D20.14, 3I10) - one card .

Columns : (1 - 20) ALPHA the constant required to evaluate the plastic zone size .

(=3. plane strain case)

(=1. plane stress case)

(21 - 30) MP Number of the plastic zone formulation.

(= 1 Dugdale model)

(= 2 Irwin model)

(31 - 40) JE Total number of flights, spectra or repeating groups of loading blocks.

(41 - 50) JA Total number of blocks.

CARD SET 11 : Control of the retardation (D20.14) - one card.
If MR is not equal to 1 omit this card.

Columns : (1 - 20) WM Wheeler exponent (retardation exponent) WM is chosen such that, similar results to the test data could be obtained .

CARD SET 12 : Stress or Load history input -(I10,2D20.14)- JA cards.

Columns : (1 -10) JB(IA) Total number of cycles in the IA'th block

(11-30) SMAX(IA) Max. stress in the IA'th block
If NFT=4 or 5 → Max. load

(31-50) SMIN(IA) Min. stress in the IA'th block
If NFT=4 or 5 → min. load

NOTE : If number of cycles in a flight or total number of blocks exceeds 900, Dimensions of JB, SMAX and SMIN in the COMMON blocks should be increased. Without any change in dimensions, JA can at most be 900.

CARD SET 13 : Output control data (I10) - one card.

columns : (1 - 10) IP Printing type
(= 1 prints out information at the end of each block)
(= 2 prints out information at the end of each flight, spectra or group blocks)
(= 3 prints out information at the end of every NP cycles. See card set 14).

NOTE : If block by block integration scheme is used, output is in a fixed form. But, You Should write output control card only to satisfy data correspondance.

CARD SET 14 : Print control (I10) - one card.
If IP is not equal to 3 omit this card.

columns : (1 - 10) NP Information is printed at the end of every NP cycles.

NOTE : Read the note written above.

D.4. Dictionary

A Magnification factor curve fitting parameter.

AMF = A * (RAB) ** R , RAB is crack length-thickness ratio in surface flaw

ACP Retardation factor in the AI direction

ADAL Linear crack growth rate in the AI direction

ADAR Retarded crack growth rate in the AI direction.

ADK Stress intensity range in AI direction

AF Final or critical crack length in AI direction

AI Initial or current crack length.

AKMAX Maximum stress intensity factor in AI direction.

AKMAXE Maximum effective stress intensity factor in AI direction.

AKMAXO Maximum stress intensity factor due to overload.

AKMIN Minimum stress intensity factor in AI direction.

AKMINE Minimum effective stress intensity factor in AI direction.

ALPHA A constant. =1 for plane stress and =3. for plane strain.

AMF Magnification factor in AI direction in surface flaw.

AO Crack length at the overload applied.

AR Cycle ratio in AI direction AR = AKMIN/AKMAX

ARPI Current plastic zone size in AI direction.

ARPO Plastic zone size due to overload in AI direction.

B Thickness of the specimen.

C Material constant used in linear crack growth equations.

CCP Wheeler retardation factor in CI direction.

CDAL Linear crack growth rate in CI direction.

CDAR	Retarded crack growth rate in CI direction.
CDK	Stress intensity range in CI direction.
CF	Stress intensity correction factor polynomial.
CI	Current or initial crack length in the major axis direction in surface flaw.
CKMAX	Max stress intensity factor in CI direction.
CKMAXE	Max. effective stress intrensity factor in CI direction.
CKMAXO	Max. stress intensity due to overload in CI direction.
CKMIN	Minimum stress intensity factor in CI direction.
CKMINE	Minimum effective stress intensity factor in CI direction.
CN	Material constant used as exponential in linear crack growth equations.
CO	Crack length at overload, in CI direction.
CR	Cycle ratio in CI direction . CR = CKMIN/CKMAX.
CRPI	Current plastic zone size in CI direction.
CRPO	Plastic zone size due to overload, in CI direction.
F	Function used in Simpson's formulation's.
H	Step size used in Simpson's formula.
IA	Current block number. IA = 1, JA.
IB	Current cycle number in the block. IB = 1, JB(JH).
IE	Current flight or spectra or group of blocks number. IE = 1, JE .
IP	Print control data . IP = 1 prints out at the end of each block , IP = 2 each flight , IP = 3 every . NP cycles.
JA	Total number of blocks in a group or total number of cycles in a flight.

JE Total number of flights, spectra or repeating groups of blocks.

JB(JH) Total number of cycles in JH - th block

MI Model of integration scheme.

MI = 1 cycle - by - cycle int.

= 2 block - by - block int.

MN Linear crack growth equation number .

MN = 1 Paris - Erdoğan equation.

= 2 Forman's equatión.

= 3 Walker's calculation formula.

MP Plastic zone size evaluation model number.

MP = 1 Dugdale model, = 2 Irwin model.

MR Retardation model number . MR = 1 Wheeler model

= 2 Willenborg model

= 3 Simpson's formula.

NFT Number of flaw type.

NFT = 1 center crack panel.

= 2 Single edge crack

= 3 Double edge crack

= 4 Bend specimen

= 5 Compact tension specimen

= 6 Surface flaw.

NI Data set number for input. NI = 5

NO Data set number for output. NO = 6

NP Print is made at the end of every NP cycles.

NT Total number of cycles.

PHI	Elliptic integral of the second Kind.
PI	PI = 3.1415927
QMAX	Flaw shape parameter due to maximum stress.
QMIN	Flaw shape parameter due to minimum stress .
R	Constant used as exponent in magnification factor evalution in surface flaw.
RAB	Crack length - thickness ratio. RAB = AI/B.
RAC	RAC = AI/2 * CI.
SKC	Fracture toughness of the specimen.
SMAX	Maximum stress.
SMIN	Minimum stress.
SYS	Yield strength of the specimen.
W	Width of the specimen.
WM	Wheeler retardation exponent.
WN	Walker's number used as exponent in Walker's calculation formula.
Z	Distance between the supports in bend specimen.

D.5 Sample data preparations

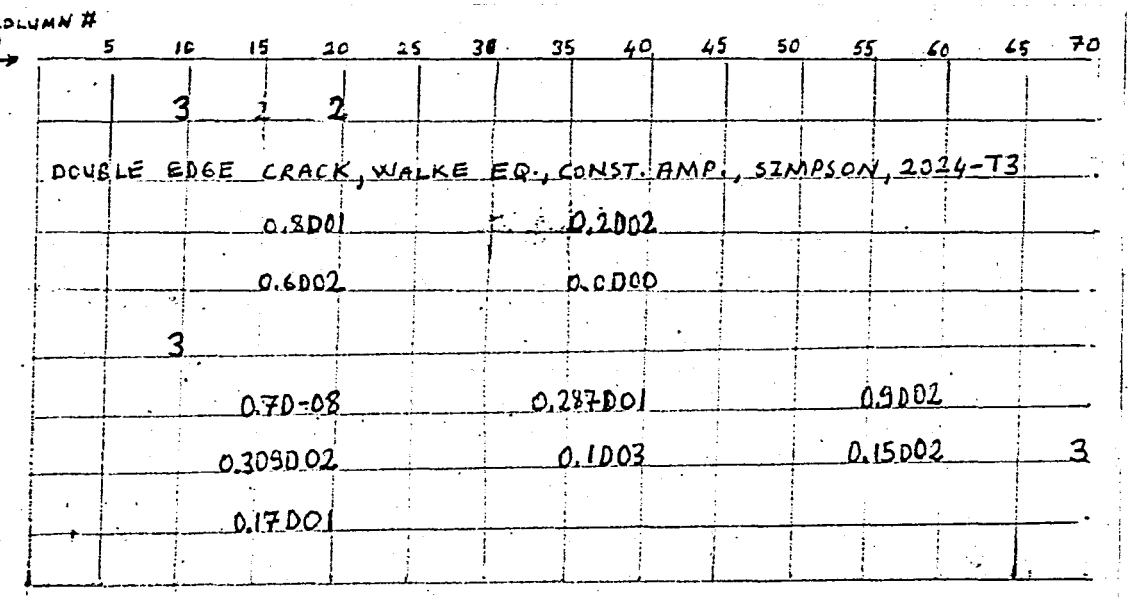

COLUMN #

5 10 15 20 25 30 35 40 45 50 55 60 65 70

1 1

CTS, PLANE STRAIN, IRWIN, WHEELER, CYCLE-BY-CYCLE, PARIS EQ, 2024-T3, KSI-I

0.5D02 0.7002

1

0.7D-08 0.287D01 0.9D02

0.309D02 0.1D03 0.15D02 5

0.3D01 2 15 5

0.24D01

5000 0.1D04 0.5D02

10000 0.75D03 0.5D02

8000 0.57D03 0.5D02

7000 0.55D03 0.5D02

39000 0.35D03 0.5D02

3

100

2 1

SURFACE FLAW, FORMAN, WILLENBORG, CYCLE-BY-CYCLE, DUGDALE, 7075-T6, KG-F

0.5D01 0.8D01

2

0.201D-08 0.27D01 0.9D02

0.354D02 0.5D02 0.2D02 6

0.15D02

0.3D01 1 2 4

2000 0.5D02 0.1D02

8000 0.6D02 0.1D02

1 0.8D02 0.1D02

60000 0.5D02 0.1D02

1

D.6. Restrictions and Limitations.

Certain restrictions have been imposed upon the analysis.

a. Compressive loads

The theory behind the crack growth rate laws and the retardation models was essentially developed for tension - tension loading . Consequently all compressive loads in the spectrum are trancated to zero.

b. Surface flaws

Surface flaws are grown under the assumption of constant shape. The current AKYÜREK - I surface flaw formulation and the magnifica - tion factor are only valid for $a/2C \leq 0.5$.

c. Unit system.

There is no restriction for unit system. But the data used in the crack growth evaluations should be consisted in. Output is set to the units of data . For example , if a , is in inches, the output of (da/dN) lin, (da/dN) ret. ai, ao are all in inches.

d. Block by block crack growth integration scheme.

This option is available only to have approximate information

about fatigue behaviour of the specimens subjected to randomized block loading . Since linear or retarded crack growth rate is assumed to be constant within the block , block by block integration scheme overestimates the cyclic life . The smaller the block size, the better the results it estimates . This integration scheme is not used for surface flaws.

APPENDIX - E

SPECIMEN ORIENTATION NOTATION.

Some of the test specimens are machined from large plates. The specimens from the same plate show different crack propagation rates under identical conditons, if their orientations are different. The orientation of a specimen is expressed with two letters (figure E.1) The first letter is the direction of the normal of crack plane. The second letter stands for the crack propagation direction.

L. Longitudinal

T. Transverse (long)

S. Short transverse

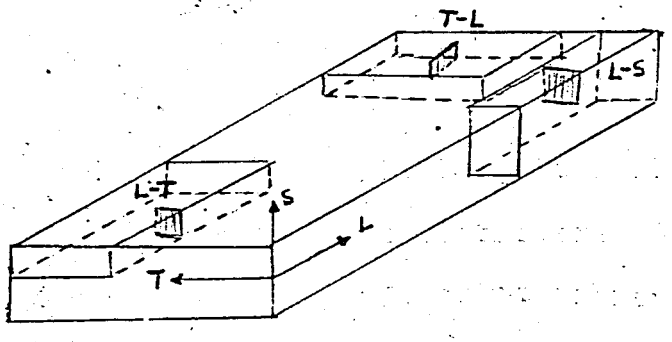

Figure E.1. Specimen orientation notation for plate materials.

BIBLIOGRAPHY

(1) Broek, D.,"Elementary Engineering Fracture Mechanics", (1974), pp.229 - 234

(2) Paris, P.C.,"The growth of fatigue cracks, due to variations in load," Ph.D.Thesis, Lehigh University (1962).

(3) Paris, P.C., Gomez , M.P. and Anderson, W.E., " A rational analytic theory of fatigue", The Trend in Engineering, 13 (1961) pp. 9 - 14.

(4) Broek, D., " The effect of intermetallic particles on fatigue crack propagation in aluminum alloys", Fracture (1969), pp.754-764, Chapman and Hall (1969).

(5) Wilhem, D.P., " Investigation of cyclic crack growth tran - sitional behavior" , ASTM STP 415, (1967) pp.363 - 383.

(6) Hudson, C.M., "Fatigue crack propagation in several titanium and stainless steel alloys and one super alloy" , NASA TN - D - 2331 (1964).

(7) Paris , P.C., Bucci ,R.J., Wessel , E.T., Clark, W.G. and Mager , T.R., "Extensive study of low fatigue crack growth ra - tes in A 533 and A 508 steels", ASTM STP 513, (1972) pp.141.176.

(8) MC Clintock, F.A., "Discussion", ASTM STP 415 , (1967) pp. 170 - 174.

(9) Hahn, G.T., Sarrat ,H. and Rosenfield, A.R.,"The nature of the fatigue crack plastic zone". Air Force Conf. on Fatigue and Fracture (1969), AFFDL TR - 70 - 144 (1970) pp.425 - 450.

(10) Schijve , J.,"Analysis of the fatigue phenomenon in aluminum alloys", Nat. Aerospace Inst. Amsterdam TR - M - 2122 (1964).

(11) Pelloux, R.M.N.,"Mechanism of formation of ductile striations", ASM Trans.62, (1969) pp.281 - 285.

(12) Bowles,C.Q. and Broek ,D.,"On the formation of fatigue Striations" Int.J.Fract. Mech ., 8 (1972) pp. 75 - 85.

(13) Bates, R.C. and Clark, W.G., "Fractography and fracture mechanics" ASM Trans. 62, (1969) pp. 380 - 388.

(14) Pelloux, R.M.N."Review of theories and laws of fatigue crack propagation", Air Force Conf. on Fatigue and fracture (1969). AFFDL - TR - 70 - 144 (1970) pp. 409 - 416.

(15) Broek,D. and Schijve,J.," The Influence of the mean stress on the propagation of fatigue cracks in aluminium alloy sheets",

Nat.Aerospace Inst. Amsterdam TR - M - 2111 (1963).

(16) Erdoğan, F.,"Crack propagation theories", NASA - CR -901 (1967).

(17) Walker,E.K., "Effects of environments and complex load history on fatigue life", ASTM STP 462, (1970) pp. 1 - 14.

(18) Walker,E.K.,"An effective strain Concept for crack propagation and fatigue with specific application to biaxial stress fatigue", AFFDL - TR - 70 - 144 (1970) pp.225 - 233.

(19) Forman,R.G., Kearney,V.E. and Engle , R.M., " Numerical analysis of crack propagation in a cyclic - loaded structure", ASME trans. J.Basic Eng. 89D , (1967) p.459.

(20) Schijve,J., NLR data.

(21) Elber,W.," The significance of fatigue crack closure", ASTM STP 486, (1971) pp. 230 - 242.

(22) Broek,D.,"Elementary engineering fracture Mechanics". 1974 pp.73 - 77.

(23) Westergard,H.M.,"Bearing pressures and cracks", J.Appl.Mech., 61 (1939) pp.A 49 - 53.

(24) Irwin,G.R.," The crack extension force for a part through crack in a plate", Trans. ASME,J.Appl.Mech., (1962) pp. 651 - 654.

(25) Koiter,W.T., " An infinite row of collinear cracks in an infinite elastic sheet", In genieur Archiv , 28 (1959) pp.168 - 172.

(26) Isida,M.,"On the tension of a strip with a central elliptical hole", Trans.Jap.Soc.Mech.Eng., 21 (1955)

(27) Paris,P.C. and Shih,G.C.,"Stress analysis of cracks", ASTM STP 391, (1965) pp. 30 - 81.

(28) Fedderson, C.E.,"Discussion", ASTM STP 410, (1967) pp.77 - 79.

(29) Sneddon,I.N.,"The distribution of stress in the neighbour. hood of a crack in an elastic solid", Proc.Roy.Soc.London A 187, (1946) pp.229 - 260.

(30) Green,A.E. andSneddon, I.N.,"The stress distribution in the neighbourhood of a flat elliptical crack in an elastic solid", Proc. Cambridge Phil.Soc., 46 (1950) pp. 159 - 164.

(31) Kobayashi, A.S., Zii,M. and Hall, L.R.,"Approximate stress intensity factor for an embedded elliptical crack near to parallel free surfaces", Int.J.Frac.Mech., (1965) pp. 81 -95.

(32) Rice,J.R.,"The line spring model for surface flaws. The surface crack : physical problems and computational solutions", pp.171 - 185. ASME, (1972).

(33) Rice,J.R. and Levy,N.,"The part. through surface crack in an elastic plate", J.Appl.Mech., (1972) pp. 185 - 194 .

(34) Grandt,A.F., and Sinclair,G.M.,"Stress intensity factors for surface cracks in bending", ASTM STP 513, (1972) pp.37 - 58.

(35) Shah,R.C. and Kobayashi, A.S.,"Stress intensity factors for an elliptical crack approaching the surface of a semi-infinite solid", Int.J.of Fracture, 9 (1973) pp. 133 - 146.

(36) Underwood,J.H.,"Comments on previous reference", Int.J. of Fracture, 9 (1973) pp.147 - 148.

(37) Shah,R.C. and Kobayashi, A.S.,"Stress intensity factor for an elliptical crack approaching the surface of a plate in bending ", ASTM STP 513, (1972) pp.3 - 21.

(38) Marrs,G.R. and Smith,C.W.,"A study of local stresses near surface flaws in bending fields, ASTM STP 513, (1972) pp.22-36.

(139) Newman,J.C.,"Fracture analysis of surface - and through.- cracked sheets and plates", Eng. Fracture Mechanics, 5 (1973) pp. 667 - 690.

(40) Bonesteel,R.M.,"Fracture of thin sections containing surface cracks", Eng.Fracture Mechanics, 5 (1973) pp. 541 - 554.

(41) Irwin,G.R.,"Fracture Mechanics", Structural mechanics, Pergomon press, London, (1960) pp. 560 - 574.

(42) Irwin,G.R.,"Plastic zone near a crack and fracture toughness", Proc. 7 th Sagamore Conf.p. IV - 63 (1960).

(43) Dugdale,D.S.,"Yielding of steel sheets containing slits", J. Mech.Phys.Sol., 8 (1960) pp.100 - 108.

(44) Burdekin,F.M. and Stone,D.E.W.,"The crack opening displacement approach to fracture mechanics in yielding materials", J.Strain Analysis, I (1966) pp. 145 - 153.

(45) Barenblatt,G.I.,"The mathematical theory of equilibrium of cracks in brittle fracture", Advences in Appl.Mech., 7 (1962) pp. 55 - 129.

(46) Bilby, B.A.,Cottrell,A.H. and Swinden,K.H.,"The spread of plastic yield from a notch", Proc.Roy.Soc.A 272 (1963) pp. 304 - 310.

(47) Bilby,B.A. and Swinden, K.H.,"Representation of plasticty at notches by dislocation arrays", Proc.Roy.Soc.A285, (1965) pp. 22 - 30.

(48) McClintock,F.A. and Irwin,G.R.,"Plasticty aspects of fracture mechanics", ASTM STP 381, (1965) pp.84 - 113.

(49) Duffy,A.R.et al.,"Fracture design practice for pressure piping", Fracture I pp. 159 - 232. Liebowitz ed., Academic press (1969).

(50) De Koning, A.V.,"Results of calculations with TRIM 6 and TRIAX 6 elastic - plastic elements", Nat. Aerospace Inst. Amsterdam, Rept. MP 73010 (1973).

(51) Rice,J.R. and Rosengren,G.F.,"Plane strain deformation near a crack tip in a power - law hardening material",J.Mech.Phys.Sol., 16 (1968) p. 1.

(52) Underwood,J.H. and Kendall, O.P.,"Measurement of plastic strain distributions in the region of a crack tip", Exp.Mechanics , (1969) pp. 296 - 304.

(53) Rice,J.R.,"The mechanics of crack tip deformation and extension by fatigue", Brown University rept. NSF GK-286/3 (1966).

(54) Swedlow,J.L., Williams,M.L. and Yang,W.H.,"Elastic - plastic stresses and strain in cracked plates", Ist ICF Conf.,I, pp. 259 -282 (1965).

(55) Gerberich,W.W. and Swedlow,J.L.,"Plastic strains and energy density in cracked plates". Experiments, Exp.Mech., 4 (1964) pp. 335 - 344.

(56) Gerberich,W.W. and Swedlow,J.L.,"PlasticStrains and energy density in cracked plates". Theory,Exp.Mech. 4 (1964) pp. 345 - 351.

(57) Oppel,G.U. and Hill,P.W.,"Strain measurements at the root of cracks and notches", Exp.Mechanics, 4 (1964) pp. 206 - 214.

(58) Hahn,G.T. and Rosenfield,A.R.,"Experimental determination of plastic constraint ahead of a sharp crack under plane - strain conditions", ASM Trans., 59 (1960) pp. 909 - 919.

(59) Broek,D.,"Elementary engineering fracture mechanics", Leyden, (1974) pp. 241 - 245.

(60) Elber,W.,"The significance of fatigue crack closure", ASTM STP 486, (1971) pp.230 - 242.

(61) Wheeler, O.E."Spectrum loading and crack growth", J. of Basic Engineering, 94 D (1972) pp. 181 - 186.

(62) Willenborg,J.D.,et al, "A crack growth retardation model using an effective stress concept", AFFDL - TM - 71 - 1 FBR (1971).

(63) Habibie ,B.J.,"Fatigue crack growth prediction", Messerschmidt - Bolkow - Blohm,Report No. Uh - 03 - 71 (1971).

(64) Hanel,J.J.,"Crack growth prediction under variable amplitude loading on the basis of Dugdale model", German Society for Materials Testing (1973).

(65) Bell,P.D.,and Creager,M.,"Crack growth analysis for arbitrary spectrum loading", AFFDL - TR - 74 - 129, (1975).

(66) Schijve,J.,"Four lectures on fatigue crack growth",Engineering Frac.Mech. Vol. II, pp.167 - 221 , (1979).

(67) Wood,H.A.,"A summary of crack growth prediction technigues", AGARD - LS - 62 , (1973) , sect.8.

(68) Shih,T.T. and Wei,R.P.,"A study of crack closure fatigue ", Lehigh university, IFSM 72-5 NASA Grant. NGL 39 - 007 - 040.

(69) Barsom,J.M., "Fatigue-crack growth under variable amplitude loading in ASTM A514 Grade B steel", ASTM STP 536,Philadelphia 1973.

(70) Rolfe , S.T., Barsom, J.M.,"Fracture and fatigue control in structures", (1977) pp. 270 - 281.

(71) Smith,S.H.,"Random loading fatigue crack growth behavior of

some aluminum and titanium alloys",structural fatigue in aircraft , ASTM STP 404, 74 (1966).

(72) Swanson,S.R., Cicci,F. and Hoppe, W.,"Crack propogation in clad 7079 - T6 aluminum alloy sheet under constant and random amplitude fatigue loading", Fatigue crack propagation, ASTM STP 415 , 312 (1967).

(73) Frost,N.E.,Marsh,K.J.,Pook,L.P.,"Metal Fatigue" , 1974 , pp. 260 - 275.

(74) Davis , S.O.,Typps, N.G. and Niemi, R.M.,"Effect of specimen type and crack orientation on fracture toughness ", AFML - TR-67 - 38 , March (1967).

(75) Barsom , J.M. and Rolfe ,S.T.,"Impact testing of metals", ASTM STP 466 , (1970) p. 281.

(76) Kanazawa, T."Correlation of brittle fracture strength and chevron notched Charpy impact test results", 3rd ICF Conf. III (1973) II - 232.

(77) Witzell,W.E. and Adsit,N.R.,"Temperature effects on fracture", Fracture IV , pp.69 - 112, Liebowitz .Ed. Academic press (1969).

(78) Schmidt,R.A. and Paris ,P.C.,"Threshold for fatigue crack propagation and the effects of load ratio and freguency", ASTM STP 536, pp. 79 - 94 (1973).

(79) Paris,P.C.,Weiss, W.,Wessel, E.T. and Anderson , A.F., "On the threshold for fatigue crack growth", presented at the Fifth International Symposium on fracture mechanics , 1971.

(80) James, L.A.,"The effect of frequency upon the fatigue - crack growth of type 304 stainless steel at 1000F ", ASTM STP 513 , pp. 218 - 229 (1972).

(81) Sprowls,D.O. and Brown, R.H.,"Resistance of wrought high strength aluminum alloys to stress corrosion", Alcoa Research Lab. Technical paper no.17, Also published in metal Progress part I, April (1962) and part II, May (1962).

(82) Broek, D.,"Elementary Engineering Fracture Mechanics", 1978) pp. 402 - 422.

(83) Porter, T.R.,"Method of Analysis and Prediction for variable Amplitude Fatigue Crack Growth", Engineering Fracture Mechanics, 1972, Vol. 4, pp. 717 - 736.

(84) Johnson,W.S.,"Multi - parameter yield zone model for predicting Spectrum crack growth", ASTM STP 748 , 1981 , pp. 85 - 102.

(85) Robin, C. and Pelloux , R.M.,"Fatigue Crack growth retardation in an aluminum alloy", Materials Science and Engineering, 44 (1980). pp. 115 - 120.

(86) Smith, F.W.,"Stress Intensity Factors for a Semi - elliptical Surface flaw", Structural Development Research Momerandum 17, The Boeing corp .,Seattle, Wash., Aug. 1966.

(87) Marrs, G.R., and Smith, C.W., " A Study of Local Stresses Near Surface Flaws in Bending Fields", ASTM STP 513 , 1971, pp. 22 - 36.

(88) Klippstein,K.H. and Schilling, C.G., "Stress spectrums for short span steel bridges " submitted for presentation at the ASTM symposium on fatigue crack growth under spectrum loads, Montreal , June 1975.